Development, optimisation, and application of ICP-SFMS methods for the measurement of isotope ratios

Sturup, Stefan

Publication date:
2000

Document Version
Publisher's PDF, also known as Version of record

Risø-R-1192(EN)

Development, optimisation, and application of ICP-SFMS methods for the measurement of isotope ratios

Stefan Stürup

Risø National Laboratory, Roskilde, Denmark
July 2000

Abstract The measurement of isotopic composition and isotope ratios in biological and environmental samples requires sensitive, precise, and accurate analytical techniques. The analytical techniques used are traditionally based on mass spectrometry, among these techniques is the ICP-SFMS technique, which became commercially available in the mid 1990s. This technique is characterised by high sensitivity, low background, and the ability to separate analyte signals from spectral interferences. These features are beneficial for the measurement of isotope ratios and enable the measurement of isotope ratios of elements, which it has not previously been possible to measure due to either spectral interferences or poor sensitivity.

The overall purpose of the project was to investigate the potential of the single detector ICP-SFMS technique for the measurement of isotope ratios in biological and environmental samples. One part of the work has focused on the fundamental aspects of the ICP-SFMS technique with special emphasize on the features important to the measurement of isotope ratios, while another part has focused on the development, optimisation and application of specific methods for the measurement of isotope ratios of elements of nutritional interest and radionuclides.

The fundamental aspects of the ICP-SFMS technique were investigated theoretically and experimentally by the measurement of isotope ratios applying different experimental conditions. It was demonstrated that isotope ratios could be measured reliably using ICP-SFMS by educated choice of acquisition parameters, scanning mode, mass discrimination correction, and by eliminating the influence of detector dead time.

Applying the knowledge gained through the fundamental study, ICP-SFMS methods for the measurement of isotope ratios of calcium, zinc, molybdenum and iron in human samples and a method for the measurement of plutonium isotope ratios and ultratrace levels of plutonium and neptunium in environmental samples were developed. The figures of merit of these methods demonstrated that isotope ratios could be measured with good precision and accuracy by ICP-SFMS.

This thesis is submitted in partial fulfilment of the requirements for the degree of Doctor of Philosophy at the Technical University of Denmark.

ISBN 87-550-2715-6; ISBN 87-550-2738-5 (Internet)
ISSN 0106-2840

Information Service Department, Risø, 2000

Contents

List of abbreviations and symbols *6*

Preface *8*

1 Introduction *10*

1.1 Isotopes, isotopic composition and isotope ratios *10*
1.2 Mass spectrometry *12*
1.3 Measurement of isotope ratios *14*
1.4 Aim of the studies *14*
1.5 Outline of the thesis *15*

2 The ICP-MS technique *15*

2.1 ICP-MS in general *15*
2.2 The ICP-SFMS instrument - an overview *17*
2.3 Sample introduction *18*
2.4 Ion source and interface *19*
2.5 The mass analyser of the PT2 ICP-SFMS instrument *20*
2.5.1 The magnetic sector *21*
2.5.2 The electrostatic analyser *22*
2.5.3 Double focusing sector field mass spectrometry *23*
2.5.4 Mass resolution, ion transmission and peak shape *23*
2.6 Scanning modes *25*
2.6.1 Magnetic scanning *25*
2.6.2 Voltage scanning *26*
2.6.3 Combined magnetic and voltage scanning *26*
2.6.4 Simultaneous magnetic and voltage scanning *27*
2.6.5 Choosing the right scanning mode *27*
2.7 The detector system *27*
2.7.1 The continuous dynode electron multiplier *28*

3 Measurement of isotope ratios using ICP-SFMS *29*

3.1 Statistics and notations *29*
3.2 Isotope ratios on the PT2 ICP-SFMS instrument *31*
3.3 Experimental evaluation of different scanning modes *31*
3.3.1 Peak hopping *32*
3.3.2 Peak scanning *32*
3.4 Mass discrimination *34*
3.4.1 Mass discrimination, theoretical considerations *34*
3.4.2 Correction for mass discrimination *36*
3.5 Detector dead time *39*
3.6 Spectral interferences *42*
3.7 Background signals, contamination, losses *44*
3.8 Signal noise *44*
3.9 Development of methods for isotope ratio measurements *46*
3.10 Characteristics of ICP-SFMS for isotope ratio measurements *49*

4 Isotope ratios and tracer experiments in human nutrition *49*

4.1 Measurement of calcium isotope ratios *51*
4.2 Measurement of zinc isotope ratios *56*
4.3 ICP-SFMS for the measurement of the $^{97}Mo/^{98}Mo$ ratio in urine *57*
4.4 ICP-SFMS for the measurement of iron isotope ratios *61*

4.5 Conclusions of the measurement of isotope ratio of nutritional elements *65*

5 Isotope and ultratrace analysis of long-lived radionuclides *66*

5.1 Isotope ratio and ultratrace determination of plutonium isotopes *68*
5.2 Ultratrace determination of neptunium *70*
5.3 Conclusions on the determination of neptunium and plutonium by ICP - SFMS *71*
5.4 Measurement of technetium by ICP-SFMS *71*

6 Measurement of lead isotope ratios using ICP-SFMS *74*

7 Conclusions and suggestions for future research *77*

7.1 Conclusions *77*
7.2 Suggestions for future research *79*

8 References *80*

Appendix 1: Peak hopping with the PT2 ICP-SFMS instrument *87*

Appendix 2: Experimental evaluation of scanning rates *90*

Appendix 3: Mass discrimination factors *96*

Appendix 4: *97*

Appendix 5: Determination of detector dead time *99*

Appendix 6: Uncertainty on calcium absorption rates *102*

Paper I *107*

Paper II *113*

Paper III *120*

List of abbreviations and symbols

$\%RSD_m$	Experimentally determined relative standard deviation of isotope ratio measurement (measurement precision)
$\%RSD_t$	Theoretical standard deviation of isotope ratio calculated from counting statistics
%XS	Relative atom enrichment
A	Abundance
AAS	Atomic absorption spectrometry
AMS	Accelerator mass spectrometry
B	Magnetic field
CRM	Certified reference material
τ	Detector dead time
E_k	Kinetic energy
ETV	Electrothermal vaporisation
F	Force
FAB-MS	Fast atom bombardment mass spectrometry
f_{md}	Mass discrimination factor
HR-ICP-MS	High resolution inductively coupled plasma mass spectrometry equals ICP-SFMS
IAEA	International Atomic Energy Agency
ICP	Inductively coupled plasma
ICP-CC-MS	Inductively coupled plasma collision cell mass spectrometry
ICP-MS	Inductively coupled plasma mass spectrometry
ICP-QMS	Inductively coupled plasma quadrupole mass spectrometry
ICP-SFMS	Inductively coupled plasma sector field mass spectrometry
ICP-TOF-MS	Inductively coupled plasma time-of-flight mass spectrometry
IUPAC	International Union of Pure and Applied Chemistry
m	Mass
ε	Mass discrimination per mass unit
MC-ICP-SFMS	Multiple collector inductively coupled plasma sector field mass spectrometry
MCN	Microconcentric nebuliser
N	Number of ion counts
n	Number of replicates
NA	Natural abundance
NIST	National institute of standards and technology
p	Momentum
PT2	PlasmaTrace2, The Micromass ICP-SFMS instrument
r	Correlation coefficient
R	Isotope ratio

r_e	Radius of the ion flight path in the electrostatic sector
RF	radio frequency
r_m	Radius of the ion flight path in the magnetic sector
RP	Mass resolution (resolution power)
R_p	Ratio between measurement and theoretical precision
RSD_t	Relative standard deviation in the Poisson distribution
SD	Standard deviation
SD_t	Standard deviation in the Poisson distribution
SEM	Standard error of the mean
t	Dwell time
TIMS	Thermal ionisation sector field mass spectrometry
TI-QMS	Thermal ionisation quadrupole mass spectrometry
U	Voltage
U_{acc}	Acceleration voltage
U_e	Voltage on electrostatic sector
U_{fl}	Voltage applied on the flight tube
u_c	Combined uncertainty
USN	Ultrasonic nebuliser
v	Velocity
$\bar{x}$	Average
z	Charge

Preface

This thesis reports the results of a Ph.D. study on measurements of isotope ratios applying ICP-SFMS. The work was carried out in the period from April 1997 to September 1999 as a joint venture between the Department of Chemistry, The Technical University of Denmark, and the Plant Biology and Biogeochemistry Department, Risø National Laboratory. The thesis consists of a report describing the development, optimisation and application of ICP-SFMS methods for the measurement of isotope ratios and three papers where details of the study are given. The three papers are:

Paper I:
Stürup S, Hansen M, Mølgaard C. *Measurement of ^{44}Ca:^{43}Ca and ^{42}Ca:^{43}Ca isotopic ratios in urine using HR-ICPMS*. J. Anal. Atom. Spectrom., 1997, 12, 919-923.

Paper II:
Stürup S, Dahlgaard H, Nielsen SC. *High Resolution Inductively Coupled Plasma Mass Spectrometry (HR-ICPMS) for Trace Determination of Plutonium Isotopes and Isotope Ratios in Environmental Samples*. J. Anal. Atom. Spectrom., 1998, 13, 1321-1326.

Paper III:
Stürup S. *Application of HR-ICPMS for the simultaneous measurement of zinc isotope ratios and total zinc content in human samples*. J. Anal. Atom. Spectrom., 2000, 15, 315-321.

I wish to thank my supervisors Professor, dr.techn. Elo Harald Hansen, Department of Chemistry, The Technical University of Denmark, and research specialist Vagn Gundersen, Plant Biology and Biogeochemistry Department, Risø National Laboratory for their guidance and support throughout the Ph.D. project. Furthermore, I would like to express my gratitude to Risø National Laboratory for providing the funds necessary and maintaining my employment as scientist during the 2½-years of the Ph.D. project.

Moreover I would like to thank:

Dr. Marianne Hansen, the Research Department of Human Nutrition, The Royal Veterinary and Agricultural University, Frederiksberg for inspiring collaboration, fruitful discussions and constructive comments to the manuscript.

Dr. Henning Dahlgaard, The Nuclear Safety Research and Facilities Department, Risø National Laboratory for inspiring collaboration and many interesting discussions.

Dr. Miranda Keith-Roach, The Nuclear Safety Research and Facilities Department, Risø National Laboratory for many interesting discussions and critical revision of the manuscript.

My fellow Ph.D. student Steffen Chen Nielsen, Department of Chemistry, The Technical University for many enjoyable hours of studying, discussions and critical revision of the manuscript.

Lis V. Kristensen, Jette B. Nielsen, Annette Møller and Ingelis Larsen, all of the Plant Biology and Biogeochemistry, Risø National Laboratory for their skilful technical assistance.

Finally, I would like to express my warm appreciation to my wife Lene and my children Andrea and Mads for their support and putting up with my long working hours.

Stefan Stürup

1 Introduction

1.1 Isotopes, isotopic composition and isotope ratios

Isotopes are atoms of the same element, which have different numbers of neutrons. All the isotopes of an element have the same atomic number, but different mass numbers. For example zinc, atomic number 30, has 5 isotopes. These are ^{64}Zn, ^{66}Zn, ^{67}Zn, ^{68}Zn and ^{70}Zn. They all contain 30 protons, but have a different number of neutrons, from 34 to 40. The number of isotopes of an element varies from 1 to 10. Most elements have one major isotope and a few minor isotopes of low abundance. In Figure 1.1 the isotopic composition of zinc is shown, the most abundant isotope is ^{64}Zn.

The natural abundance of each isotope is shown in percent over the bar. Since all isotopes of an element have the same number of electrons they have the same chemical properties, but they have different physical properties.

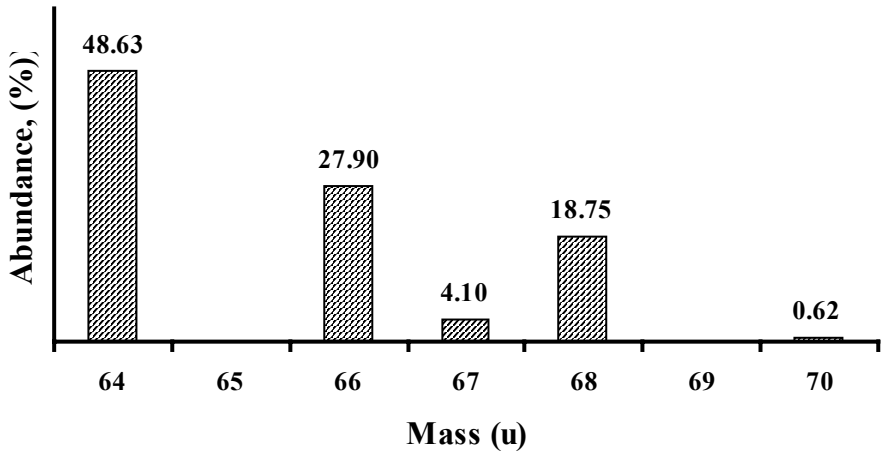

Figure 1.1 *The isotopic composition of zinc*

The amount of the different stable isotopes of most elements, the natural abundance, is constant in nature. The best measurements of the isotopic composition of the natural occurring elements are frequently evaluated by IUPAC and the best estimates of isotopic natural abundances are published[1]. These values are considered the true isotopic abundances for materials of natural terrestrial origin. Although the isotopic abundances are constant for most elements, small variations are found for some 20 elements in nature. The differences in isotopic composition of light elements such as lithium, boron, sulfur are caused by physico-chemical fractionation processes (also known as mass fractionation). The main factor controlling the fractionation is the relative mass difference of the

isotopes. Boron, for example, has a complex chemistry and a large relative mass difference between its two isotopes; consequently large variation of the $^{11}B/^{10}B$ ratio is found in nature, ranging from 4.28 to 3.92[1]. For the heavier elements, such as strontium, neodynium and lead, the isotopic composition varies because one or more of the isotopes are the end-product of radioactive decay. The isotopic composition is dependent of the age and composition of the original material. For lead, three of the isotopes originate from radioactive decay and all have long-lived radioactive parents; ^{232}Th ($t_{½} = 1.4 \cdot 10^{10}$ y) is the parent of ^{208}Pb, ^{235}U ($t_{½} = 7 \cdot 10^{8}$ y) of ^{207}Pb and ^{238}U ($t½ = 4.5 \cdot 10^{9}$ y) of ^{206}Pb. The last lead isotope, ^{204}Pb does not have a long-lived radioactive parent. The isotopic abundance of ^{206}Pb, for example, varies between 20.84 and 27.48 % in nature[1]. Knowledge of the isotopic compositions in nature is therefore useful in investigating and understanding geochemical processes and the origin and age of materials. Differences in isotope abundances are also seen between terrestrial and extraterrestrial materials[2,3].

The isotopic composition of an element can be changed artificially and materials are formed, which usually have enriched abundance of one isotope and depleted abundances of the other isotopes. As an example, the zinc used for method validation in this work, contained 98.3 % ^{68}Zn, where natural zinc only contains 18.75 %[III]. Materials enriched with isotopes are useful because the enriched isotope can be used as a tracer in environmental and biological systems, the same way as radioactive isotopes are used. Enriched stable isotopes are also useful in analytical chemistry were they are used for method validation and very accurate quantitative determination of total element content, i.e. isotope dilution. Isotope dilution excels as one of the most accurate methods for elemental analysis only surpassed by neutron activation analysis. Long-lived radioactive elements (and thereby isotopes) are formed artificially by fission. Among these man-made elements plutonium and technetium are probably the best known. They are both produced during nuclear fission processes.

The applications of isotope analysis are many and they are often divided into three groups; isotope ratio measurements, tracer experiments and isotope dilution[4]. The possible applications of isotope analysis are shown in Figure 1.2.

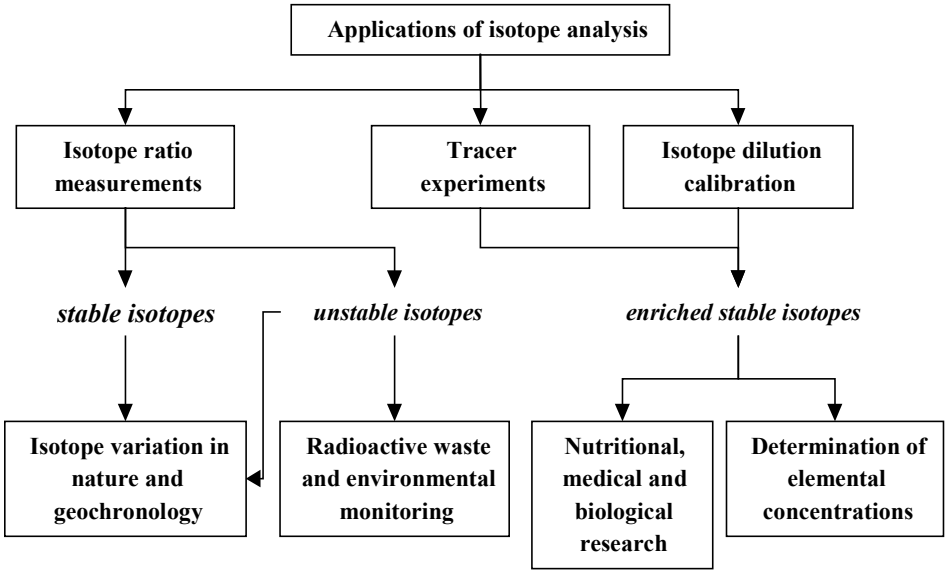

Figure 1.2 *Applications of isotope analysis*

The different possible applications cover a broad range from the determination of elemental concentrations to nutritional research and geochronology. Therefore isotope ratio measurements are useful in many different scientific disciplines. Application of isotope analysis within these scientific disciplines is only useful if accurate, precise and reliable analytical techniques for measurement of isotopes are available.

1.2 Mass spectrometry

The majority of analytical techniques used to determine stable isotopes are based on mass spectrometry. In 1912 Thompson proved the existence of isotopes. He used a "positive ray" detector to determine the isotopes of neon[5,6]; the first single magnetic sector mass analysers were build in the late 1910s by Aston and Dempster, respectively[5,7]. Right from the start Thompson was aware of the great potential of isotope measurements. In the preface to his book from 1913 *Rays of positive electricity and their application to chemical analysis*[8] he wrote:

"One of the main reasons for writing this book was the hope that it might induce others, and especially chemists, to try this method of analysis. I feel sure that there are many problems in chemistry, which could be solved with far greater ease by this than any other method. The method is surprisingly sensitive – more so than that of spectrum analysis, requires an infinitesimal amount of material, and does not require this to be specially purified; the technique is not difficult if appliances for producing high vacua are available."

Even today chemists give the same reasons for the application of mass spectrometry. Even though the instrumentation of mass spectrometry has undergone tremendous technological development since the 1910s, all mass spectrometry instruments still operate on the same principle. This is to handle and measure ions, atoms and molecules on the basis of a very

simple but fundamental property – their mass. Today there are two main types of mass analyser that are applied to the measurement of stable isotopes. These are magnetic field (sector field) and quadrupole mass analysers of which both were developed in the 1940s and 1950s[6]. The majority of mass spectrometers in use today are quadrupole based instruments. Modern mass spectrometry instruments consist of two main parts, the ion source and the mass analyser. Different combinations of ion source and mass analyser produce different instruments, which have their advantages within different areas of research.

The most frequently used techniques in the measurement of stable isotopes in biological and environmental samples are TIMS (thermal ionization mass spectrometry), equipped with either quadrupole or magnetic field mass analysers, FAB-MS (fast atom bombardment mass spectrometry) equipped with magnetic field mass analysers and ICP-QMS (inductively coupled plasma quadrupole mass spectrometry). During the last 10 years, new types of ICP-MS instruments have been introduced on the market. Among these are ICP-MS instruments with a magnetic field mass analyser and either a single detector (ICP-SFMS) or multiple detectors/collectors (MC-ICP-SFMS). Instruments applying time-of-flight mass analysers (ICP-TOF-MS) and instruments with a collision cell in front of the mass analyser (ICP-CC-MS) are now also commercially available. All of these instruments have been developed with the aim of solving one or more of the problems encountered in ICP-QMS, especially the problem of spectral interferences. The main advantage of applying magnetic field mass spectrometry is that analyte peaks can be separated from spectral interferences applying a high mass resolution, therefore more isotopes can be measured free of intereferences than when using ICP-QMS. With both MC-ICP-SFMS and ICP-TOF-MS several isotopes can be measured simultaneously, therefore possible isotope ratios can be measured with very good precision. In collision cell instruments, the argon or oxygen ions in the ion beam can be stripped of by an appropriate collision gas, resulting in removal of either argon or oxygen containing spectral interferences. The recent developments in the instrumentation of ICP-MS has opened the way to certain isotope ratio applications, which had previously been beyond the reach of ICP-MS. However, since the more advanced ICP-MS instruments are still only used in a small number of laboratories around the world, the potential of these techniques has not yet been explored in full, and many aspects of the measurement of isotope ratios with these instruments are still to be investigated in detail. The new applications can be illustrated by looking at the developments in the measurement of sulfur isotope ratios using ICPMS. With ICP-QMS the sulfur isotopes cannot be measured directly because of spectral interferences, instead the $^{32}S^{+}/^{34}S^{+}$ ratio can be measured indirectly as the $^{32}SO^{+}/^{34}SO^{+}$ ratio[9]. Applying ICP-SFMS, the $^{32}S^{+}/^{34}S^{+}$ ratio can be measured directly using a high mass resolution[10]. Most recently the spectral interferences have been almost eliminated with the application of ICP-CC-MS and the $^{32}S^{+}/^{34}S^{+}$ ratio can be measured directly using low mass resolution[11]. This again illustrates the breadth of the potential of these new ICP-MS techniques

and that many new applications of the ICP-MS technique are now within reach.

1.3 Measurement of isotope ratios

The validity and usefulness of an analytical technique for the measurement of isotope ratios depends upon the accuracy and precision by which a ratio can be measured. It is therefore important that the mass spectrometric technique used possesses sufficient accuracy and precision for the specific application. Different applications require different accuracy and precision. Typical a measurement precision better than 0.05 % is required for geological dating purposes[12]. For other applications like tracer experiments, environmental studies, studies on radioisotopes or isotope dilution for the measurement of total concentrations, a measurement precision in the range of 0.1 to 1 % is required[12,13]. The latter can in principal be achieved with most techniques available today for the measurement of isotope ratios in biological and environmental samples, while a measurement precision better than 0.05 % is more difficult to obtain, and so far it can only be obtained on a routine basis using TIMS[12,14] or MC-ICP-MS[15-17].

All mass spectrometry analyse are to some extent are prone to spectral interferences and instrumental mass discrimination. As a result the measured isotope ratios are often inaccurate and need to be corrected in order to achieve sufficient accuracy. Accuracy and precision are not the only factors of importance when isotope ratios are measured. Sample preparation procedures, ease of operation and cost also have to be taken into account when the choice of mass spectrometric technique is made.
Among the new ICP-MS techniques mentioned especially ICP-SFMS posseses characteristics that potentially are advantageous for the measurement of isotope ratios. The use of magnetic field mass analysers opens up for the opportunity to apply a high mass resolution and thereby resolve analyte peaks from interfering ionic molecules of the same nominal mass. Therefore, potentially, isotope ratios of almost any element can be measured with a high degree of accuracy. If interferences are resolved during the analysis there is no need for a separation of the analyte from the sample matrix during the sample preparation, which significantly simplifies the sample preparation. Furthermore flat-topped peaks can be obtained, which improves precision when repetitive sweeps are used. These features make it interesting to investigate the potential of ICP-SFMS for the measurement of isotope ratios.

1.4 Aim of the studies

The scope of this Ph.D. study was to investigate the potential of the single detector ICP-SFMS technique for the measurement of isotope ratios in biological and environmental samples. The investigation includes both fundamental aspects and applications. In order to meet these general goals the work was directed towards:

- Characterisation and optimisation of the ICP-SFMS instrument
- Development of a range of ICP-SFMS methods for the measurement of isotope ratios of different elements requiring different analytical approaches in order to achieve good accuracy, good precision, and high sensitivity and selectivity.
- Investigation and optimisation of the factors that control the accuracy and precision of isotope ratio measurements, including estimations of the combined method uncertainties for measurement and use of isotope ratios.
- Identification of spectral interferences in different sample matrices.
- Application of the developed ICP-SFMS methods with the purpose of solving different analytical problems within biological and environmental science.

1.5 Outline of the thesis

The first part of the thesis (chapter 2 and 3) is a discussion of the fundamental aspects of the ICP-SFMS technique. The theory given strives to be thorough and detailed on the aspects that have major influence on the measurement of isotope ratios, and when possible, supported by experimental data. The second part of the thesis (chapter 4, 5, and 6) describes the methods developed for the measurement of isotope ratios. The three papers included mainly describe the developed methods and their application. However, they also contain more fundamental discussions, especially on the occurrence and formation of spectral interference[I,III] and optimisation of acquisition parameters[II].

Throughout the thesis the focus is on the ICP-SFMS technique and measurement of isotope ratios. Related areas of research like other mass spectrometry techniques, measurement of total elemental content, development of sample preparation procedures, experimental designs for method optimisation, human nutrition and the chemistry of radionuclides are not covered in detail. These subjects are only discussed when appropriate for the discussion and evaluation of the obtained results.

2 The ICP-MS technique

2.1 ICP-MS in general

In general all ICP-MS instruments consist of the same four basic elements, the sample introduction system, the ion source (inductively coupled plasma), the mass analyser and the detector. In Figure 2.1 a schematic drawing of an ICP-MS instrument is shown.

Normally the sample introduction system consists of a peristaltic pump, which delivers the sample solution to the nebuliser, where the sample aerosol is formed with the aid of a small stream of argon gas. The sample aerosol then passes through a spray chamber, which only allows droplets below a certain size (< 10 μm) to pass through to the argon plasma. The ion source is common to all ICP-MS instruments. The ICP is an argon plasma (6-8000°C), running at atmospheric pressure, into which the sample aerosol is introduced. In the plasma the analyte is desolvated, vaporised, atomised and ionised. The analyte ions are transported through the mass analyser to the detector.

Different types of ICP-MS instruments apply different kinds of mass analysers and detector systems. The role of the mass analyser is to separate the analyte ions from all other ions and direct only the analyte ions towards the detector; a separation based on the m/z ratio. The detector simply counts the ions that arrive at a given time, and the signals from the detector are send to a computer, where the data are processed and a mass spectrum formed.

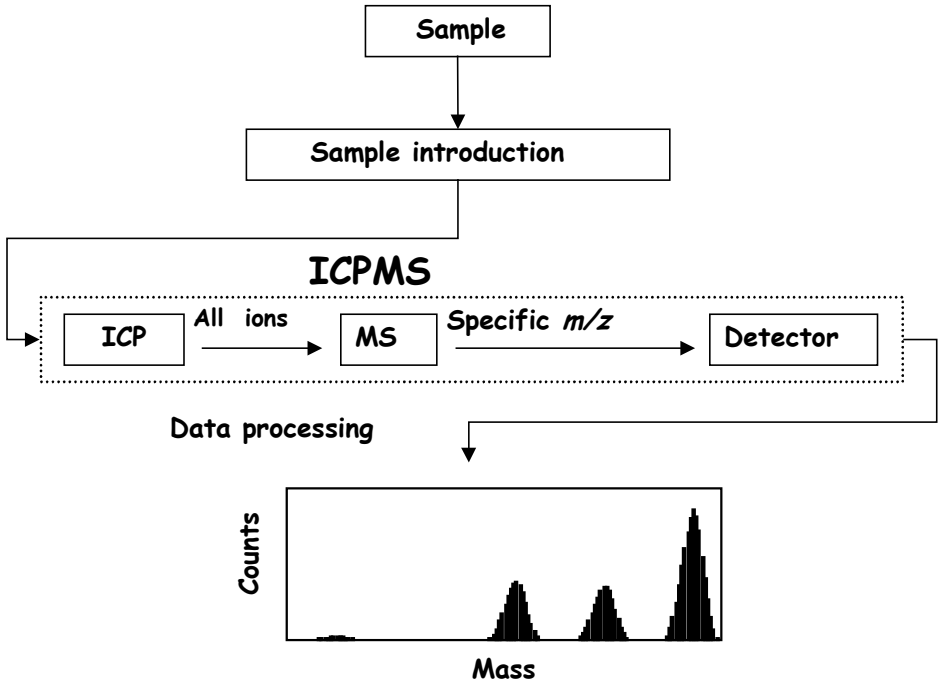

Figure 2.1 *General schematic of an ICPMS instrument*

The combination of ICPs with mass analysers (quadrupoles at first) are relatively new, the first paper was published by Houk et al. in 1980[18]. The technique quickly proved to be a breakthrough for elemental analysis and has a great potential for elemental determinations, i.e. excellent sensitivity, nearly complete elemental coverage, wide linear range, and isotopic information. The main weaknesses are interferences and limited precision on isotope ratios due to signal noise. Today ICP-MS instruments are widespread and used in thousands of laboratories throughout the world.

2.2 The ICP-SFMS instrument - an overview

The ICP-MS instrument applied for the experimental work in this project is a single detector inductively coupled plasma sector field mass spectrometer (ICP-SFMS). This type of instrumentation is often referred to as high resolution inductively coupled plasma mass spectrometry (HR-ICP-MS) due to its ability to separate analyte signals from spectral interferences of the same nominal mass. Since the first abbreviation is more accurate and covers all possible usage of the instrument (also analysis using low mass resolution setting) the term ICP-SFMS is used throughout this thesis. The instrument used is a PlasmaTrace2 ICP-SFMS instrument from Micromass Ltd, Manchester, England. An overview of the instrument is shown in Figure 2.2

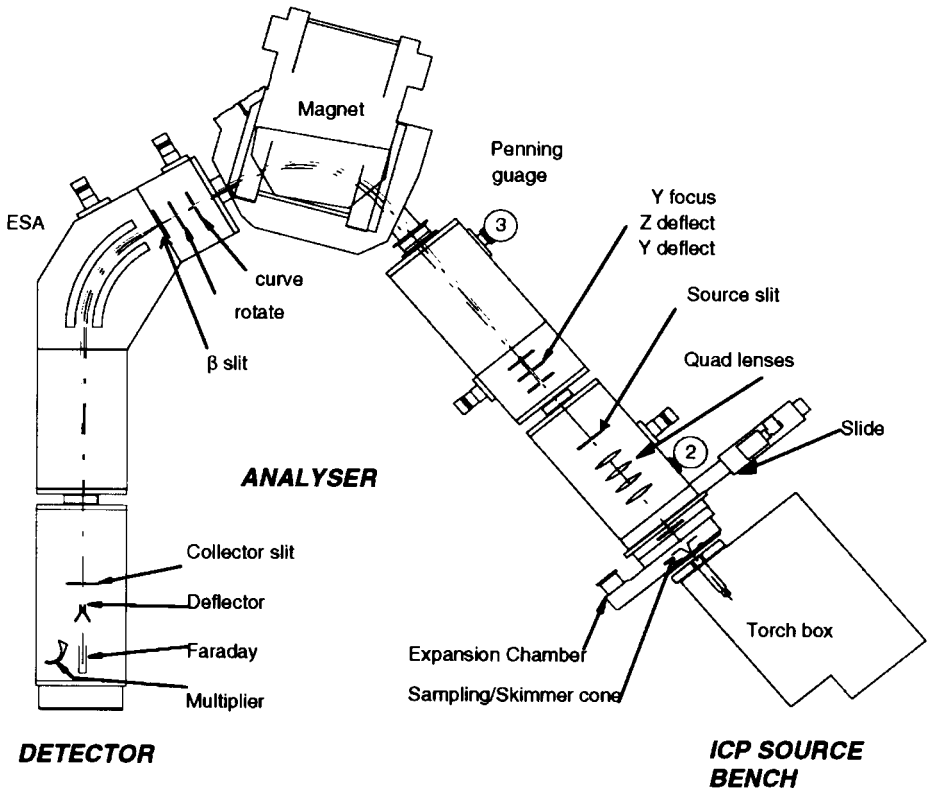

Figure 2.2 *An overwiev of the PT2 ICP-MS instrument, reprinted from the PT2 manual*

In the argon plasma a circular ion beam is formed. Via apertures in the sampler and skimmer cones held at 6000 V, the extraction lens (4200 V) and a grounded ion lens the ion beam is accelerated towards the quadrupole lens stack, where the ion beam is focused. Afterwards it passes through the source slit, which together with the collector slit determines the mass resolution setting. Between the source slit and the magnet, the position and width of the ion beam is adjusted by 3 electrostatic lenses so that it enters the magnet at exactly the right position. Only ions with the selected m/z ratio are allowed to pass

through the magnet and enter the electrostatic analyser (ESA), in which the energy spread of the ion beam is cancelled. Two ion lenses between the magnet and the electrostatic analyser adjust the shape of the ion beam. The ion beam then passes through the collector slit and enters the detector section. Here the ion beam reaches the faraday detector, which is placed directly behind the collector slit. Applying a voltage of approximately 900 V to the deflector plate, the ion beam is directed towards the electron multiplier.

It is important to understand how the instrument operates in detail in order to setup and optimise the analytical procedures for isotope ratio measurements. Therefore in the next chapters the sample introduction system, the ion source, the mass analyser and the detector system are explained in detail with special emphazise on features important for the measurement of isotope ratios.

2.3 Sample introduction

In the experimental work of this thesis two different sample introduction systems have been used. The normal instrument set-up, consists of a peristaltic pump, a concentric nebuliser and a spray chamber maintained at 5°C. The peristaltic pump delivers the sample solution to the centre glass capillary of the nebuliser, where a small stream of argon facilitates the formation of a sample aerosol (pneumatic nebulisation). In the spray chamber only aerosols with a diameter below 10 μm are allowed into the plasma, droplets with a larger diameter are send to drain. The sample uptake rate is approximately 0.5 ml/min. The benefits of this sample introduction system are that it is simple, robust, reliable, and easy to operate. The main disadvantage is that only 1-3 % of the sample solution reaches the plasma, which limits the overall sensitivity. Therefore when ultratrace analysis is performed a different sample introduction system is used.

For this purpose an ultrasonic nebuliser (USN, U-5000AT$^+$, CETAC, USA) was employed. Via the peristaltic pump the sample solution is introduced onto the surface of a piezoelectric transducer, where the aerosol is formed. From the spray chamber an argon gas transports the sample aerosol through the heating chamber (140°C) and the condenser (3°C) whereby the solvent is almost completely removed. The sample uptake rate is approximately 1.1 ml/min and the analyte transport efficiency of the ultrasonic nebuliser is approximately 20 %. Therefore a significant better overall sensitivity is obtained relative to the instrument set-up with a concentric nebuliser. Normally, a 10-fold increase in sensitivity is obtained. A further advantage is that the solvent is removed, which significantly reduces the occurrence of oxygen and hydrogen containing interferences.

For the experimentally work performed in this project pneumatic nebulisation was used for most applications, while an ultrasonic nebuliser was applied for the measurement of radionuclides.

2.4 Ion source and interface

The PT2 instrument is equipped with an inductively coupled argon plasma as the ion source. The plasma is formed at atmospheric pressure in a stream of argon (≈ 15 l/min) flowing through a concentric quartz torch. A load coil connected to a radiofrequency (RF) generator operated at 27 MHz encircles the torch, see Figure 2.3. The magnetic field generated by the RF current through the load coil induces a current in the argon stream. When the argon stream is seeded with energetic electrons from a Tesla discharge the plasma is formed. The plasma has an annular configuration, this ensures the efficient introduction of the sample aerosol into the central channel of the plasma, where the sample aerosol is desolvated, vaporised, atomised and ionised.

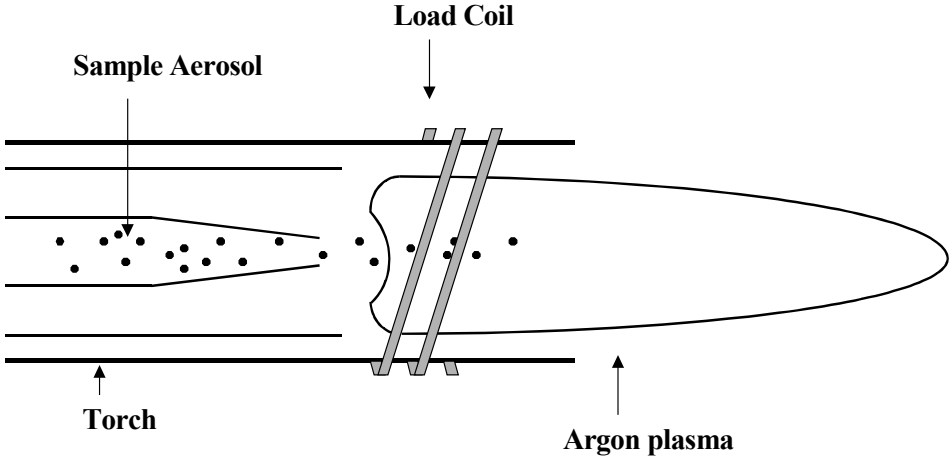

Figure 2.3 *The argon plasma*

There are many analytical advantages of using the ICP as an ion source. It has a high electron density (1-3 · 10^{15}/cm^3) and a high electron temperature (8000 – 10000 K) ensuring efficient ionisation of a wide range of elements[19]. Argon has a first ionisation potential of 15.76 eV, which is higher than the first ionisation potential and lower than the second ionisation potential of most elements. Therefore the majority of ions formed are single positively charged ions, which makes the resulting mass spectra relatively simple. However, low levels of doubly-charged ions and charged molecules (polyatomic ions) are also seen in the plasma, which appear as spectral interferences in the resulting mass spectra.

The ions have to be extracted from the ion source into the mass spectrometer, maintained at a vacuum. This is done via an interface, which on the PT2 instrument consists of a sample cone, skimmer cone, extraction lens, cylindrical ground lens and quadrupole lens stack. The ions are sampled from the plasma by means of the sampler cone (normally a nickel cone), which is held at 6000 V and water-cooled. A rotary pump evacuates the region behind the sampler cone (the expansion chamber) to a pressure of approximately 2 mBar. The ions form a shock wave structure behind the sampler cone (known as the zone of silence). The second cone, the skimmer cone, “skims” the analyte ions from the

zone of silence. Behind the skimmer cone the ions are extracted by a cylindrical electrode (held at ≈ 4200 V, the extraction voltage) and focused towards a cylindrical ground lens (held at 0 V), the ions pass through a hole in its centre. From the ground lens the ions are directed towards the quadrupole lens stack (4 small quadrupoles). The quadrupoles are used the transform the circular profile of the ion beam coming from the plasma to an ion beam having a ellipsoid shape as it passes through the rectangular source slit placed directly behind the quadrupole lens stack, the ion beam at this point enters the mass analyser. In the quadrupole lens chamber a pressure of 10^{-4} mBar is maintained, while on the other side of the source slit, inside the mass analyser, a pressure of 10^{-8} mBar is maintained.

The ion source and the interface have characteristics that must be taken into account when measuring isotope ratios. The most important being noise from the ion source, which has an impact on the precision of isotope ratio measurements, and space charge effects leading to mass discrimination, which in turn affects the accuracy of the isotope ratio measurement. Both these aspects will be discussed in more detail in chapter 3.

2.5 The mass analyser of the PT2 ICP-SFMS instrument

The mass analyser of the PT2 instrument is a double focusing sector field mass spectrometer, which has two analyser sectors. The magnetic sector, in which the ions are separated according to momentum, resulting in dispersion in both mass/charge ratio and energy, and the electrostatic sector, which provides dispersion in energy only. The two sectors are combined in reverse Nier-Johnson geometry in which the energy dispersion is exactly cancelled out. The mass spectrometer then provides dispersion in mass to charge ratio (m/z) only. A schematic of the PT2 ICP-SFMS mass analyser is shown in Figure 2.4.

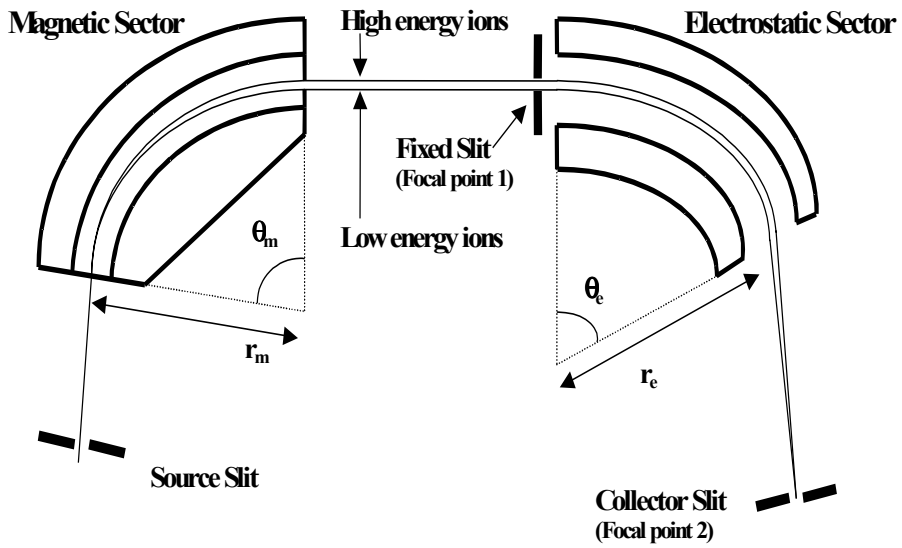

Figure 2.4 *Principle of the PT2 ICP-SFMS mass analyser*

2.5.1 The magnetic sector

The magnetic mass analyser on the PT2 instrument consists of a curved flight tube located between the poles of an electromagnet, the curvature of the flight tube is 81.6° (θ_m). The magnetic field is 0.9 tesla, when m/z = 238 is measured[20]. The magnetic field being perpendicular to the flight direction of the ions. When a moving charged particle experience a magnetic field it is deflected. Thus, a charged *(z)* ion of mass ***m***, moving through a magnetic field ***B*** with the velocity ***v*** will experience a force ***F*** perpendicular to both the flight direction and the magnetic field. This force is given by:

$$F = Bzv \qquad (2.1)$$

This results in a deflection from the initial straight flight path of the ions into a circular motion where the magnitude of the force ***F*** equals the centripetal force acting on the ion:

$$mv^2/r_m = zBv \quad or \quad mv/z = Br_m \qquad (2.2)$$

where r_m is the radius of the circular motion of the ion. The second part of equation 2.2 shows that ions of equal momentum ($p = mv$) and charge follows the same circular motion in a magnetic field. The magnetic field serves as a momentum analyser for the ion beam passing through the magnet, i.e. separation in both mass and energy is achieved. The kinetic energy (E_k) of the ion is equal to the energy gained through acceleration from the ion source.

$$E_k = ½mv^2 = Uz \quad or \quad ½mv^2 = (U_{acc} + U_{fl} + \delta U)z \qquad (2.3)$$

where U is the total acceleration voltage experienced by the ions, U_{acc} is the initial acceleration voltage of 6000 V applied to the interface, U_{fl} is the voltage applied to the flight tube inside the magnet, which can be

varied between ± 100 V and δU accounts for the initial energy spread (in eV), which the ions obtain during the formation process in the ICP. The ions formed in the ICP have an energy spread of approximately 12 eV. Combining equation 2.2 and 2.3 eliminating the velocity yields:

$$\frac{m}{z} = \frac{B^2 r_m^2}{2U} = \frac{B^2 r_m^2}{2(U_{acc} + U_{fl} + \delta U)} \tag{2.4}$$

If only ions with a single charge are considered, then with a constant field strength and constant acceleration voltage the radius of the ions circular motion depends on mass as follows:

$$r_m = \sqrt{\frac{2mU}{B^2}} \tag{2.5}$$

Low mass ions will perform a greater deflection than ions with a high mass, i.e. ions of different mass will leave the magnetic field at different positions. It is more convenient for monitoring and collection of ions that they all arrive at the same point; therefore r_m is kept constant. On the PT2 instrument r_m is 20 cm[20]. This means that by varying B and/or U ions of different mass can be brought into focus at the same point (focal point 1) sequentially. The following relationships exist between m and B and U.

$m \propto B^2$ (U constant) or $m \propto 1/U$ (B constant) or $m \propto B^2/U$ (2.6)

Again, from these relationships it can be seen that if either the magnetic field, or the voltage or both are scanned, the whole range of masses of the ions can be brought into focus sequentially at a given point, the focal point. On the PT2 instrument a slit with a fixed width of 1.8 mm is located at the focal point in between the magnetic sector and the electrostatic sector[20]. A further property of the magnetic sector is that it is also directional (or angular) focusing. The ion beam has an angular width of ± α leaving the source slit, and although the ion beam further diverges in the first flight tube between the source slit and the magnet, the beam is converged into focus at the focal point between the magnet and the electrostatic analyser. The energy dispersion of the magnetic sector limits the mass resolution to about 300 RP[21]. Therefore, to achieve high mass resolution (up to 10000 RP) a electrostatic sector is used to compensate for the energy dispersion.

2.5.2 The electrostatic analyser

The electrostatic analyser of the PT2 instrument consists of two coaxial cylindrical plates with a curvature of 60° (θ_e) with the outer and inner plate held at a positive and negative voltage of 450 V, respectively. The ion beam is injected midway between the plates. In the electrostatic sector the centripetal force acting on the ion is given by:

$$zU_e = \frac{mv^2}{r_e} \tag{2.7}$$

where r_e is the radius of the circular motion of the ion in the electrostatic sector and U_e is the difference in voltage between the plates. Combining this equation with equation 2.3 for the kinetic energy of the ion, the following relationship is obtained:

$$r_e = \frac{2U}{U_e} \quad , \quad U = U_{acc} + U_{fl} + \delta U \tag{2.8}$$

No mass or charge appears in this equation, therefore in the electrostatic sector the circular motion of the ion depends only on the voltages of the electrostatic sector (U_e) and the acceleration voltage (U), i.e. the energy of the ion (see equation 2.3). Ions of the same mass but different energies injected between the two plates of the electrostatic analyser are then brought into focus at the focal point, where the collector slit is positioned. As with the magnetic sector the electrostatic sector is directional focusing, whereas an ion beam entering the electrostatic analyser under some diverging angel is brought into focus at the focal point (the collector slit). On the PT2 instrument the voltages applied to the two plates of the electrostatic analyser are held constant at all times.

2.5.3 Double focusing sector field mass spectrometry

Combing a magnetic sector with an electrostatic sector creates a double focusing sector field mass spectrometer, a mass spectrometer that focuses in both energy and direction and gives dispersion as a function of the mass to charge ratio of the ions. The whole range of mass to charge ratios are then brought into focus at the collector slit, sequentially, by varying either or both the magnetic field of the magnetic sector and/or the voltage applied to the flight tube. On the PT2 instrument the two sectors are placed in reverse Nier-Johnson geometry, that is, the magnetic sector in front of the electrostatic sector, see Figure 2.4. With this geometric design aberrations from the ideal ion path through the mass spectrometer are minimised[22,23]. The reverse Nier-Johnson geometry is particularly appropriate when ICPs are used as ion sources as it ensures a very low noise level. The reverse Nier-Johnson design allows for a mass resolutions up to 10000, the limiting factor being the initial energy spread of the ion beam (≈ 12 eV).

2.5.4 Mass resolution, ion transmission and peak shape

The mass resolution is defined as:

$$RP = \frac{m}{\Delta m} \tag{2.9}$$

Where m is the nominal peak mass and Δm is the mass difference between peaks. Two peaks of equal size are considered resolved if the valley between them is 10 % of the peak height. A mass resolution of 10000 is required to separate m/z = 100.00 from m/z = 100.01. If full separation of the peaks is required or if one peak is considerably larger than the other a mass resolution higher than RP is required. For a given

mass (***m***) and mass resolution setting (***RP***) the peak width is defined as ***Δm*** at all resolution settings. The mass range scanned by the PT2 instrument is set by the number of chosen peak widths. On the PT2 instrument the mass resolution is controlled by restricting the width of the ion beam. This is done by controlling the widths of the source and collector slits. When the slits are fully opened the mass resolution is 400. Narrowing the slit widths the mass resolution is increased. At RP = 4000 the width of the slits is approximately 30 µm, while it is approximately 10 µm at RP = 10000, ignoring the effects of aberrations. At high resolution aberrations become significant and slit widths smaller than those calculated theoretically are needed. Even though a slit width of 10 µm is small, still approximately 80000 Pb^{2+} ions can pass side by side.

Clearly, the ion transmission of the mass spectrometer is a function of mass resolution, since the ion beam is restricted at the source slit and the collector slit. The ion transmission is inversely proportional to the mass resolution. A typical transmission versus mass resolution curve is shown in Figure 2.5. As seen on the figure the ion transmission, and with that the sensitivity, decreases as the mass resolution is increased.

Therefore, in order to maintain highest possible sensitivity unnecessarily high mass resolution settings should be avoided. The ion transmission at RP = 10000 is approximately 3 % of that at RP = 400. One further advantage of the double focusing sector field mass spectrometer is that flat-topped peaks can be obtained in low resolution mode (RP = 400) by controlling the widths of the source and collector slits.

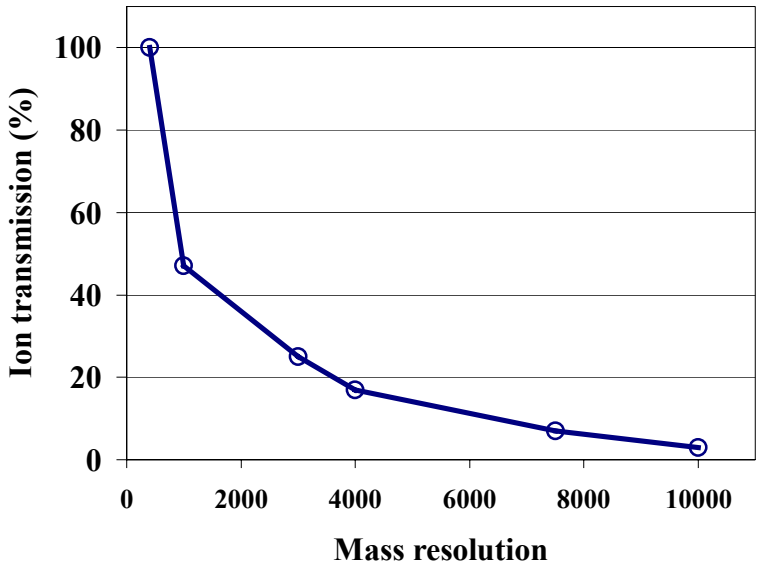

Figure 2.5 *Ion transmission versus mass resolution setting for the PT2 instrument.*

This can be achieved by applying a smaller width of the source slit than that of the collector slit[24] and/or by balancing the acceleration voltage and the deflector voltage[21]. Flat-topped peaks are of particular

importance when isotope ratios are measured, as it enables peak hopping. Applying a higher mass resolution the peak shape always becomes gaussian and peak hopping is not possible without degrading accuracy on the isotope ratio measurement.

2.6 Scanning modes

The double focusing sector field mass spectrometer of the PT2 instrument can be scanned in four different ways; magnetic scanning, voltage scanning, combined magnetic and voltage scanning and simultaneous magnetic and voltage scanning. To measure isotope ratios with sufficient precision it is important that fast scanning is possible without compromising the accuracy of the jumping between m/z ratios, in order to cancel the signal noise and maintain good accuracy.

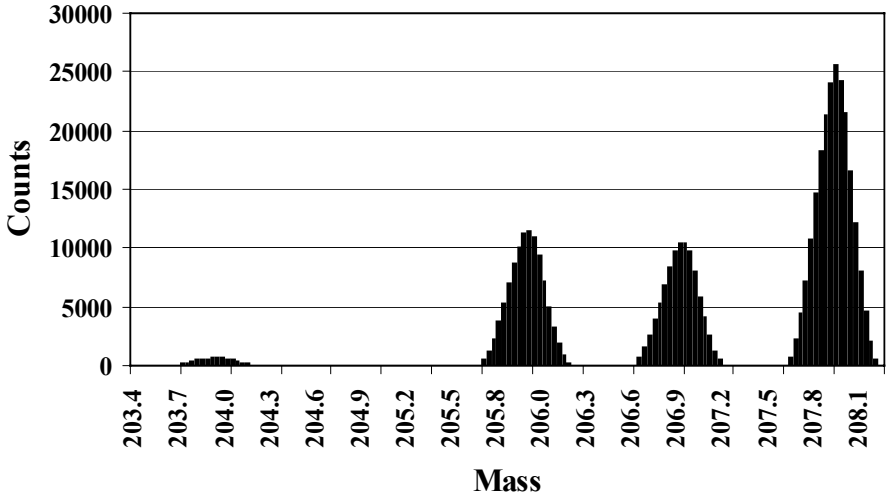

Figure 2.6 *Spectrum of lead isotopes applying magnetic scanning*

As the PT2 ICP-SFMS is a single detector instrument, it is not possible to measure the signals for more than one mass at the time. For the determination of isotope ratios the measurement of the individual isotopes is therefore sequential. Figure 2.6 shows a magnetic scan of the lead isotopes measured in a 2 µg/l solution of NIST CRM 981, natural lead isotopes. Each line in the spectrum represents a measurement point, at each point the ions arriving at the detector of that particular mass are counted for the duration of the dwell time, 5 ms is used in the spectrum in the figure. The points are separated in time by the small jump settle time. If successive sweeps are applied the counts from each sweep are summed in the final spectrum. The spectrum in the figure is the sum of 50 sweeps.

2.6.1 Magnetic scanning

In magnetic scanning no voltage is applied to the flight tube. The magnet is scanned in small jumps, the size of which are determined by the

number of points chosen per peak width. The jump settle time between points is 1000 µs. Scanning the magnet can be done in two ways either by jumping to a fixed current or a to a fixed magnetic field. Jumping to a fixed current is more precise with regard to mass than jumping to a fixed magnetic field, which on the other hand is faster[25]. Thus, jumping to a fixed magnetic field can be advantageous when measuring isotope ratios, where fast scanning is desired. Repeating a scanning sequence a full hysterisis loop of the magnet has to be performed, which includes a high and a low hysterisis settle time. The low hysterisis settle time (B = 0) is set lower than the high hysterisis loop (B = 1.0 tesla), since settling is faster when no field is present. Normally values of 10000 and 5000 µs are used for the high and low hysterisis settle time, respectively. One spectrum including all the chosen peaks are obtained from a magnetic scanning, i.e. the same dwell time is applied to all peaks, which is a disadvantage for some applications. Magnetic scanning is only useful when RP = 400, as the majority of the measurement time would be spent measuring the baseline between the narrow peaks applying a higher mass resolution. When two or more analyte peaks are present in the same spectrum, as is the case of magnetic and voltage scanning, they cannot be integrated automatically from the instrument computer.

2.6.2 Voltage scanning

In voltage scanning the magnetic field is held constant at a value corresponding to the nominal mass chosen, while the voltage applied to the flight tube placed inside the magnet is scanned in small jumps. The number of points chosen per peak width again sets the size of the jumps. For quantitative determinations the voltage on the flight tube can be scanned over a range of 120 V (± 60 V), which correspond to a scan of 2 % of the mass chosen (120 V out of 6000 V). Scanning more than 120 V on the flight tube the signal becomes non-linear due to losses of ions onto the surface of the flight tube[25]. If a mass range larger than 2 % of a given mass is chosen the instrument automatically shifts to magnetic scanning. For qualitative determinations scans over 200 V (± 100 V) are allowed, since small inaccuracies are not crucial. Voltage scanning is faster than magnetic scanning, since no settle time after changing the voltage on the flight is necessary. In a spectrum from a voltage scanning the same dwell time is applied to all peaks. As with magnetic scanning, voltage scanning is only useful for RP = 400, for the same reasons.

2.6.3 Combined magnetic and voltage scanning

A combined magnetic and voltage scanning is used in analyses applying high resolution (RP > 1000) or analysis of isotopes separated by several mass units. This scanning mode is the instrument default. The magnetic field is changed to perform the relatively large jump between nominal masses, while the voltage is ramped in small jumps to scan across the individual peaks. For large jumps of the magnetic field a large jump settle time of 100 ms are used. If sweeps across the chosen masses are repeated a full hysterisis loop, including the high and low hysterisis settle times, is performed between sweeps. The magnetic field is changed many

times using this scanning mode, and it is by far the slowest scanning mode. However, it does have advantages. First of all high mass resolutions can be applied. Secondly, different dwell times can be assigned to different nominal masses allowing a larger fraction of the total measurement time to be spent on low abundance isotopes, which significantly improves the precision on the measurement of isotopes ratios involving low abundance isotopes. Furthermore, peak hopping is also possible, defining only a fraction of a peak width to be measured on each nominal mass. Finally, it is possible to integrate all peaks automatically from the instrument software.

2.6.4 Simultaneous magnetic and voltage scanning

Very fast mass scanning is achieved by changing the magnetic field and the voltage applied to the flight tube simultaneously. This scanning mode is therefore called sprint. In this scanning mode a small jump settle time of zero, a large jump settle time of 10 μs, and a dwell time as low as 0.5 ms can be applied. Both scanning of the whole peak or a few points at the peak top (peak hopping) is possible. The main disadvantage of this scanning mode is that, as the large jump settle time is very small, the accuracy of the jumping between masses is poor compared with the other scanning modes, which might degrade the accuracy of isotope ratios measurements. Other, more practical, disadvantages are that an autosampler can not be used in this scanning mode, and data cannot be integrated automatically, which makes analysis and data handling very tedious and time-consuming. However, this scanning mode provides by far the fastest scanning and is as such useful for certain applications.

2.6.5 Choosing the right scanning mode

All the scanning modes described in the previous chapter have both advantages and disadvantages. The choice depends on the analysis to be performed. If a high mass resolution is needed in order to eliminate interferences, the choice is simple, only the combined magnetic and voltage scanning mode is a reasonable choice. If there are no interferences and a low mass resolution can be applied the choice is more complicated. In order to evaluate these four different scanning modes in practice an experiment was set up to measure the isotopic ratios of lead in a material with a certified isotopic composition using the different scanning modes, see chapter 3.3.

2.7 The detector system

The PT2 ICP-SFMS instrument is a single detector instrument. The instrument is equipped with a dual detector system consisting of an ion counting detector (a continuous dynode electron multiplier) for count rates up to 10^6 ions/second and an analogue detector (a faraday cup) for higher count rates. The default detector is the faraday cup, which is placed directly behind the collector slit. When the continuous dynode electron multiplier is used a deflector voltage of 900 V is applied to

direct the ion beam to the detector. The faraday cup has not been used in the experimentally work and will therefore not be discussed in more detail.

2.7.1 The continuous dynode electron multiplier

The continuous dynode electron multiplier is an ion counting detector, where the incoming ions from the mass spectrometer are directed onto the surface of the detector, which is held at a high negative voltage. On impact, electrons are released from the surface, which again hit the surface and release new electrons. This process is repeated many times resulting in a gain of the signal, the gain is typically of the order of 10^8 [24]. A high voltage of approximately - 2500 V across the detector surface supplies energy to the released electrons. At the end of the detector surface the electrons are directed to a collector electrode. The resultant pulse charge is send through a discriminator, where it is compared with a pre-set discriminator level. A pulse below the discriminator level is considered as noise and is not processed. Pulses above the discriminator level are send to the instruments data system, the duration of an output pulse is approximately 15 ns, during this period of time, the detector dead time, no new incoming ions are detected.

The advantages of the electron multiplier are that is has a very low noise level (0.12 count/second on the PT2 instrument in use) and a linear response up to 10^6 ions/second. As such it is useful for determinations in a wide concentration range, from fg/ml to µg/ml. However, it does have limitations, which are of special importance when isotope ratios are measured. Since the process time of a signal is finite (≈15 ns), and no new ions are detected in this interval, signals with a high ion counts rate will be negatively biased. At a count rate of 10^6 ions/second this error is approximately 1 %[24]. When measuring isotope ratios of isotopes of unequal abundance a bias is introduced if the count rate of the most abundant isotope approaches 10^6 ions/second. A correction for detector dead time is therefore needed. At even higher count rates the gain of the multiplier decreases as the number of incoming ions increases, because the fraction of output pulses falling below the discriminator level increases, therefore an increasing number of ions are not detected. This effect is called “sag” and leads to a significant increase of the measured (apparent) dead time[26]. Furthermore, the gain of the detector has also been reported to be dependent on the m/z ratio of the incoming ions, fewer secondary electrons are released from the detector surface for heavy ions than for light ions[24,26]. Since the m/z ratio is related to the ion kinetic energy an apparent dependence on m/z ratio might in fact be energy dependent. Therefore, when measuring isotope ratios, a small difference in detector gain of the two isotopes measured result in a bias on the observed isotope ratio. This effect will be encountered as a mass discrimination and corrected as such.

3 Measurement of isotope ratios using ICP-SFMS

In this chapter the factors that control the accuracy and precision of the measurement of isotope ratios with ICP-SFMS are discussed on the basis of both theory and experiments leading to a general protocol for the development of analytical methods for the measurement of isotope ratios using ICP-SFMS. Many of the aspects discussed have been investigated experimentally on the PT2 ICP-SFMS instrument in use. Before the different factors are discussed the notations and statistics used for isotope ratios are presented.

3.1 Statistics and notations

The isotope ratio between two isotopes is calculated as the ratio of the integrated counts for the two isotopes:

$$R = N_1 / N_2 \tag{3.1}$$

where N_1 and N_2 are the observed number of counts for isotope 1 and 2, respectively. Normally N_1 is the isotope of lowest mass. Ion counting in mass spectrometry is a discrete counting process and as such it follows the Poisson distribution. The Poisson distribution approximates to the Normal distribution at high count rates. The precision calculated from the Poisson statistics is referred to as the theoretical precision, since it only takes into account the uncertainty of the counting process, it is therefore the ultimate attainable precision. The standard deviation (SD) and the relative standard deviation (RSD) on the number of counts measured for a single isotope are:

$$SD_1 = \sqrt{N_1} \quad , \quad RSD_1 = \sqrt{N_1} / N_1 \tag{3.2}$$

Therefore the relative standard deviation (%RSD) on the measurement of an isotope ratio is:

$$\%RSD_t = 100 \cdot \sqrt{RSD_1^2 + RSD_2^2} = 100 \cdot \sqrt{1/N_1 + 1/N_2} \tag{3.3}$$

The relative standard deviation ($\%RSD_t$) is also referred to as the theoretical precision. In the case of two equally abundant isotopes, 2 million counts for each isotope results in a theoretical precision of 0.1 %. When the two isotopes are not of equal abundance, longer measurement time should be spend on the less abundant isotope in order to optimise the theoretical precision. The optimum ratio of counting times follows the inverse square root of the ratio of abundances[27]:

$$t_1 / t_2 = \sqrt{A_2 / A_1} \tag{3.4}$$

Where t_1, A_1 and t_2, A_2 are the dwell time and abundance of isotope 1 and 2, respectively.

Several different notations are used in the literature to present isotope ratio data with regard to both the actual ratio and the precision of the measurement. In environmental and biological sciences isotope ratios are normally presented as the absolute value with four decimal places, regardless of the actual precision of the measurement, e.g. $^{42}Ca/^{43}Ca$ = 4.7862. In geochemistry and related areas the elements encountered are often affected by mass fractionation (i.e. variable isotope ratio in nature). The variation in isotope ratio is given as a difference to a certified isotope ratio in a standard material, e.g. $\delta^{11}B$ = - 30 ‰, where $\delta^{11}B$ is defined as:

$$\delta^{11}B(^{0}/_{00}) = \left[\frac{(^{11}B/^{10}B)_{\text{sample}}}{(^{11}B/^{10}B)_{\text{Standard}}} - 1 \right] \cdot 1000 \qquad (3.5)$$

In this thesis isotope ratios are presented as the absolute value.

The precision of the measurements of isotope ratios is presented in terms of the standard deviation. In the literature, often the exact way the standard deviation is calculated is not given and some confusion between terms like short-term precision, long-term precision, internal precision, external precision, standard deviation and standard error of the mean exist. In this thesis the following definition are used for the different ways of expressing the precision on the measurement of isotope ratios. The standard deviation is defined as follows:

$$SD = \sqrt{\frac{\sum_i (x_i - \bar{x})^2}{(n-1)}} \qquad (3.6)$$

Where x_i is the individual measurement, $\bar{x}$ the average and n the number of measurements. The standard error of the mean is defined as:

$$\text{SEM} = \text{SD}/\sqrt{\text{n}} \qquad (3.7)$$

And the relative standard deviation as:

$$\%RSD_m = 100 \cdot SD/\bar{x} \qquad (3.8)$$

In this thesis $\%RSD_m$ is referred to as the measurement precision of isotope ratios. The ratio between the measurement precision and the theoretical precision R_p ($R_p = \%RSD_m/\%RSD_t$) is also an important measure, as it allows comparison of the precision of different methods regardless of the number of counts measured for the two isotopes. If n represents measurements within one day, the resulting $\%RSD_m$ is referred to as the short-term precision, if n represents measurements from

different days, the resulting $\%RSD_m$ is referred to as the long-term precision.

In this thesis results are in general presented as the absolute value of the ratio, along with the measurement precision $(\%RSD_m)$ and the R_p value.

3.2 Isotope ratios on the PT2 ICP-SFMS instrument

Numerous factors have influence on the precision and accuracy of the measurement of isotope ratios. Since the two isotopes are not measured simultaneously any change of the noise level in between the measurement of the two isotopes will degrade the precision of the result. In Table 3.1 a list of the most common sources of noise and error, when measuring isotope ratios, is shown. In addition to the factors shown in the table any factor that has an influence on the signal intensity has an impact on the measurement precision due to a change of the underlying Poisson statistics, which controls the theoretical precision.

Sources of noise and error	
Spectral interferences	Ion source noise
Detector dead time	Sample introduction system
Mass discrimination	Mass resolution
Background signals	Contamination/losses
Matrix effects	Analyte concentration

Table 3.1 *Sources of noise and error*

Beyond the factors already mentioned the choice of scanning mode also influences both accuracy and precision. The optimum conditions for the measurement of isotope ratios using ICP-SFMS is a fast scanning alternating between the two isotopes, summing up the counts in one spectrum. At the same time all factors influencing accuracy and precision need to be controlled. In the following chapters the most important factors and how to control them will be discussed in more detail.

3.3 Experimental evaluation of different scanning modes

As discussed in chapter two there are four basic ways by which the PT2 ICP-SFMS instrument can be scanned; *magnetic* scanning, *voltage* scanning, *combined* magnetic and voltage scanning or *simultaneous* magnetic and voltage scanning. These four scanning modes can be set up in many different ways.

The different scanning modes were evaluated experimentally measuring the lead isotopes in a material with a certified lead isotope composition (NIST CRM 981, natural lead). Lead was chosen since the spectrum of the lead isotopes is very simple and only one interference needs to be

considered (the isobaric overlap of ^{204}Hg on ^{204}Pb). Thus, a low mass resolution of 400 can then be used. The scanning modes were evaluated upon accuracy, precision and time consumption.

3.3.1 Peak hopping

The first experiment was set up to evaluate the peak hopping capability of the instrument. A simultaneous scan (sprint) was performed, measuring between 1.7 and 0.15 peak widths, corresponding to a full peak, 5, 3 and 1 points per peak. The experiment is described in detail in Appendix 1. In conclusion the precision was best when scanning the full peak ($Rp \approx 1$). The scanning was very fast, 500 sweeps across the peaks were completed in 3 min. However, the accuracy was poor and a deviation of up to 13 % from the established value was found for the ^{208}Pb/^{206}Pb ratio. Such a large error cannot be ascribed to mass discrimination, which normally is < 5 %[I,III,28]. The two main reasons for this large bias are probably inaccuracies on the exact mass position using this very fast scanning mode and the fact that the peaks have rounded tops and are not truly flat-topped. The fast scanning involves a small jump settle time of zero, even though the magnetic field is changed, which may explain part of the inaccuracy in the measurement. However, if the peaks were truly flat-topped this would not affect the accuracy. Measuring only 1-5 points at the top of the peak when the position is not exact, introduces an error, which is not easily corrected for. In theory flat-topped peaks should be obtained applying a low mass resolution. In practise it is very difficult or even impossible to obtain truly flat-topped peaks. Even if slit widths, acceleration voltage and deflector voltage are optimised as recommended rounded peak tops are usually obtained, see Figure 2.6. In conclusion, peak hopping is not a reasonable scanning mode in the measurement of isotope ratios because of an unacceptable poor accuracy and a worse precision than when the full peak is scanned. Therefore only whole peak scanning was used in the rest of the experimental work in this project.

3.3.2 Peak scanning

The different whole peak scanning modes were evaluated for the measurement of lead isotope ratios in a 2 µg/l nitric acid solution of CRM 981. This concentration was chosen as the count rates then would be well below 10^6 counts per second, and therefore the impact of detector dead time on the measurements is insignificant. The four different modes were *magnetic* scanning, *voltages* scanning, *combined* and *simultaneous* magnetic and voltage scanning. For the combined scanning two different dwell times were applied, short (5 ms) and long (250 ms), in order to see if a long dwell time can be applied to cancel noise in the same way as applying many successive sweeps and a short dwell time. The five different scanning modes were set up to measure an equal amount of ions of the individual isotopes in order to make comparison of the results more straightforward. The experimental details are given in Appendix 2. The results are summarised in Table 3.2, where RSD_m is the relative standard deviation in percent of 10 successive measurements, R_p is the

measured precision divided by the theoretical precision and f_{md} is the mass discrimination factor, the true isotope ratio divided by the measured isotope ratio.

Scanning mode	Time, s	$^{204}Pb/^{206}Pb$			$^{207}Pb/^{206}Pb$			$^{208}Pb/^{206}Pb$		
		RSD_m	R_p	F_{md}	RSD_m	R_p	F_{md}	RSD_m	R_p	f_{md}
Combined, 5ms	275	1.11	1.6	0.97	0.55	1.2	1.00	0.51	1.3	0.99
Combined, 250 ms	65	1.21	1.8	0.96	1.03	2.1	1.00	1.75	4.2	1.00
Simultan.	90	1.37	1.0	0.98	0.60	1.3	1.00	0.39	1.0	0.94
Voltage	150	-	-	-	0.45	0.9	1.00	0.40	1.0	1.05
Magnetic	190	1.91	1.5	0.97	0.46	1.0	1.00	0.51	1.3	1.00

Table 3.2 *Scanning mode for isotope ratio measurements*

The most obvious conclusion to draw from these data is that the *combined* scanning with a long dwell time results in considerably poorer precision than the other scanning modes do both in relative terms and in absolute values. This means that the noise cannot be cancelled out using a 250 ms dwell time, i.e. some of the noise components are oscillating with a amplitude longer than 250 ms. The voltage scan also has its limitations because the scan is restricted to a mass range of 2 % of the chosen mass. Therefore, it is not possible to have both a full m/z = 204 and m/z = 208 signal in the window at the same time. Other manufactures have solved this problem by applying a broader flight tube (Finnigan Element ICP-SFMS) and scanning the acceleration voltage (similar to scanning the flight tube voltage). Through this a voltage scan of up to 30 % of the given mass can be performed[29]. The best absolute precision for the $^{204}Pb/^{208}Pb$ ratio was obtained with the combined (5 ms) scanning mode. The reason being that a longer dwell time of 25 ms was chosen for the ^{204}Pb isotope in order to accumulate more counts and thereby ensure better counting statistics. This is not possible with either *simultaneous*, *voltage* or *magnetic* scanning. For the $^{207}Pb/^{206}Pb$ ratio the best precision, in terms of both absolute and relative values, was achieved with *voltage* and *magnetic* scanning. For the $^{208}Pb/^{206}Pb$ ratio the best precision was obtained for *simultaneous* and *voltage* scanning. However, these scanning modes introduce a bias of 5 %. The reason for this is unknown.

None of the scanning procedures are fast compared with ICP-QMS, were 50 sweeps across the lead isotopes easily can be performed within one minute. The reason for this is first of all that scanning a magnet is slower than scanning a quadrupole, simply because a magnetic field needs a longer settle time than the voltages applied to the rods of the +quadrupole, secondly that peak hopping can be performed with quadrupoles. Simultaneous scanning is fastest (90 second) and combined scanning slowest (275 seconds), as expected from the theoretical considerations presented in chapter 2.

In general there are no big differences between the scanning modes (leaving out the combined, 250 ms). The choice therefore depends on the

analytical task. If a high mass resolution is needed or if a low abundant isotopes has to be measured the combined scanning should be chosen otherwise magnetic, voltage or simultaneously should be preferred.

3.4 Mass discrimination

Mass discrimination processes affect the ion beam on its way from the plasma to the detector. These are physical processes which alter the travelling ions of different mass to charge ratio differently, resulting in different transport efficiencies for ions of different mass to charge ratio. Therefore in the measurement of isotope ratios the apparent ratio is biased. A mass discrimination correction has to be performed in order to ensure sufficient accuracy on the results. Different correction schemes can be applied: mathematical corrections[30,31], internal correction, a correction using a constant isotope ratio of another element present in the sample solution[17,32-35], or external correction, a correction using the given isotope ratio measured in reference materials, standards or samples with known isotopic composition[I,III,36-43]. Even though the mass discrimination processes are not fully understood, under constant investigation and often intensely debated, some understanding of the underlying physical processes are helpful in the selection of correction scheme.

3.4.1 Mass discrimination, theoretical considerations

Mass discrimination is believed to take place mainly during the extraction of ions from the skimmer cone to the ion lenses, in the ion lenses (and quadrupoles on the PT2 instrument) and in the electron multiplier[24,26,44]. The sector field mass analyser is free of mass discrimination[45,46], while mass discrimination similar to that of the ion lenses is seen in quadrupole mass analysers. Mass discrimination processes are related to the kinetic energy of the ions. Changes in the ion kinetic energy distribution therefore change the magnitude of space charge effects.

In between the sampler and the skimmer cones the motion of the neutrals, ions and electrons are determined by the gas kinetics of the neutral argon atoms. The velocity of neutrals, ions and electrons reaching the skimmer is uniform (approximately $2.3 \cdot 10^5$ cm/second) and independent of charge, mass and kinetic energy. The mass discrimination processes in this area are under normal conditions not significant[44].

Coming through the skimmer cone the ion beam expands into the second vacuum stage. In this area between the skimmer and the first ion lens the electrons diffuse away from the ion beam[46]. An ion beam consisting mostly of positive ions are then formed. Between the skimmer and the ion lenses significant mass discrimination processes (space charge) take place. Space charge is the repulsion of like charges when a high charge density occurs. The positive ions are present at a high density in the ion beam, above the space charge limit, so they repel one another. Light ions with a low kinetic energy can be deflected out of the ion beam much

more easily than heavy ions. Thus, adding a concentrated matrix ion to the ion beam (e.g. analysing a sample with major concentration of a few elements), the total ion current and the space charge is increased. Thereby also the fraction of light ions lost is increased. As a result the transport efficiency of the ions between the skimmer and first ion lens depends on the mass to charge ratio[47]. The magnitude of the space charge effect is, as mentioned before, dependent on the total ion current produced by a sample and with that the sample matrix. Therefore, the sample matrix has an influence on the mass discrimination observed when measuring isotope ratios.

The magnitude of the mass discrimination furthermore depends on the acceleration or extraction voltage applied[24,48]. If the applied voltage is significantly greater than the initial ion kinetic energies (3-12 V) the ion kinetic energy becomes nearly independent of mass and more uniform across the mass range. If a lower voltage is applied, i.e. of the same magnitude as the initial ion kinetic energy, the ion kinetic energy remains proportional to mass, as within the plasma[44]. Therefore mass discrimination processes between the skimmer and the ion lenses are less significant for ICP-MS instruments in which a high acceleration voltage is used, e.g. ICP-SFMS instruments. Also ICP-MS instruments with other interfaces designed to reduce the spread in ion kinetic energies are supposedly less affects by mass discrimination processes, e.g. ICP-CC-MS instruments[25]. Similar mass discrimination processes (space charge) also affect the ion beam within the ion lenses, the mass discrimination being most significant between the first and second ion lens[46]. The mass discrimination then favours higher transport efficiency for heavier ions between the skimmer cone and the mass analyser.

In a quadrupole acting as a mass filter (ICP-QMS) or as an ion focusing device (ICP-SFMS) mass discrimination of the reverse tendency is observed[24,49], that is, towards a lower transport efficiency for heavy ions. The reason being that heavier ions spend more time in the fringing fields at the entrance to the quadrupoles and therefore have a greater dispersion when entering the quadrupole, which result in a higher loss than for light ions[49]. The mass discrimination within the quadrupole is small compared with the mass discrimination from space charge[49].

When the ions reach the detector, mass discrimination processes are possibly also present. Here the tendency is towards a lower signal gain of heavier ions in the detector resulting in an apparent lower sensitivity of heavy ions than for light ions, as the yield of secondary electrons of the detector surface is mass dependent[24].

A more uniform ion kinetic energy distribution across the mass range reduces mass discrimination for all of the different mass discrimination processes. Therefore, the observed mass discrimination is supposedly smaller for ICP-SFMS instruments than for ICP-QMS instruments.

The deviation from the true isotope ratio observed when measuring isotope ratios is a result of the different mass discrimination processes all adding up as the ion beam travels through the instrument. As indicated above, the magnitude of the mass discrimination processes are highly dependent on the exact design of the ICP-MS instrument and on the voltages that are applied across the ion lenses. In the PT2 ICP-SFMS instrument used in this study, a high acceleration voltage of 6000 V and a mass analyser free of mass discrimination are applied along with a detector, in which mass discrimination was found to be negligible. In conclusion, the main mass discrimination processes occur in the area between the skimmer and the quadrupole lens stack.

3.4.2 Correction for mass discrimination

The total mass discrimination for a mass spectrometer can be experimental determined and expressed by the mass discrimination factor f_{md}, where R is the isotope ratio of the light over the heavy isotope[49].

$$f_{md} = \frac{R_{true}}{R_{measured}} \tag{3.9}$$

If $f_{md} > 1$ it indicates that space charge effects are dominant (loss of low mass ions), while $f_{md} < 1$ indicates that mass discrimination processes in the detector or quadrupole are dominant (loss of high mass ions). The mass discrimination is normally found to decrease with increasing mass to charge ratio in ICP-QMS instruments[49], where space charge effects are the dominant source. For the PT2 ICP-SFMS instrument used in this thesis f_{md} values were found to vary within days and between days, with values both above and below 1, see Appendix 3. Similar finding have be reported for both ICP-QMS and ICP-SFMS instruments[41,42,50]. These results indicate that on the PT2 instrument there is no dominant mass discrimination source. The reason for this might be that the high acceleration voltage applied on the PT2 instrument reduces the space charge effect between the skimmer and the ion lenses, which is often considered as the major source of mass discrimination[49]. Also no mass dependence on the magnitude of the mass discrimination was found, which again indicates that the mass discrimination between the skimmer and the ion lenses is not the dominant source. The lack of systematism in the behaviour of the observed mass discrimination makes corrections difficult.

When correcting for mass discrimination the sum of mass discrimination processes are corrected for and not the individual processes. As mentioned above there are different ways to correct for mass discrimination (mathematically, internally or externally) the most commonly applied correction being the mathematically correction. The mathematically corrections assumes that a mathematical relationships exists between the observed mass discrimination f_{md} and the mass difference between the two isotopes (Δm). There are three algorithms, which may be applied in correction of mass discrimination. These are

based upon a linear, power law and exponential relationship[30,34], respectively. The linear function is described as:

$$f_{md} = 1 + \Delta m \varepsilon_{lin} \tag{3.10}$$

The power law function as:

$$f_{md} = (1 + \varepsilon_{pow})^{\Delta m} \tag{3.11}$$

And the exponential relationship as:

$$f_{md} = e^{(\Delta m \varepsilon_{\exp})} \tag{3.12}$$

Where ε_{lin}, ε_{pow} and ε_{exp} are the mass discriminations per mass unit. From the observed ratio and the true (certified) ratio, these ε values are calculated and subsequently used to correct the future observed values or a different ratio of the same element measured in the same sample[30]. Which of the three functions that results in the most accurate correction can be evaluated experimentally. Taylor et al.[30] found that the power law or the exponential function resulted in the best results for measurement of uranium isotope ratios, while Begley and Sharp[34] and Alonso[51] found that the linear function were most suitable for lead isotope ratios and zirconium, molybdenum, ruthenium and palladium isotope ratios, respectively. A mathematical correction has the advantage that it does not involve the analysis of other solutions than the sample solutions, when a value of ε first has been established (besides a regular check that the value is still valid). The results from this study show that the power law function is slightly better than the others for correcting iron isotope ratios, although the difference between the different methods was very small, see Appendix 4.

A different approach is a correction utilising a constant isotope ratio of another element measured at the same time in the same sample solution as the ratio of interest. This correction is known as internal correction. Examples of such pairs of an internal ratio and analyte ratio(s) are the use of $^{203}Tl/^{205}Tl$ for correction of lead isotope ratios[17,32,43,35] and $^{67}Ga/^{69}Ga$ for the correction of the zinc isotope ratios[33]. One prerequisite for a successful internal correction is that the isotope ratio used as the reference is constant in nature, i.e. that no mass fractionation occurs. Furthermore, two important assumptions need to be fulfilled. First of all that the two elements involved respond equally to matrix effects and changes in plasma conditions, secondly that all signals are free from interferences or corrected appropriately. The first assumption can be regarded as valid with some confidence if the two elements involved have similar ionisation potentials and are of similar mass, while the second assumption needs to be proved experimentally for the given sample matrix.

One disadvantage of the approach is that the measurement time has to be split between the analyte isotopes and the reference isotopes. If the sample volume is limited, this will limit the number of ions accumulated of the analyte isotopes and, with that, on the precision (counting statistics). The advantage of this approach is that the validity of the correction is not affected by long- or short-term changes of the mass discrimination. Internal correction was not used in the experimental work of this study, since it was decided to spend as long time as possible on the analyte isotopes in order to increase measurement precision.

The final correction scheme considered is external correction in which the correction is performed using the isotope ratio of interest measured in reference materials, standards or samples with known isotopic composition. In the analytical procedure isotopic standards and unknown samples are measured in between each other, e.g. one standard for every 6 samples. The isotope ratios measured in the unknown samples are then corrected using the average of the f_{md} value calculated for the two standard solutions bracketing the unknown samples. This approach has the advantage of being very simple and relies only on the assumptions, that the mass discrimination is the same for the standard solution and the unknown samples, and that it does not vary in the time it takes to analyse the sample and standards. If certified reference materials or real samples with the same sample matrix as the unknown samples are used, the first assumption will be fulfilled. Otherwise single elements standard solutions of known isotopic composition can be used diluted to an element concentration similar to that of the unknown samples. External correction is not affected by changes over time of the magnitude of mass discrimination provided that standard solution is analysed frequently. Due to its simplicity and the very few assumptions involved this approach is often used[I,III,36-43]. The correction scheme was compared with mathematical correction for the measurement of iron isotope ratios. The results obtained were similar for both approaches and it is impossible, on the basis of these results, to conclude which correction scheme is the best. The choice of correction scheme also depends on practical considerations.

In conclusion the choice of correction scheme depends on the nature of the mass discrimination on the instrument in use. If the mass discrimination is constant and a mathematical relationship can be found between f_{md} and Δm, this approach is the best choice, since it does not prolong the analysis sequence significantly. On the other hand the external correction is always a reasonable choice even though the analysis sequence is prolonged. When using internal correction, great care must be taken to make sure that the mass discrimination is the same for the two isotope ratios involved. Throughout this study external correction has been applied.

3.5 Detector dead time

The dead time of the electron multiplier induces a bias in the observed isotope ratio if the abundance of the two isotopes is far from equal and the count rate of the most abundant isotope approaches 10^6 counts/second. As a high ion count rate is desirable in order to increase the precision of the isotope ratio measurement, isotope ratios are often measured using analyte concentrations that results in ion count rates higher than 10^6. Consequently the signals needs to be corrected for detector dead time, before the final calculation of the isotope ratio. The observed number of counts for the two isotopes are corrected using the following equation:

$$N_c = \frac{N_m}{(1 - N_m \tau)} \tag{3.13}$$

Where N_c and N_m are the corrected and measured number of counts, and τ is the detector dead time (s). The detector dead time is not a known constant and needs to be measured experimentally. The dead time is different for different batches of electron multipliers and has also been reported to change during the lifetime of the detector[26]. It is therefore advisable to determine the dead time regularly. In the literature two experimental methods for the determination of the detector dead time are described: a graphical method[28] and a method based on least square fitting[51], the graphical method being the most frequently used. Both methods are based on the measurement of the given isotope ratio in standard solutions of different concentrations. The concentration levels have to be chosen to produce ion count rates high enough to be influenced by the dead time and below the level where "sagging" occurs. Both methods also provide a measure of the apparent mass discrimination, as the difference between the true and the corrected isotope ratio.

For the graphical method the isotope ratio of interest is measured in a number of standard solutions with different concentrations. For each concentration level the normalised isotope ratio (the isotope ratio corrected for dead time divided by the natural isotope ratio) is plotted against the dead time producing a curve for each concentration level. The dead time for which the curves intersect is the correct dead time of the detector. Ideally all curves should intersect in the same point, but in practice there are small deviations. The average dead time is then calculated as the average between the estimated values. The difference between the estimated values can be used as a measure of the precision on the determination of the detector dead time, see Appendix 5.

The method based on least square fitting minimising the error between the true and measured isotope ratio was originally developed for a simultaneous determination of detector dead time and mass discrimination[51-53]. However, a similar approach have been generated for the determination of the dead time only, minimising the standard

deviation of the isotope ratios measured at different concentration levels, see Appendix 5.

Essentially, the two methods are alike both minimising the difference between the isotope ratios measured at different concentration levels. Therefore similar values of the detector dead time are found applying both methods, e.g. a detector dead time of 10.5 ns was found for the applied detector using both the graphical and the least square fitting method, see Appendix 5. The advantage of the graphical method is that it is simple, and in addition, provides a measure of the precision on the determined detector dead time. The disadvantage is that it depends on a visual interpretation of the graphs. The advantage of the least square fitting method is that it is more accurate and the disadvantage that it does not provide a measure of the precision on the detector dead time. A specific detector dead time can be found for a given electron multiplier. Even though the dead time changes gradually with the lifetime of the detector (1-3 years), it can be considered constant within a short time span, e.g. months.

However, some difficulties arise in the interpretation of the dead times determined by the above described methods. First of all, the precision of the determination of the dead time is not very good. As an example, for the electron multiplier on the ICP-SFMS instrument used in this study, detector dead times in the range of 10 – 23 ns with an average of 15 ± 4 ns (± 1 SD) were found for isotope ratios covering the mass range from m/z = 24 –208[III]. Similar results were found by Vanhaecke et al.[26] for an ICP-SFMS instrument equipped with a discrete dynode electron multiplier. In this case the dead time varied in the range of 18 – 29 ns across the mass range. Alonso et al.[53] found that the apparent dead time for an electron multiplier on a ICP-QMS instrument varied between 100 and 168 ns with an average of 131 ± 20 ns (±1 SD) for tin isotope ratios. Such deviations of the dead time have a significant impact on the calculated isotope ratio. As an example the absolute value of the $^{42}Ca/^{43}Ca$ ratio measured in a 500 µg/ml calcium standard solution was changed by 0.7 % changing the dead time from 10.5 to 20.5 ns, see Appendix 5 for details. A bias of 0.7 % is crucial if high accuracy and precision is needed. The reason for the poor precision in the determination of the detector dead time is that many factors other than dead time affect the observed number of counts in an analyte peak, i.e. sensitivity drift, matrix effects. These factors are therefore included in the determination of the dead time.

Mass dependence of the apparent detector dead time has been reported for continuous dynode electron multiplier detectors on ICP-QMS instruments[24,26,53], while the detector dead time for a conversion dynode secondary electron multiplier on an ICP-SFMS instrument was found to be constant over the whole mass range[26]. The explanation suggested by the authors[26] is that since all ions in the ion beam are accelerated by the high negative voltage applied to the detector the difference in the ion kinetic energy of incoming ions is negligible for both ICP-QMS and ICP-

SFMS instruments. They argue that the mass dependence found for ICP-QMS is therefore not related to the ion kinetic energy of the incoming ions, but to the use of the conversion dynode in front of the electron multiplier on the ICP-SFMS instrument[26]. Using a conversion dynode, incoming ions are not allowed directly onto the surface of the detector, but onto an electrode held at a high negative voltage (conversion dynode) from which secondary electrons are released and accelerated into the detector when an ion strikes the conversion dynode. The gain of multipliers equipped with conversion dynodes has been reported to be less affected by differences in energy and velocity of the incoming ions than continuous dynode electron multipliers, and therefore a smaller or no mass dependence is seen on conversion dynode electron multipliers[24,26].

However, this argumentation cannot explain the findings in this study, where the detector dead time was found to be constant over the whole mass range for a continuous dynode electron multiplier on an ICP-SFMS instrument[III]. This detector is the same as applied on the ICP-QMS instruments discussed above. It is therefore more likely that the differences seen in mass dependence between detectors on ICP-QMS and ICP-SFMS instruments are related to the ion kinetic energy of the incoming ions and not to the use of different detectors. In ICP-QMS the ions are normally accelerated over a potential difference of a few hundred volts[49]. This means that the kinetic energies of the ions leaving the quadrupole are a few hundred eVs (approximately 200 eV), with a spread in energy of approximately 12 eVs. The difference in ion energy of the ions is significant and mass dependent, as lighter ions pick up a higher velocity than heavier ions in the ion lenses and the quadrupole[47]. Apparently this mass dependent energy spread is not eliminated by the high negative voltage on the detector and causes the mass dependence on the output pulses of the detector. On the PT2 ICP-SFMS instrument the ions are accelerated over a potential difference of 6000 volts and have a kinetic energy of approximately 6000 eV leaving the collector slit[25]. The energy spread in the ion beam is still 12 eV, but this is now a relatively small energy spread compared with the ion kinetic energy of 6000 eV. In conclusion the ion beam leaving a double focusing sector field mass spectrometer is more uniform in ion kinetic energy (relatively) than the ion beam leaving a quadrupole mass analyser, therefore no mass dependence of the gain of the continuous dynode electron multiplier on a ICP-SFMS instrument was found.

No matter how the detector dead time behaves, it is necessary to correct for it when ion count rates approach 10^6 count/second. The correction will to some extent affect the precision of the measurement of isotope ratios and also the accuracy if not corrected properly.

The easiest way to avoid the possible uncertainty from the correction for detector dead time is to design the experiments so that all ion count rates are well below 10^6 count/second, i.e. analysing more dilute samples. If the isotope ratio to be measured is close to unity the majority of the error

induced is cancelled out when the ion counts for the two isotopes are divided. The precision induced by counting statistics is degraded when measuring a low count rate, but applying many sweeps across the isotopes (50-100) accumulating the counts from each sweep this effect is cancelled out. The cost is that the analysis time per sample is prolonged as the number of sweeps increases.

The ultimate way to solve the problem is to use or develop detectors that are not affected by dead time. Such a detector is the Daly detector in which a photomultiplier is used. No dead time correction is needed and the mass discrimination is small[23]. Such detectors are now used on several new instruments such as the Micromass ICP-CC-MS instruments[11].

3.6 Spectral interferences

One of the major limitations of the ICP-MS technique is the presence of spectral interferences in the mass spectra. If the isotopes of interest coincide with interferences the accuracy on the measurement is degraded. One of the key features of ICP-SFMS instruments is the ability to use a high mass resolution by which most spectral interferences can be eliminated. The mass resolution needed to separate a spectral inteference from the analyte peak can be calculated from equation 2.9. Spectral interferences can be divided into three groups based on their origin: i) isobaric overlap ii) doubly-charged ions and iii) polyatomic ions.

Isobaric overlap is the overlap of two elements, which both have an isotope at the same nominal mass, e.g. the overlap between $^{64}Ni^{+}$ and $^{64}Zn^{+}$. Normally the mass difference between two isobars is very small and generally they cannot be separated. The mass difference between $^{64}Ni^{+}$ and $^{64}Zn^{+}$ is 0.0012 mass units, thus a mass resolution setting of 54296 is required to separate them, which is not possible with ICP-SFMS.

In the argon plasma singly positive charged ions are formed mainly, but some elements do have a second ionisation potential below the first ionisation potential of argon (15.76 eV) and therefore significant levels of doubly-charged ions are formed. The doubly charged ions are transported through the mass spectrometer, appearing at a mass of half their actual mass (m/z, z = 2), e.g. doubly charged strontium ions interfere on the calcium isotopes[I]. Some of the doubly-charged ions have masses very close to the mass of the isotope of interest and thus they cannot always be eliminated applying a high mass resolution setting. As an example, the doubly-charged strontium ions interfering at the calcium isotopes cannot be resolved, and therefore a mathematical correction is needed[I], while the doubly-charged barium ions interfering with the zinc isotopes can be resolved applying a mass resolution setting of approximately 2500[III].

Polyatomic ions are matrix-induced molecular species such as oxides, argides, nitrides, dimers etc., which are formed (or not cleaved) in the argon plasma and in the interface between the ion source and the mass spectrometer. The presence and formation rate of polyatomic ions is dependent on the sample matrix, and therefore the interference pattern varies for different sample matrices. The majority of polyatomic ions can be separated from analyte peaks by applying a high mass resolution. As explained, the ion transmission decreases when the mass resolution is increased. The choice of mass resolution consequently affects both accuracy and precision. However, the mass resolution setting is used primarily to ensure a good accuracy on the measurement of isotope ratios. The main advantage is that matrix elements which form interfering ions of the same nominal mass as the analyte ions do not need to be removed in the sample preparation step, but can be eliminated using an appropriate mass resolution setting. Through the application of different mass resolution settings during the method development the interference patterns can be mapped[I,III], and an appropriate mass resolution setting for analysis decided on. As some of the interferences are formed from matrix ions, the interference pattern changes between different sample matrices. An example is shown in Figure 3.1 for the ^{70}Zn isotope in urine, faeces and serum.

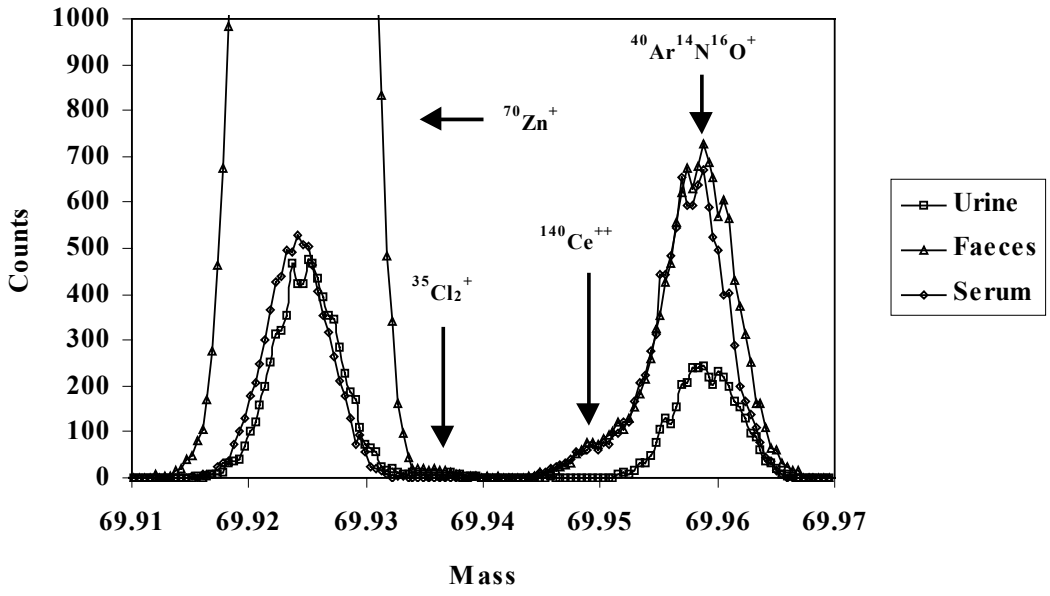

Figure 3.1 *Spectra of $^{70}Zn^{+}$ in faeces, serum and urine. Faeces was digested and diluted to a total dilution factor of 1000, while a direct 50-fold dilution with 0.14 % nitric acid were applied for serum and urine*

Three different interferences were found on $^{70}Zn^{+}$: $^{140}Ce^{++}$, $^{40}Ar^{14}N^{16}O^{+}$, and $^{35}Cl_2^{+}$, which were all found analysing faeces, while $^{140}Ce^{++}$ and $^{40}Ar^{14}N^{16}O^{+}$ are found in serum and only $^{40}Ar^{14}N^{16}O^{+}$ in urine. Consequently different mass resolutions are needed to achieve baseline separation of analyte and interference for the different sample matrices.

While a mass resolution of 6000 is needed analysing faeces, only 3000 and 2500 are needed for serum and urine, respectively[III].

A method developed for the measurement of isotope ratios in one particular sample matrix cannot necessarily be applied to the analysis of other sample matrices without any further investigation to assess the interference patterns in the new sample matrix.

It is important that the chosen mass resolution is not too high, in order not to degrade the measurement precision unnecessarily. The optimum mass resolution setting is where baseline separation of analyte and interference peaks is just achieved. For example a mass resolution setting of 4000 is used to achieve baseline separation between interferences and calcium isotopes even though a mass resolution of 2688 is sufficient according to the tabulated value[I].

3.7 Background signals, contamination, losses

As in all other analytical chemical procedures background signals, contamination and analyte losses affect the measurements. If the ratio to be measured is not constant in nature or is different from that of the natural ratio, precautions have to be taken in order to ensure a good accuracy on the measurement. Background signals will have a different isotope ratio than that of the sample, so will the ratio of an analyte contamination, whereas losses from the sample do not affect the measurement. For some applications, where both isotope ratios and total concentrations are needed[III], such analyte losses should be avoided. For a specific application it therefore has to be considered carefully if background signals, contamination and losses are of importance in the analysis.

3.8 Signal noise

Noise in the ICP-MS signal often limits the precision of isotope ratio measurements[34,43,54]. If the signals were free from noise the precision would only be limited by counting statistics and the resulting R_p value would equal 1. However, in practise R_p is most often in the range 1-3[I-III,43,51,52,54,55]. Careful selection of acquisition parameters and reduction of the individual noise components can improve the precision.

The noise in ICP-MS spectra has been studied using noise power spectra[56,57]. These studies showed that the noise could be divided into three types of noise. White noise, which is the noise present throughout the range of possible frequencies. Flicker noise, which is random noise originating mainly from the plasma and the aerosol formation[58], and frequency dependent noise which originates from pulsing in the sample introduction system and other discrete noise sources[56-58]. By educated selection of acquisition parameters (in particular, dwell time and the number of sweeps) the majority of the noise can be eliminated, resulting

in R_p values approaching 1 [56]. For example a high number of sweeps is beneficial, since the summation of sweeps is an effective means of noise reduction as isotope profiles are added coherently, while noise components are reduced by smoothing[56].

In an effort to optimise the measurement precision by reduction of the signal noise it is important to consider the individual noise components. The white noise cannot be eliminated, but it can be significantly reduced by use of syringe pumps, which are free of pulsation[58]. The choice of dwell time also influences the random noise and the frequency dependent noise. Decreasing the dwell time is beneficial in the reduction of random noise, while increasing the dwell time is beneficial in the reduction of frequency dependent noise. Since random noise is most noticeable in ICP-MS a short dwell time is preferred for the measurement of isotope ratios[56]. Optimisation of acquisition parameters is therefore important in order to achieve the best possible precision (lowest noise level).

The main component of the frequency dependent noise originating from the sample introduction system is pulsation caused by the peristaltic pump. This can be eliminated almost completely by the use of a syringe pumps[58,59]. However, the aerosol formation in the nebuliser, and transport and filtering of aerosols in the spray chamber also influence the frequency dependent noise. A uniform aerosol with regard to droplet size produces less noise than an aerosol containing many large droplets[58]. The choice of nebuliser, spray chamber and spray chamber temperature therefore have an influence on the noise in the spectrum.

The dwell time, the number of sweeps and the sample uptake rate was optimised using a 2^3 central composite design in order to eliminate noise and improve measurement precision of the measurement of the $^{240}Pu/^{239}Pu$ ratio[II]. The sample uptake rate was included, since it has been shown that it has a significant influence on the frequency dependent noise[56]. The optimisation showed that the application of a sample uptake rate of 1.0 - 1.2 ml/min and more than 70 sweeps produces the most precise results, that is, %RSD = 1.2. The dwell time has no influence, as long as it is in the range of 1 – 5 ms. With these settings, R_p values approaching 1 are obtained, indicating that random noise and frequency dependent noise are effectively eliminated and that precision is limited by counting statistics only[II]. Applying the same principle of a small dwell time and a high number of sweeps similar results ($R_p \approx 1$) was obtained for the measurement of Pb isotope ratios using the PT2 instrument in its basic configuration, see Table 3.2. Showing again that flicker noise and frequency dependent noise can be effectively eliminated.

Measuring isotope ratios at higher mass resolution settings (RP = 4000 – 6000) R_p values in the range of 1.5 - 4 is found, see chapter 4, indicating that other noise components than the counting statistics contribute significantly to the precision. Even though a small dwell time and a large number of sweeps is applied in these methods as in the Pu and Pb

methods, the random noise and/or frequency dependent noise is apparently not completely eliminated.

As no changes are made at the front-end of the instrument (plasma conditions and sample introduction system) when a higher mass resolution setting is applied, this indicates, that the increase in noise has to be related to the physical restriction imposed on the ion beam by the slits. In addition this "unknown" noise phenomena at the slits needs to possess a frequency which is not eliminated by the use of a large number of sweeps and a low dwell time. A visual inspection of the mass spectra obtained at different resolution settings reveals that the peak profile is less reproducible at high resolution (RP > 2000) than at low resolution (RP = 400), again indicating that narrowing the slit width induces additional fluctuations in the ion beam. Performing a noise power spectra analysis could reveal more definite information about this noise component.

3.9 Development of methods for isotope ratio measurements

In the development of a method for the measurement of isotope ratio using ICP-SFMS all the factors discussed in the previous sections need to be considered, i.e. acquisition parameters, scanning mode, spectral interferences, mass discrimination, detector dead time, background signals, contamination, analyte losses and noise. In this study a systematic procedure for the method development has been generated, the procedure is shown in the flow diagram in Figure 3.2. The procedure is based on the initial choice of a small dwell time (1 – 5 ms) and a large number of sweeps ($n \geq 50$). Some of the aspects discussed above are left out. The simultaneous voltage/magnetic-scanning mode and the internal correction of mass discrimination is not considered, because they are of little practical value.

In the flow diagram two types of figures are used; boxes for questions that need to be considered or investigations to be performed and ovals for the resulting decisions. The main components of the procedure outlined in the flow diagram are the mapping of the spectral interference pattern, choice of scanning mode, detector dead time correction, mass discrimination corrections and evaluation of accuracy and precision. For the method development to be successful, it is important that a full investigation of the spectral interferences found in the sample matrix of interest is performed, otherwise the accuracy might be affected. The scanning mode chosen needs to be appropriate in order to optimise the measurement time, so that the longest possible fraction of the measurement cycle is spent on the analyte isotopes and not on background or isotopes without interest. Whether or not to apply a dead time correction needs to be decided on, and a proper mass discrimination correction also has to be applied. The easiest way to judge the accuracy is to compare the isotope values obtained for standards and samples with

the true value. If any significant deviations are found the interference mapping, detector dead time correction and mass discrimination correction have to be re-evaluated.

Finally, the measurement precision has to be evaluated. For methods applying low mass resolution (RP = 400) a R_p value approaching 1 is optimum, while R_p values in the order of 1 to 3 are acceptable for methods were high mass resolutions settings are used. If acceptable R_p values are not achieved, the choice of acquisition parameters has to be re-evaluated. As the acquisition parameters are interrelated, a statistical approach for optimisation is advantageous, e.g. applying central composite designs[II], simplex optimisation[60] or other methods.

Also the sample introduction systems has to be looked at and set-up to avoid unnecessary pulsation from the peristaltic pump and the nebuliser. The absolute value of the measurement precision needs to be judged too. The necessary precision varies from one application to another and is a function of the uncertainty allowed on the final result. The easiest way to improve the absolute precision is to increase the number of sweeps, whereby the theoretical precision is improved and with that the measurement precision.

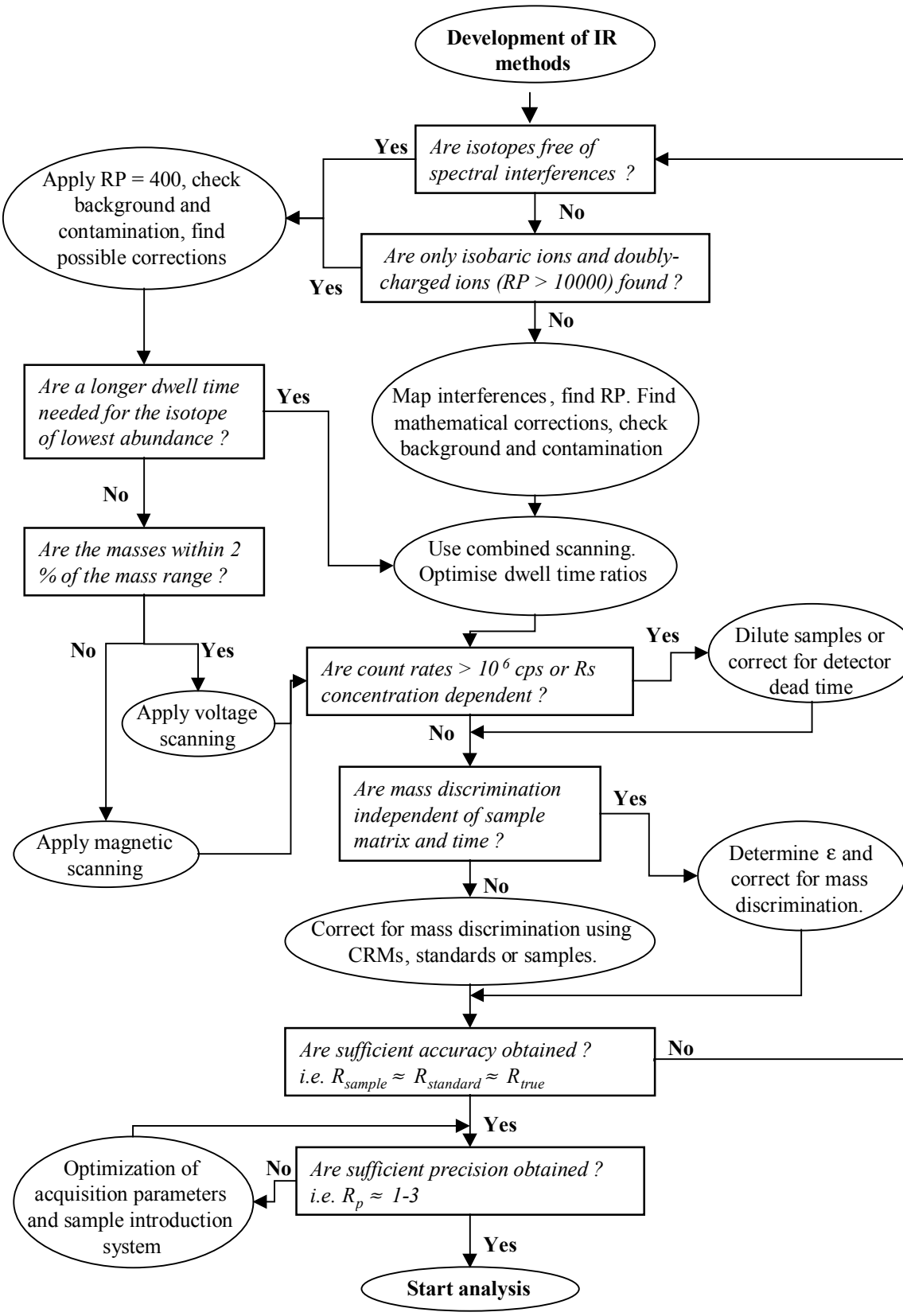

Figure 3.2 *Flow diagram for the development of ICP-SFMS methods for the measurement of isotope ratios*

The depicted procedure for method development is useful for all the measurements where isotope ratios are involved either directly or

indirectly, that is, direct measurements of the ratios themselves, and also isotope dilution measurements. More indirectly isotope ratios are also applied when internal standards are applied to correct for instrumental drift.

3.10 Characteristics of ICP-SFMS for isotope ratio measurements

From the above discussion it is possible to outline the advantages and disadvantages of the ICP-SFMS technique for the measurement of isotope ratios. The main advantages are that the majority of the spectral interferences can be eliminated, that the technique possesses high selectively, and that good accuracy and precision can be obtained. However, the precision is in general limited by the single detector design, and it is not possible to match the precision obtained by TIMS and MC-ICP-SFMS. The main disadvantages are that the scanning is slow and that flat-topped peaks not can be obtained on a routine basis. Also mass discrimination and detector dead time corrections affect the overall performance. Means to reduce or eliminate these effects would be advantageous.

There are several ways by which the detection of isotope ratios can be improved. The application of a syringe pump system instead of the peristaltic pump would significantly reduce the noise and improve precision. The exchange of the electron multiplier detector with a detector based on photomultiplication would also improve both accuracy and precision, since no detector dead time correction is necessary. Finally, lowering the spread of the ion kinetic energies of the ions leaving the plasma can reduce the mass discrimination effects. This can be achieved using a shielded torch, that is, a grounded circular thin metal plate placed in between the load coil and the plasma. A shielded torch reduces the ion kinetic energy spread from 12 eV to 1-2 eV. Furthermore, it has the advantage that the sensitivity is increased[61].

4 Isotope ratios and tracer experiments in human nutrition

The use of inorganic stable isotopes as tracers in human nutrition experiments has increased rapidly since the first experiments were performed in the 1960s[62]. Stable isotope tracers are now used in studies of the metabolism, bioavailability, requirements and toxicity of essential and toxic elements. Traditionally TIMS or FABMS are used for the measurement of stable isotopes, but since 1985, where ICP-QMS became commercially available, a large number of papers utilising ICP-QMS in human nutrition experiments have been published[63-78]. The reason for this is that the ICP-QMS technique in general is simpler and easier to

use, still the technique possesses sufficient precision to be useful in metabolism experiments (%RSD_m < 1), even though the precision is poorer than for TIMS. However, the ICP-QMS technique has one major drawback, that is, the mass spectra of the elements of nutritional interest (Mg, Ca, Zn, Fe, Se, Mo among others) have significant interferences from polyatomic ions and doubly-charged ions. Great attention therefore has to be paid to identification and correction of interferences during the method development, and often matrix separation or complicated mathematical corrections have to be applied in order to achieve sufficient accuracy[65,66,69-73]. ICP-SFMS possesses several features that are believed to be beneficial in the measurement of isotope ratios. First of all the ability to apply a high mass resolution setting and thereby resolve the analyte peaks from the interference. Secondly simple sample preparation procedures can be used if spectral interferences are eliminated. It was therefore hoped that with the introduction of the ICP-SFMS technique, simple and very precise methods, which eliminate spectral interferences, could be developed for the measurement of isotope ratios[79]. More modest expectations for the use of ICP-SFMS in nutritional applications were expressed by Crews et al.[80] in the book "Stable Isotopes in human nutrition – Inorganic nutrient metabolism" from 1996 where they wrote:

"There appears to be no great advantage to high resolution ICP-MS over quadrupole ICP-MS in many nutritional applications; ICP-MS based on quadrupole mass analysers is adequate for most measurements. There may be advantages to high-resolution techniques in resolving some of the isobars in the Ca region (although not the $^{40}Ar^+/^{40}Ca^+$ isobar, separation of which would require an unacceptably high resolution) and in the Fe region. In order to take full advantage of the potentially higher precision conferred by high-resolution ICP-MS a multicollector detection system of sufficient sensitivity is required. This adds to the expense of an already costly system. Given that the overall precision on absorption measurements is frequently limited by sample collection techniques (in the case of faecal monitoring, for example), increased mass spectrometric precision might not yield significant improvements in the quality of most biological data, with the exceptions noted above."

This quote very accurately pinpoints the advantages and limitations of the ICP-SFMS technique. The main advantage being that spectral interferences can be resolved, and the main limitation being that the precision is limited by the single detector system applied. Also, another very important point is made in this quote, that the final precision on absorption measurements often is limited by the sampling process and not the actual measurement of isotope ratios in the samples. In the beginning of 1997 (when this research project was started) only two papers had been published, which discussed in detail the use of single collector ICP-SFMS for measurement of isotope ratios[54,81]. These papers, both written by Vanhaecke et al., showed that with a mass resolution setting of 300 (similar to that of ICP-QMS) lead and magnesium isotope ratios could be measured with a precision < 0.1 %RSD[54]. Precisions in the range of 0.3 – 0.6 %RSD are achieved by applying a mass resolution

setting of 3000 for the $^{65}Cu^{+}/^{63}Cu^{+}$ ratio in an antarctic sediment sample and a human serum reference material[81]. As can be inferred from the above, very little information was available on the measurement of isotope ratios using ICP-SFMS. One of the aims of this thesis was therefore to exploit the potential of ICP-SFMS for the measurement of isotope ratios of elements of nutritional interest.

The validity of the ICP-SFMS technique for the measurement of isotope ratios of elements of nutritional interest was demonstrated by the development of analytical methods for the measurement of Ca isotope ratios in human urine[I], Zn isotope ratios in faecal sample digests[III] and the $^{97}Mo/^{98}Mo$ ratio in human urine (data not published yet). These methods were developed with the aim of being used to measure isotope ratios in human samples from nutritional experiments set-up by the Research Department of Human Nutrition at the Royal Veterinary & Agricultural University, Denmark. Furthermore, isotope ratios of Fe have been measured in faecal samples. In the following chapters the methods for the four elements and their applications within human nutrition will be discussed in detail.

4.1 Measurement of calcium isotope ratios

The analytical method has been published[I] and therefore only a short summary of the analytical aspects will be given here. That paper was the first published on the application of ICP-SFMS for isotope ratio measurements in a human metabolic experiment. In the method developed, the $^{42}Ca^{+}/^{43}Ca^{+}$ and $^{44}Ca^{+}/^{43}Ca^{+}$ ratios are measured. The ratios can be measured with precisions ($\%RSD_m$) of 0.41 and 0.33, respectively, corresponding to R_p values of approximately 3, following a 50-fold dilution of the urine with 0.14 M nitric acid. The calcium concentration in the sample solutions is in the range of 1- 2 mg/l. Using a mass resolution setting of 4000 the calcium peaks were resolved from interfering polyatomic ions, while a mathematical correction was used to correct for overlap between the calcium peaks and doubly-charged strontium ions. The $^{43.5}Sr^{++}$ signal was measured simultaneously with the calcium isotopes to facilitate this correction. These corrections ensured a good accuracy of the measurements.

The ICP-SFMS method was evaluated using a double stable isotope method for the determination of calcium absorption in humans and compared with a radioisotope method based on whole body counting[82]. In this experiment fifteen adults received a test meal containing 377 mg calcium. The meal was extrinsically labelled with 8.9 or 16.7 mg ^{44}Ca and 0.2 MBq ^{47}Ca. One hour after ingestion of the meal, 1.7 or 3.3 mg ^{42}Ca was administered intravenously. Stable isotope ratios were measured with the method described above in urine collected immediately before (baseline) and 24-48 hours after the test meal. The calcium absorption was estimated to 25.1 ± 6.7 % (mean ± SD) with the stable isotope method and 20.3 ± 5.3 % with the radioisotope method.

There was a moderately good correlation between the two methods (r = 0.68) see Figure 4.1, redrawn from the data presented in the paper[82].

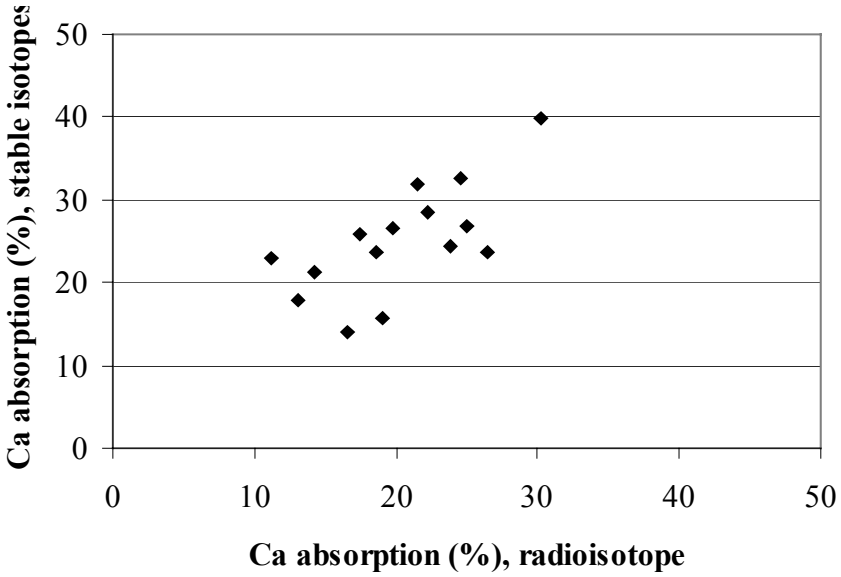

Figure 4.1 *Comparison of Ca absorption determined by a radioisotope method and a stable isotope method*

However, calcium absorption values estimated by the stable isotope method were in average 4.8% higher. The overall precision of the calculated calcium absorption value was approximately 16% and 6% for the stable isotope and radioisotope method, respectively. This is though considered acceptable.

This study proves that ICP-SFMS methods can be used successfully for the measurement calcium isotopes in human metabolic studies. However, it also points out one of the problems using double stable isotopes methods in human nutrition, that is, the precision on the final result (the absorption rate) is large (16 %) compared with the precision on the individual measurement of isotope ratios (0.3 to 0.4 %). The following equation is used for the calculation of the absorption rate in double stable isotope studies[83]:

$$Absorption(\%) = 100 \cdot \frac{na^{44}Ca}{na^{42}Ca} \cdot \frac{^{42}Ca(i.v)}{^{44}Ca(oral)} \cdot \frac{\%XS^{44}Ca}{\%XS^{42}Ca} \qquad (4.1)$$

Where $na^{44}Ca$ and $na^{42}Ca$ are the natural abundances of ^{44}Ca and ^{42}Ca, respectively, $^{42}Ca(i.v.)$ and $^{44}Ca(oral)$ are the doses of the isotopes administered in mmol and $\%XS^{44}Ca$ and $\%XS^{42}Ca$ are the % atom enrichment defined as:

$$\%XS = \frac{(R_{enriched} - R_{baseline})}{R_{baseline}} \qquad (4.2)$$

Here $R_{enriched}$ and $R_{baseline}$ are the isotope ratios (^{42}Ca/^{43}Ca or ^{44}Ca/^{43}Ca) in the enriched and baseline sample, respectively. The combined

uncertainty for the calculated absorption rate can be estimated using the laws of error propagation[84]. It has been shown that more than 99% of the uncertainty in the absorption rate originates from the third term in Equation 4.1, the ratio between the calculated atom enrichments. The uncertainty on this term was again shown to originate mainly (> 99 %) from the two calculations of the differences between enriched and baseline ratios ($R_{enriched} - R_{baseline}$), see Appendix 6. The conclusion from this uncertainty analysis is that the uncertainty is completely controlled by the uncertainty on the two terms $R_{enriched} - R_{baseline}$. Two factors control this uncertainty; the precision on the measurement of the isotope ratios and the % atom enrichment in the enriched sample, where the latter one is controlled by the amount of the stable isotope administered and absorbed. The amount of the administered dose absorbed is affected by the bioavailability as well as the total amount of calcium in the test meal due to the reverse correlation between relative absorption and total amount of calcium. Improving the precision on the meaurements, increasing the isotope doses or decreasing the amount of natural calcium given in the food therefore improves the uncertainty on the absorption rate. It is therefore very important that these three factors are considered in the set-up of nutritional experiments.

In the study cited above, the estimated combined uncertainty was 16 %. The stable isotope doses applied resulted in average atom enrichments in the urine samples of 2 % and 4 %, for ^{44}Ca and ^{42}Ca, respectively. The isotope ratios used in the calculations were averages of triplicate measurements resulting in % RSDs of 0.19 and 0.24 for $^{44}Ca/^{43}Ca$ and $^{42}Ca/^{43}Ca$, respectively. In the next study performed (determination of calcium absorption from meals containing different food oils) the ^{44}Ca dose was increased and the total amount of natural calcium given with the food oil decreased in order to obtain an uncertainty on the absorption rate better than the 16 % obtained in the first study. Doses of 2.3 mg ^{42}Ca and 19.5 mg ^{44}Ca were applied and %XS values of 5 and 4 % were achieved for ^{44}Ca and ^{42}Ca, respectively. The amount of natural calcium in the food was 150 mg[85]. The estimated uncertainty on the calcium absorption rate was 10 %, which is in good agreement with the experimentally determined precision of 8 %, see Appendix 6.

Having derived the equation for the combined overall uncertainty on the calcium absorption rate, it is possible to estimate the uncertainty for given values of measurement precision and urinary atom enrichment. Also, if a specific combined uncertainty on the absorption rate is wanted, the measurement precision and the % atom enrichment needed to achieve this can be calculated. It is important to notice that several combinations of measurement precision and atom enrichment result in the same uncertainty. The measurement precision can be improved by doing more replicates in one measurement of an isotope ratio, by re-optimising the ICP-SFMS method or by measuring the isotope ratios using a mass spectrometric technique that possesses a better precision. As mentioned earlier, the size of the stable isotope doses and the total amount of calcium in the test meal control the atom enrichment. No exact

relationship exists between these factors, since the human absorption varies with weight, calcium status, genetic predisposition and perhaps adaptation to different calcium intakes. In practise there is also an upper limit on size of the isotope doses, as they should not significantly increase the daily intake of the elements in order not to change the natural uptake mechanisms. Therefore some experience from nutritional experiments is needed in order to estimate the isotope doses needed to produce certain atom enrichments.

Since different combinations of measurements precision (number of replicates) and atom enrichment are suitable to produce a given combined uncertainty on the absorption rate, it is necessary to decide which combination is the preferred. This decision can (among other things) be made on the basis of the total cost of the measurement of the absorption rate for one subject. A function for the total cost can be made, and then the different combination can be evaluated.

$$Total\ Cost = (A_b + n \cdot A_r) + (N_b + w_{44} \cdot N_{44} + w_{42} \cdot N_{42}) \qquad (4.3)$$

Where A_b is the basic cost of the one replicate analysis of the baseline and enriched urine samples, n the additional number of replicates and A_r the cost per additional replicate. N_b is the basic cost per subject setting up the nutritional experiment, w_{44} and w_{42} are the mg isotope administered and N_{44} and N_{42} are the cost of the isotopes per mg. As an example if a combined uncertainty of 7 % is needed, this can be achieved with I) 3 replicates, 8 % $XS^{44}Ca$ and 6 % $XS^{42}Ca$ or II) 6 replicates, 6 % $XS^{44}Ca$ and 4 % $XS^{42}Ca$, providing that the measurement precision on one replicate measurements is 0.33 and 0.41 % RSD for $^{44}Ca^{+}/^{43}Ca^{+}$ and $^{42}Ca^{+}/^{43}Ca^{+}$, respectively. It is assumed (estimated) that 8 and 6 % $XS^{44}Ca$ can be achieved applying a dose of 25 and 20 mg ^{44}Ca and that 6 and 4 % $XS^{42}Ca$ can be achieved with 3.0 and 2.3 mg ^{42}Ca in adult subjects from a meal with medium high calcium bioavailability, respectively. The cost factors are set as follows: A_b = 800 Dkr, A_r = 200 DKr, N_b = 500, N_{44} = 150 DKr and N_{42} = 550 DKr. These figures are approximate and not exact values, but are given to illustrate the principle. The cost of the two different combinations is 7300,- DKr for the first and 6765,- for the second combination. Therefore the second combination is preferred.

This uncertainty analysis provide useful information on the factors that control the combined uncertainty on the calculation of the absorption rate from double stable isotope experiments and on the economical factors that in the end decides how many subjects can be included in a nutritional experiment with a fixed budget. The uncertainty analysis also shows that an experimental set-up (choice of isotope doses etc.) developed for one analytical technique (e.g. TIMS) cannot be used directly with another analytical technique (e.g. ICP-SFMS) if the precision by which the isotope ratios are measured are different. The set-up of the nutritional experiment has to be adjusted to the analytical technique used.

A more general and simple rule based on detection limits is normally used to estimate the atom enrichment needed for nutritional experiments. While the detection limit for measuring a change in isotope ratio is 3 times the relative standard deviation (measurement precision as % RSD), it is customary to design nutritional experiments to result in an average shift in isotope ratio of approximately 10 times the % RSD[13]. The advantage of this approach is that it is simple and straightforward, while the limitations are that no knowledge is gained on uncertainty and the factors that controls the uncertainty or on the economy of the experiments. Even though the uncertainty analysis and the economical considerations outlined in this thesis are more time-consuming they should be preferred over the detection limit approach, since a figure on the combined uncertainty is provided and a more detailed understanding of the experiments to be performed is achieved. Applying the detection limit approach to the calcium experiments performed reveals that the % $XS^{44}Ca$ achieved in the original experiment[82] is below the recommended atom enrichment ($10 \cdot 0.33$ % RSD = 3.3 % $XS^{44}Ca$), while both the % $XS^{44}Ca$ and % $XS^{42}Ca$ values obtained in the food oil experiment are considered sufficient. From the detection limit approach it can also be concluded that the atom enrichments achieved in the first set-up is not sufficient, so as a first approximation this approach also provides good guidance, but no details.

In relation to nutritional experiments it has been shown that double stable isotope experiments, in which the isotope ratios were measured with ICP-SFMS, provided calculated human absorption rates in reasonable good agreement with absorption rates achieved using a calcium radiotracer. As such, ICP-SFMS is a valid analytical technique for nutritional experiments. The uncertainty analysis performed outlines a procedure for optimising the overall performance of nutritional tracer experiments, taking into account both the analytical technique and the design of the nutritional experiment.

The above discussion, of the uncertainty of the final result and the economical considerations, also opens a discussion about the appropriate choice of analytical method for a given analytical problem (fitness for purpose). Many definitions have been given on fitness for purpose, but most precise is probably that of Thompson and Fearn[86] who write:

"Fitness for purpose demands sufficient but only necessary accuracy in analysis. Purely scientific requirements may be constrained by financial considerations"

This quote very clearly states that both scientific and economical considerations have to be taken into account when an analytical problem has to be solved. This also implies that it is not necessarily the "state-of-the-art" technique, which employs front-line science that is best choice. Taking the determination of human calcium absorption rates as an example, a valid evaluation of the application of the double stable isotope technique using ICP-SFMS for the isotope ratio measurements is

presented, including both scientific and economical considerations. However, in order to choose the best method for the purpose, other methods and techniques should be considered. If the task is to determine absorption rates with an combined uncertainty of 7 %, this could be achieved using the method outlined above for a cost of approximately 6765,- DKr per subject. Similar evaluations should be performed for TIMS, FABMS or ICP-MCMS if they were to be used for the analysis, and also the radioisotope method, which is a completely different approach, should be evaluated on basis of both scientific and economical considerations. So the choice of the method best suited for the purpose is very complex, and it is definitely not just the choice of the method that shows the "best" figures of merit. Even though the combined uncertainty and economical analysis is a very complex procedure, some factors are, in part, left out. For example, the time-consumption is only indirectly included, as a part of the basic costs. A more direct time factor should probably be included. Also, the ethical aspect is not covered. In studies with pregnant women or infants/children stable isotopes are almost always preferred over radioisotopes due to the radiation exposure (although it is minimal). So again the choice is complex, but doing considerations on the overall uncertainty and fitness for purpose of the analytical method in use would probably improve the quality of many analytical results.

4.2 Measurement of zinc isotope ratios

As for the method for calcium isotope ratios, the zinc method has been published[III] and only a summary of the results will be given here. Using the method described zinc isotope ratios ($^{64}Zn^+/^{66}Zn^+$, $^{67}Zn^+/^{66}Zn^+$, $^{68}Zn^+/^{66}Zn^+$ and $^{70}Zn^+/^{66}Zn^+$) and the total zinc content are measured simultaneously in human faeces, urine and serum using ICP-SFMS. Relative standard deviations (RSD) of 0.7 % were found for $^{67}Zn^+/^{66}Zn^+$, $^{68}Zn^+/^{66}Zn^+$ and $^{70}Zn^+/^{66}Zn^+$, while a RSD of 1.2 % was found for $^{64}Zn^+/^{66}Zn^+$, corresponding to R_p values in the range of 2 - 4. The method was shown to be accurate by analysing faecal sample solutions spiked with zinc enriched in ^{68}Zn. Using a mass resolution of 6000, all zinc isotopes could be measured free from interferences, except for $^{64}Zn^+$, where the overlap from $^{64}Ni^+$ had to be corrected for mathematically. The use of different mass resolution settings ensured a positive identification of all spectral interferences found at the zinc isotope masses in faeces, urine and serum. The total zinc content was determined using the sum of the counts for the five zinc isotopes. These measurements showed fairly good agreement with atomic absorption spectrometry (AAS) data (r = 0.95).

As for the calcium method, the zinc method proves that ICP-SFMS can be used for reliable measurements of isotope ratios, again with a measurement precision of 2- 4 times that of the theoretical precision. In addition, the accuracy was shown to be good over a range of ratios and not only for the natural values. This is of importance when samples with enriched isotopes are measured, as in tracer experiments. It was shown

that a positive identification of all the spectral interferences is possible, and that the pattern of the spectral interferences changes between different sample matrices. It is therefore of great importance during method development to carry out an analysis of the spectral interferences for each sample matrix. Finally, a good selectivity was obtained for all five zinc isotopes applying a mass resolution setting of 6000. Therefore, the total zinc content could be determined along with the isotope ratios. This is a major advantage of this ICP-SFMS method, since both the isotope ratios and the total content are needed when human absorption is calculated from the faecal monitoring technique[87]. Hence, until now two analytical techniques had to be used to determine human absorption; one for the measurement of isotope ratios and one for the measurement of total content. With this new ICP-SFMS method only one analysis per sample is needed, which makes it much simpler and cheaper.

4.3 ICP-SFMS for the measurement of the ^{97}Mo/^{98}Mo ratio in urine

The method presented was developed in order to measure the ^{97}Mo/^{98}Mo ratios in human urine samples as part of a tracer experiment estimating molybdenum absorption. ^{97}Mo was used as the tracer.

Molybdenum has 7 isotopes, all of which coincide with spectral interferences. Therefore ICP-MS analysis of molybdenum is difficult. In Table 4.1 some of the potential spectral interferences on ^{96}Mo, ^{97}Mo, ^{98}Mo and ^{100}Mo are shown. The interference pattern is complex and many of the interferences cannot be separated from the molybdenum peak, even with a mass resolution setting of 10000.

Isotope	Abundance(%)	Spectral Interferences
^{96}Mo	16.68	$^{40}Ar^{56}Fe^{+}$ (13041), $^{36}Ar^{60}Ni^{+}$ (14538), $^{96}Ru^{+}$ (32839), $^{96}Zr^{+}$ (26667), $^{80}Se^{16}O^{+}$ (14189), $^{79}Br^{16}OH^{+}$ (5849), $^{192}Pt^{2+}$ (1265), $^{192}Os^{2+}$ (1262)
^{97}Mo	9.55	$^{38}Ar^{50}Co^{+}$ (9605), $^{40}Ar^{57}Fe^{+}$ (11761), $^{81}Br^{16}O^{+}$ (18683), $^{40}Ar_2{}^{16}OH^{+}$ (4516), $^{194}Pt^{2+}$ (1288)
^{98}Mo	24.13	$^{40}Ar^{58}Ni^{+}$ (12755), $^{40}Ar^{58}Fe^{+}$ (10047), $^{98}Ru^{+}$ (829706), $^{82}Se^{16}O^{+}$ (15744), $^{81}Br^{16}OH^{+}$ (7187), $^{196}Pt^{2+}$ (1271), $^{196}Hg^{2+}$ (1264)
^{100}Mo	9.63	$^{40}Ar^{60}Ni^{+}$ (6985), $^{36}Ar^{64}Zn^{+}$ (9265), $^{100}Ru^{+}$ (30688), $^{84}Sr^{16}O^{+}$ (114837), $^{200}Hg^{2+}$ (1304)

Table 4.1 *Potential interferences on Mo isotopes*

The interferences at ^{97}Mo, ^{98}Mo and ^{100}Mo from the urine matrix were investigated. Only one spectral interference of importance could be positively identified using mass resolution settings between 2000 and 10000, the overlap between $^{97}Mo^{+}$ and $^{40}Ar_2OH^{+}$. The mass difference, Δm, between the two peaks is 0.0215 mass units, therefore a mass resolution setting of 4516 is needed to separate the $^{97}Mo^{+}$ signal from the $^{40}Ar_2OH^{+}$ signal. The two peaks are of similar size in the mass spectra of diluted urine samples. Baseline separation of the peaks was achieved using a mass resolution setting of 6000, see Figure 4.2.

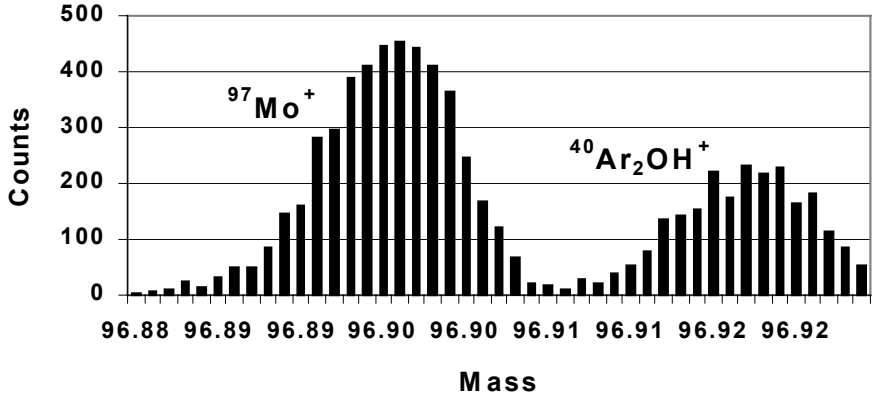

Figure 4.2 *Spectra on m/z = 97 analysing a urine sample containing 1.5 µg/l total molybdenum*

The figure show the m/z = 97 spectrum from a natural human urine sample solution containing 1.5 µg/l of total molybdenum, acquired by applying 100 sweeps and a dwell time of 10 ms. Approximately 11000 counts was acquired for $^{97}Mo^{+}$.

The isotope ratios shown in Table 4.2 were obtained through analysing a urine sample using a mass resolution setting of 6000.

Ratio	Observed	Natural
$^{97}Mo/^{98}Mo$	0.3906	0.3959
$^{97}Mo/^{100}Mo$	0.8772	0.9917
$^{98}Mo/^{100}Mo$	2.2457	2.5057

Table 4.2 *Observed Mo isotope ratios in urine*

The observed ratios indicate that there are still interferences at the ^{100}Mo peak, since the $^{97}Mo/^{100}Mo$ and $^{98}Mo/^{100}Mo$ ratios are significantly lower than the natural values. Combining this information with Table 4.1 suggests that the most likely interference at $^{100}Mo^{+}$ is $^{84}Sr^{16}O^{+}$, since the mass resolution setting needed to separate the "unknown" interference is higher than 10000. Also, strontium is present in urine in high concentrations, approximately 0.2 mg/l[88] and since typically MO^{+}/M^{+} ratios are in the range of 0.01 to 0.10[44], some formation of $^{84}Sr^{16}O^{+}$ can be expected. However, the interference cannot be positively identified. The $^{97}Mo/^{98}Mo$ ratio was therefore selected to monitor the excretion of ^{97}Mo in urine.

The molybdenum concentration in urine is low, resulting in total molybdenum concentrations in the diluted urine sample solutions in the order of 0.5 – 2 ng/ml. One hundred sweeps were applied, the counts were summed and the majority of the signal noise was eliminated. However, the number of counts acquired was still low. A molybdenum concentration of 1 ng/ml in the sample solution resulted in approximately 7500 counts for ^{97}Mo and 18250 counts for ^{98}Mo. This is far below 10^{6}

count per second therefore no detector dead time correction was needed. The data was corrected for mass discrimination using the ratios measured in molybdenum standard solutions (1 or 5 ng/ml) analysed frequently in between the samples. A small constant molybdenum background signal was found throughout the study. The background signal corresponded to a total molybdenum concentration of approximately 50 pg/ml and had an isotope ratio similar to that of natural molybdenum. A background correction was therefore necessary in order not to introduce a bias on the isotope ratio measurement in samples enriched with ^{97}Mo. The results obtained for the measurement of ^{97}Mo/^{98}Mo in standard solutions and urine samples are presented in Table 4.3.

Matrix	Mo_{conc}, (ng/ml)	Ratio	SD	%RSD	R_p	f_{md}
Standard	1	0.4026	0.0050	1.2 (n = 15)	1.5	0.98
Urine	0.5 – 2	0.3943	0.0126	3.2 (n = 11)	2.0	-

Table 4.3 *Measurement of ^{97}Mo/^{98}Mo ratios using ICP-SFMS*

The sample solutions were analysed over 3 days, %RSD is the long-term measurement precision. R_p is the ratio between the measurement precision and the theoretical precision, and f_{md} is the mass discrimination factor. The R_p values are similar to those in the range of 2 – 4 found for calcium and zinc isotope ratios. The observed mass discrimination is approximately 2 %, the f_{md} is not calculated for the urine samples, since these data were mass bias corrected using the standard solutions bracketing the samples in the analysis sequence.

To my knowledge only two papers have been published previously on the measurement of molybdenum isotope ratios using ICP-MS. These papers were both published by Soltani-Neshan et al.[89,90] and reports on the measurement of molybdenum isotopes in human urine and feaces by ICP-QMS. They found that ^{96}Mo, ^{98}Mo and ^{100}Mo could be measured free of interferences in urine, but only ^{98}Mo and ^{100}Mo in faeces. Consequently the ^{98}Mo/^{100}Mo ratio was measured in the samples, which was performed with a measurement precision of 0.1 – 1%[90]. No information was given on the exact molybdenum concentrations in the sample solutions or on the number of counts acquired. The differences in the interference pattern between the work by Soltani-Neshan et al.[89,90] and this work can probably be explained by the different sample preparation procedures applied. Soltani-Neshan et al. apply freeze-drying followed by a nitric acid digestion, while in this work the urine is simply diluted with weak nitric acid. During a nitric acid digestion the majority of the organic molecules present in the urine decompose, therefore less spectral interference should be encountered in the ICP-MS analysis. However, the very simple dilution of the urine with nitric acid has the advantage that it contains very few sample handling operations, therefore the risk of contaminating the enriched samples and introducing a bias in the measured ratios are significantly smaller than when the freeze-drying and nitric acid digestion is applied. Also differences in instrumental design and plasma conditions might change the interferences pattern.

All of the molybdenum isotopes can be measured free of interferences using TIMS, after a thorough sample preparation procedure. As an example, Turnlund et al.[91] measured the $^{94}Mo/^{98}Mo$, $^{97}Mo/^{98}Mo$ and $^{100}Mo/^{98}Mo$ ratios in human urine and faeces. The sample preparation procedure included drying, ashing in a muffle furnace, dissolving in hydrochloric acid, and a double column ion-exchange separation of the molybdenum from the sample matrix. Performing 10 replicates on samples containing 1 µg molybdenum the isotope ratios could be measured with excellent accuracy, a within run precision below 0.1 % and a between sample precision in the range of 0.1 – 0.6 %[91]. These data show that TIMS is superior in terms of the precision of the molybdenum isotope ratio measurement.

The above discussion emphasizes that ^{97}Mo is not an ideal tracer isotope, because it is severely interfered, forcing the use of a high mass resolution setting. This in turn limits the number of counts acquired and the absolute precision obtained. The measurement precision of 3 % for the $^{97}Mo/^{98}Mo$ ratio in the urine samples is not sufficient to be used in an double-stable isotope experiment, for example, where a very good measurement precision is crucial (below 1 % RSD).

However, for the purpose at hand, where the isotope ratios and total concentrations measured in both urine and faeces have to be used to estimate absorption, the results are useful. The urinary excretion of the ^{97}Mo tracer is shown for one subject from the molybdenum absorption experiment in Figure 4.3. The subject received a meal containing 100 µg molybdenum on day 1, a dose similar to that of the typical daily intake of 130 µg[92]. The error bars represent ± 1 standard deviation (3.2 %RSD). The horizontal line at 0.3958 show the true $^{97}Mo/^{98}Mo$ ratio.

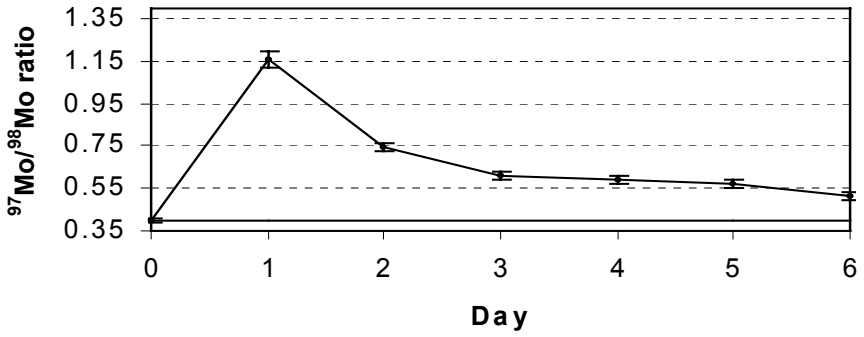

Figure 4.3 *Urinary excretion of ^{97}Mo*

Even though the measurement precision is relatively poor, it is evident that the $^{97}Mo/^{98}Mo$ ratio can be measured with sufficient precision to see the variation in ^{97}Mo excretion over time. The analysis of the urine and faecal samples and subsequent calculation of molybdenum absorption have not yet been completed. However, the above preliminary results show that ICP-SFMS has the potential to be used to measure molybdenum isotope ratios. The measurement precision may potentially

be improved by a different choice of isotopes. According to Soltani-Neshan et al.[89,90] the use of the ^{96}Mo isotope as tracer would be a wiser choice.

The overall instrument sensitivity can be improved by the use of an ultrasonic nebuliser (USN), shown by a test analysis of the sample analysed earlier, shown in Figure 4.2. The sensitivity increased by a factor of 4.5, when using the USN (48500 counts for $^{97}Mo^+$ and 117000 for $^{98}Mo^+$). In addition the formation of $^{40}ArOH^+$ was reduced due to the desolvation of the sample aerosol, so the $^{97}Mo^+/^{40}ArOH^+$ ratio was increased from 2 to 6. This shows that applying an USN can potentially improve the precision on the $^{97}Mo^+/^{98}Mo^+$ ratio due the increased number of counts acquired. Thus, the theoretical precision is improved by a factor of two by applying the USN. If this can be achieved in general, a measurement precision of approximately 1.5 % should be within reach, simply by using the USN instead of the concentric nebuliser.

Even though some investigations and developments still remain to be done, the preliminary results show that ICP-SFMS has the potential to measure molybdenum isotope ratios in human samples for nutritional tracer experiments.

4.4 ICP-SFMS for the measurement of iron isotope ratios

A method for the measurement of iron isotope ratios was developed in order to participate in an intercomparison study. This study involved comparing ICP-MS techniques and TI-QMS for the measurement of isotope ratios in faecal sample solutions. The method comparison was initiated by Dr. H. Crews and Dr. L. Owen from the Central Science Laboratory, York, UK. The method comparison involved measurements of iron, zinc, calcium and magnesium isotope ratios in faecal sample solutions. The data evaluation have not yet been finished, therefore only the comparison of the iron isotope ratios measured by ICP-SFMS (this work) and TI-QMS is presented here. Dr. T. Fox, Institue of Food Research, Norwich Laboratory, UK, performed the TI-QMS measurements and provided the data. The $^{57}Fe/^{56}Fe$ and $^{58}Fe/^{56}Fe$ ratios were measured by the two methods in 16 faecal sample solutions.

Iron has four stable isotopes, one major isotope (^{56}Fe) and three minor isotopes (^{54}Fe, ^{57}Fe, ^{58}Fe). A mass resolution setting of 4000 was applied to resolve the iron signals from all spectral interferences, except the isobaric overlaps from $^{54}Cr^+$ on $^{54}Fe^+$ and $^{58}Ni^+$ on $^{58}Fe^+$. These interferences were corrected for mathematically using the signals on $^{52}Cr^+$ and $^{60}Ni^+$, which were measured in the same run as the analyte peaks. A dwell time of 2 ms, 50 sweeps, 3 peak widths and 20 points per peak width were applied. The results in Table 4.4 were obtained for 10 repetitive measurements of the iron isotope ratios in a 30 ng/ml single elements standard solution.

Ratio	True	Measured	%RSD$_m$	R_p
$^{54}Fe/^{56}Fe$	0.0637	0.0630	0.99	2.7
$^{57}Fe/^{56}Fe$	0.0231	0.0232	0.87	1.5
$^{58}Fe/^{56}Fe$	0.0031	0.0029	11.3	6.8

Table 4.4 *Iron isotope ratios in 30 ng/ml standard solution*

The precision and accuracy of the $^{54}Fe/^{56}Fe$ and $^{57}Fe/^{56}Fe$ ratios are comparable to those of the calcium, zink and molydenum isotope ratios. The precision of the $^{58}Fe/^{56}Fe$ ratio is not very good, a R_p value of 6.8 is not acceptable under normal conditions. The reason for this poor precision is two-fold, first of all very few counts were acquired for the ^{58}Fe isotope, because of its very low abundance (0.28 %). This problem could be minimised by applying a longer dwell time on m/z = 58 in the future. However, the largest nickel isotope also overlaps with the ^{58}Fe signal and this overlap is significant even in an single element iron standard, therefore a correction is necessary, which does degrade the precision. Even though the above-described method can be improved it was used in the method comparison. Since all the iron isotopes were measured the total iron content can also be assessed, by summing the counts acquired for the four isotopes. Total iron concentrations have also been determined in the faecal sample solutions analysed for the method comparison, but since the data are not evaluated yet, they are not presented here.

Sixteen faecal sample solutions were analysed in the comparison of ICP-SFMS and TI-QMS. The results obtained for the $^{57}Fe/^{56}Fe$ ratio is shown in Table 4.5. At a first glance there is a good agreement between the two methods and the relative deviations are below 4 %, except for one sample (number 16).

Sample	TI-QMS	ICP-SFMS	Deviation (%)
1	0.023103	0.0237	-2.58
2	0.023206	0.0234	-0.84
3	0.023283	0.0234	-0.50
4	0.023411	0.0231	1.33
5	0.023460	0.0237	-1.02
6	0.023553	0.0237	-0.62
7	0.023572	0.0237	-0.54
8	0.023818	0.0235	1.34
9	0.023915	0.0235	1.74
10	0.024013	0.0239	0.47
11	0.024043	0.0234	2.67
12	0.024570	0.0244	0.67
13	0.026406	0.0254	3.81
14	0.057495	0.0552	3.99
15	0.065616	0.0660	-0.59
16	0.148855	0.1256	15.6

Table 4.5 *$^{57}Fe/^{56}Fe$ ratios measured by TI-QMS and ICP-SFMS*

It is difficult to perform a statistical analysis of the data, due to the very skewed distribution of the absolute values of isotope ratios measured, 13 out of 16 measurements are in the range of 0.023 – 0.026 and the

remaining 3 measurement are significantly above this range. The average standard deviation of the individual TI-QMS measurements is 1.8 %, while the ICP-SFMS measurement precision for repetitive measurement of a standard solution is 0.9 %. These figure show that the precisions of the two methods are comparable. Due to the skewness of the data set neither a paired t-test nor a linear regression is fully appropriate for comparison of the two methods.

Performing a linear regression taking into account the uncertainty on both variables[93,94] the following equation was obtained: *ICP-SFMS = 0.839·TI-QMS + 0.004, r = 0.997*, the confidence interval on the slope is 0.808 – 0.872, indicating that the ICP-SFMS method produces significant lower values than the TI-QMS method. Even though the above linear regression looks fine, it does not truly describe the variation of the 3 samples that have significant higher ratios. This was revealed by a residual analysis, in which the residual values (the observed ICP-SFMS values subtracted the estimated value) were plotted against the 16 observations in ascending order, see Figure 4.3. Here the residual plot is shown along with the plotted data and the regression line. It is clear that for the first 13 observations, where the residuals are close to zero, the linear regression is a valid description of the variation. However, for the last 3 observations, large residuals are obtained, indicating the variation between these observations is not accounted for in the regression analysis. A residual plot, as shown in Figure 4.4, normally indicates that a weighted linear regression should be performed, but the linear regression applied taking into account the uncertainty in both variables does also include a weighting[94].

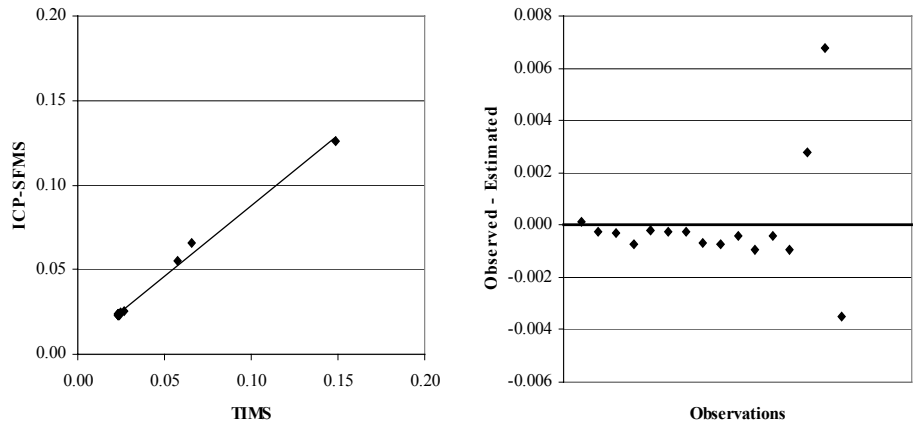

Figure 4.4 *Plotted data and residual analysis for the $^{57}Fe/^{56}Fe$ measurement*

So the only way to obtain a more sound regression is to analyse more faecal sample solutions with high $^{57}Fe/^{56}Fe$ ratios and then obtain a data set which is more evenly distributed across the observation range.

As an alternative to the linear regression a Wilcoxon signed rank test was performed on the data. In this test the deviation between the TI-QMS and ICP-SFMS observations are ranked in ascending numerical order and

assigned ranks from 1 to 16. The positive ranks are added and the negative ranks are added the lower of these two numbers is the test statistics. The binomial theorem will give the probability of this number occurring[95]. For the above data set the sum of positive ranks is 91 and the sum of negative ranks is – 45, the critical value is 34. Since 45 > 34, the null hypothesis cannot be rejected, i.e., according to this test there is no significant difference between the TI-QMS and the ICP-SFMS measurements. Therefore, the conclusion is that there seems to be a good agreement between the two techniques for the measurement of the $^{57}Fe/^{56}Fe$ ratio, but that more samples have to be analysed in order to do a valid statistical treatment of the data.

For the measurement of the $^{58}Fe/^{56}Fe$ ratios the precision is poor using both TI-QMS and ICP-SFMS. The average RSD on the 16 measurements by TI-QMS is 10 %, while the measurement precision for ICP-SFMS is similar, 11.3 %. Performing a linear regression taking into account the uncertainty in both variables the following equation was obtained: *ICP-SFMS = 1.171·TIMS + 0.001, r = 0.998*. The confidence interval on slope was 1.140 – 1.202. This indicates that higher values were found with the ICP-SFMS technique. A residual analysis was also performed, but no problems were encountered. The residuals were evenly spread below and above zero. In this case therefore the regression analysis was valid for the comparison of the two methods. The plotted data, the regression line and the residual plot are shown in Figure 4.5. The results from the two methods show a good correlation, despite the very low abundance of the ^{58}Fe isotope and the poor measurement precision of both techniques. There was an additional problem associated with the ICP-SFMS measurements, as a correction had to be applied to account for the $^{58}Ni^+$ overlap with the $^{58}Fe^+$ signal. Approximately 75 % of the observed counts an m/z = 58 in faecal sample solutions are due to nickel, so 75 % of the total signal is subtracted. In conclusion, there is good agreement between TI-QMS and ICP-SFMS for the measurement of $^{58}Fe/^{56}Fe$ ratios, even though slightly higher values are obtained with ICP-SFMS.

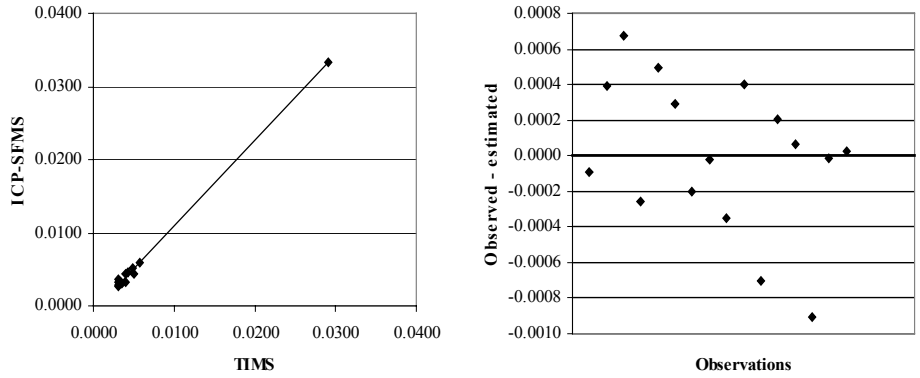

Figure 4.5 *Plotted data and residual analysis for the $^{58}Fe/^{56}Fe$ measurement*

The measurement of iron isotope ratio by ICP-QMS is difficult because of the many spectral interferences encountered, this problem has been

solved by the use of electrothermal vaporisation (ETV), which significantly reduces the formation of certain polyatomic interferences[64] or by careful instrument optimisation and analysis of sample solutions containing high levels of iron (> 5 μg/ml)[68]. Applying these approaches measurement precisions ($\%RSD_m$) in the range of 0.2 – 0.6 % for $^{57}Fe/^{56}Fe$ and $^{58}Fe/^{56}Fe$[68] and 0.9 – 1.5 % for $^{54}Fe/^{56}Fe$ and $^{57}Fe/^{56}Fe$ was found for the measurement of iron isotope ratios in blood[64]. These figure are comparable with the precision obtained in this work of 0.9 – 1.0 % for the $^{54}Fe/^{56}Fe$ and $^{57}Fe/^{56}Fe$ ratios in solutions containing 30 ng/ml. The precision obtained in this work for the $^{58}Fe/^{56}Fe$ ratio is considerably worse, but can probably be improved.

Iron isotopes have frequently been analysed using TIMS by which presicions in the range of 0.1 – 1.6 % have been reported[14]. It is here important to make a distinction between internal and external precision, i.e., within and between sample precision. As an example Kastenmayer et al.[96] reports internal precision of < 0.5 % for the $^{57}Fe/^{56}Fe$ ratio and < 1 % for the $^{58}Fe/^{56}Fe$ ratio in blood, while the external precision is 0.7 % and 1.6 %, respectively. The latter figures are comparable with the figures cited above for ICP-QMS and with the figures for the $^{57}Fe/^{56}Fe$ ratio obtained in this work, showing that TIMS do not posses superior precision for all applications.

The results obtained in this work show that ICP-SFMS has the potential for the measurement of iron isotope ratios, but that further developments and investigations still remain.

4.5 Conclusions of the measurement of isotope ratio of nutritional elements

The above development, evaluation and application of the ICP-SFMS methods for the measurement of calcium, zinc, molybdenum and iron isotope ratios show that reliable, accurate and precise measurements of isotope ratios with ICP-SFMS are possible. Most spectral interferences can be resolved by applying a high mass resolution setting, and precisions in the order of 2-3 times the theoretical precision can be obtained. The accuracy of these methods has been demonstrated both by spiking with enriched stable isotopes (zinc) and by comparison with TI-QMS (iron). For elements where all isotopes can be measured reliably the total element content can be measured independently of the isotopic composition in the sample. It has also been shown that using stable isotopes and ICP-SFMS for the measurement of human absorption rates, results similar to those obtained through the use of radioisotopes (calcium) can be produced. Finally it has been shown that the major sources of uncertainty on the final results can be identified, means of optimising both the analytical method and the experimental set-up simultaneously were found, which potentially can improve the overall results significantly.

The fact that both isotope ratios and total content can be measured simultaneously, as is required for some tracer experiments, means that the use of ICP-SFMS imposes a significant reduction in the total costs, as only one analytical technique is needed. Furthermore, no complex matrix separation is needed, because the cost per subject in tracer experiments hereby is reduced, and more subjects can be involved in the tracer experiments. Consequently conclusions may be drawn on the basis of a larger data material, rather than if other techniques like TIMS or ICP-QMS were used.

Another interesting point can be made that expertise within both analytical chemistry and human nutrition is required to explore the potential of human nutritional tracer experiments in full. This is probably one of the main reasons that the use of stable isotopes in human nutrition is still limited.

It has been shown that also ICP-SFMS can also be used in human nutritional tracer experiments along with TIMS, FABMS and ICP-QMS. The very rapid growth in laboratories applying ICP-SFMS instrumentation during the last five years will probably result in a more extensive use of stable isotopes as tracers in human tracer experiments.

5 Isotope and ultratrace analysis of long-lived radionuclides

Radionuclides are highly toxic elements that are released into the environment mainly through nuclear weapons tests, by satellite and reactor accidents, from nuclear facilities and nuclear fuel processing. The levels of radionuclides in the environment are very low, often in the low pg/kg range. Therefore the availability of very sensitive analytical techniques for the analysis of radionuclides are required in order to perform reliable analysis of environmental samples. Not only total concentrations are of interest, but also isotopic composition, elemental ratios and isotope ratios, since they for some radionuclides can be used to determine the origin of the radionuclides. As an example the $^{240}Pu/^{239}Pu$ ratio gives an opportunity to distinguish between plutonium from different sources. Plutonium originating from nuclear weapons has a $^{240}Pu/^{239}Pu$ ratio below 0.06, while it is approximately 0.20 for plutonium originating from nuclear power facilities and global fallout. Analytical techniques that provide information on both total concentrations and isotopic composition are therefore needed in order to investigate the pathways of radionuclides in nature. Traditionally analytical techniques for the determination of long-lived radionuclides are based on the measurement of alpha, beta or gamma radiation. But also ICP-QMS is a well-established technique for the measurement of long-lived radionuclides[31,51,53,97-121]. Since ICP-SFMS is a relatively new technique only a few papers have so far been published on the use of this technique

for the measurement of radionuclides[II,4,31,104,121]. The main advantage of the ICP-MS technique, and especially the ICP-SFMS technique, is the high sensitivity approaching or even surpassing that of the radiation techniques and the low background signals, resulting in better detection limits than for radiometric methods[II,116,122]. It has been estimated that for radionuclides with a half-life above 1000 years, better detection limits are obtained with ICP-MS methods than with radiometric methods[116]. The half-life of the radionuclides measured in this study is shown in Table 5.1.

Radionuclide	Half-life, years
^{99}Tc	$2.1 \cdot 10^5$
^{237}Np	$2.1 \cdot 10^6$
^{239}Pu	$2.4 \cdot 10^4$
^{240}Pu	6550
^{241}Pu	14
^{242}Pu	$3.8 \cdot 10^4$

Table 5.1 *Half-life of radionuclides*

Also ICP-MS possesses a better selectivity, the signals for the individual isotopes being completely separated, whereas overlap between the signals form different isotopes are seen, e.g., in α-spectrometry[123]. For ICP-SFMS instruments this means that only the use a low mass resolution setting is valid in order to maintain a high sensitivity. Often even higher sensitivity is desired and action is taken to further increase the instrument sensitivity, e.g., the use of a ultrasonic nebuliser[II,119] or a shielded torch[29,61].

This means that all possible spectral interferences have to be dealt with during the sample preparation procedure. This involves different separation procedures and most often also pre-concentration steps in order to bring the radionuclide concentrations in the final sample solution above the detection limit of the analytical method in use. The sample preparation procedures used for the determination of long-lived radionuclides in environmental samples are therefore both time-consuming and complex[116,124]. The validity of the ICP-SFMS technique for the determination of radionuclides in this thesis has been shown by the development of a method for the measurement of isotope ratios and ultratrace levels of plutonium. The method has been published[II]. This method was later extended to measure neptunium as well. Preliminary work on the development of a method for the determination technetium will also be presented below. Unless otherwise stated all samples were provided by the Nuclear Safety Research and Facilities Department, Risø National Laboratory, Denmark. Also all sample preparations were performed there.

The method described below for the simultaneously determination of neptunium and plutonium has been applied for the measurement of total plutonium, plutonium isotope ratios and plutonium/neptunium elemental ratios in marine samples from the Thule nuclear weapons accident site

and sediment samples from the river system draining the Russian nuclear weapons production facility "Mayak" in the Urals[125]. The very low concentrations of plutonium and neptunium in the Danish seawater have been determined by the developed ICP-SFMS methods. The concentrations in Danish seawater are below 1 ng/m^3 [126].

5.1 Isotope ratio and ultratrace determination of plutonium isotopes

The analytical method has been published[II] therefore only a short summary on the analytical aspects will be given here. The ultrasonic nebulisation (USN) ICP-SFMS method was set-up to measure the ^{239}Pu, ^{240}Pu and ^{242}Pu isotopes and the ^{240}Pu/^{239}Pu ratio. The combined magnetic and voltage scanning mode was applied, since a longer dwell time is used for $^{240}Pu^+$ in order to improve counting statistics and precision on the ^{240}Pu/^{239}Pu ratio. Using the ultrasonic nebuliser a sensitivity of $8 \cdot 10^8$ counts/s for $^{238}U^+$ in a 1 μg/ml standard was obtained, an increase in sensitivity of 10 compared with the normal instrument set-up applying a concentric nebuliser. The potential interference form $^{238}UH^+$ on $^{239}Pu^+$, which could degrade the accuracy on both total measurement and isotope ratio measurements, was almost completely eliminated during the sample preparation where plutonium is separated from uranium and americium[II,124]. Total Pu concentrations ($^{239+240}$Pu) measured in reference materials and environmental samples were in good agreement with certified values and α-spectrometry measurements, showing that the ICP-SFMS method possesses good accuracy. Quantification was performed by both external calibration and isotope dilution calibration. The best agreement between α-spectrometry and ICP-SFMS was found applying isotope dilution. This was expected as isotope dilution is often considered the most accurate method of quantification in ICP-MS. Since isotope dilution is based on spiking of the samples with enriched stable isotopes and measurement of isotope ratios in samples and standards, the same considerations regarding accuracy and precision as discussed for the measurement of isotope ratios in chapter 3 needs to be taken into account for the quantification to be successful. Good accuracy was also found on the measurement of the ^{240}Pu/^{239}Pu ratio comparing the results from α-spectrometry with the results applying the ICP-SFMS method.

The accuracy of the Pu ratio measurements have been further investigated by the analysis of two samples provided by Dr. D. Oughton, The Agricultural University of Norway, that had previously been analysed by different ICP-QMS methods and by AMS (accelerator mass spectrometry). The preliminary results from this comparison are shown in Table 5.2 below. Considering that only one replicate was performed, the agreement between the ICP-SFMS method and the other methods are acceptable. The agreement between ICP-SFMS and AMS for the ^{242}Pu/^{239}Pu ratio in sample 1 is surprisingly good considering that less than 100 counts were acquired for the ^{242}Pu isotope.

Sample	Technique	$^{240}Pu/^{239}Pu$	SD	N	$^{242}Pu/^{239}P$	SD	n
	ICP-QMS (MCN)	0.1132	0.00097	6			
	ICP-QMS (USN)	0.112	0.0019	6			
1	ICP-QMS (ETV)	0.109	0.0044	6			
	AMS	0.1108	0.0021	5	0.0171	0.0012	1
	ICP-SFMS[a]	0.1011	0.0047[b]	1	0.0176		1
2	**AMS**	0.01585	0.00065	1	< 0.0002		1
	ICP-SFMS[a]	0.0171	0.0007[b]	1	0.002		1

Table 5.2 *Comparison of analytical techniques for Pu isotope ratios measurements. [a]results obtained applying the published ICP-SFMS method. [b]The standard deviation is calculated from counting statistics*

Recently data from another ICP-SFMS method has been presented by Bruneau et al.[121]. The method employed is similar to the ICP-SFMS method described here utilising a Micromass PT2 ICP-SFMS instrument but with pneumatic nebulisation. A reference material (IAEA 135 Intertidal sediment from eastern Irish Sea) has been analysed by both ICP-SFMS methods with results that for both methods are in good agreement with the reference values and results from TIMS and α-spectrometry analysis[121], see Table 5.3. Concentration values are given in Bg/kg dry weight as the average with one standard deviation. The results from this work are the average of four determinations. Isotope ratios are calculated as atom ratios.

Quantity	ICP-SFMS (This work)	ICP-SFMS[a]	TIMS[a]	α-spec[a]	Reference Interval
$^{(239+240)}Pu$	217 ± 7	219 ± 20	222 ± 4	219 ± 2	205 – 221
^{241}Pu	2290 ± 181	2630 ± 256	2610 ± 41	2700 ± 50	2265 – 3015
$^{240}Pu/^{239}Pu$	0.209 ± 0.006	0.218 ± 0.019	0.2083 ± 0.0004	0.198 ± 0.005	

Table 5.3 *Determination of plutonium in IAEA 135. [a]Results from Bruneau et al.[121]*

These data show that the accuracy is good and that the developed method also can be used for the measurement of the ^{241}Pu isotope. Although better figures of merit are probably found by radiometric methods due to the half-life of only 14 years. Together the above results show that the accuracy of the developed ICP-SFMS is excellent even when very low levels of plutonium isotopes are determined.

The experimental precision (%RSD) on the measurement of the $^{240}Pu/^{239}Pu$ ratio was shown to be approximately 2 % in sample solutions containing 2 – 10 pg/ml plutonium. A precision close to the theoretical precision which indicates that the precision is limited mainly by counting statistics. The precision can probably be improved by applying a large number of sweeps or analysing more concentrated sample solutions. Detection limits of 5, 1 and 1 fg/ml for ^{239}Pu, ^{240}Pu and ^{242}Pu were published[II]. The reason for the higher detection limit for ^{239}Pu was carry-

over from samples to blanks, this problem has now been solved applying a wash solution with a nitric acid concentration of 5 % instead of 1%. Detection limits of 0.5, 0.2, 0.1 and 1.5 fg/ml is now found for ^{239}Pu, ^{240}Pu, ^{241}Pu and ^{242}Pu, respectively. The detection limits were determined by analysis of 8 blank solutions performed in between real samples. The average absolute number of counts acquired for the blank solutions are in range of 0.5 to 4. These detection limits are among the best ever published for the measurement for Pu by ICP-MS[98,118,119]. In conclusion it has been shown that ICP-SFMS is a valid technique possessing high sensitivity, excellent accuracy, excellent detection limits and good precision for the measurement of total plutonium and plutonium isotope ratios in environmental samples.

5.2 Ultratrace determination of neptunium

The method described above for the measurement of plutonium has been extended to also measure ^{237}Np. The sample preparation procedure is the same as applied for plutonium. A detection limit of 0.4 fg/ml was found for neptunium, a value similar to that of the plutonium isotopes. The detection limit was determined by measurement of blank solutions analysed in between real samples. The sensitivity for neptunium was $2.5 \cdot 10^9$ counts for 1 µg/ml neptunium. Very few papers have been published on the measurement of neptunium by ICP-MS[97,118,119,121]. One paper by Kim et al.[97] describes a ICP-SFMS method for the measurement of ^{237}Np. They applied a PT1 ICP-SFMS instrument and an ultrasonic nebuliser and found a detection limit of 2 fg/ml and a sensitivity of $1.8 \cdot 10^9$ counts for 1 µg/ml. Figures of merit slightly poorer than those obtained in this study. Bruneau et al.[121] also measured neptunium along with plutonium. Detection limits are not given, but a neptunium content of 0.28 ± 0.03 Bq/kg was reported for the IAEA 135 material, which is somewhat lower than the 0.85 ± 0.04 Bq/kg found in this work. The level of neptunium is not certified in IAEA 135. It is difficult to draw any exact conclusions on the accuracy of the results other than the values found by the two methods are of the same order of magnitude.

Two studies comparing the use of different types of sample introduction systems for the determination of radionuclides by ICP-QMS have been published by Becker et al.[118,119]. They compared the use of a ultrasonic nebuliser, a cross flow nebuliser, a microconcentric nebuliser and a direct injection high efficiency nebuliser. For neptunium the best detection limit (80 fg/ml) was found applying the microconcentric nebuliser, while the best sensitivity ($8.5 \cdot 10^8$ count for 1 µg/ml neptunium) was found applying the ultrasonic nebuliser[119]. Significantly better results were found for the ICP-SFMS instrument applied in this work, demonstrating the very high sensitivity and very low background of the ICP-SFMS technique.

In conclusion ICP-SFMS seems to have been a valid choice for the measurement of neptunium, but still there is a need for further developments and validation.

5.3 Conclusions on the determination of neptunium and plutonium by ICP-SFMS

The levels of plutonium and neptunium in environmental samples are extremely low and more reliable measurements require even more sensitive analytical methods than the ICP-SFMS methods presented above. The possible improvements fall into two groups, improvements of the sample preparation procedure and improvement of the sensitivity of the analytical technique. The sample preparation procedure will only be briefly discussed here, as a detailed discussion is outside the scope of this thesis. The sample preparation procedure used here (and in most other ICP-MS methods) was originally developed for the purpose of producing samples to be analysed by α-spectrometry. The goal therefore was to develop a sample preparation procedure, which matched the demands of α-spectrometry, i.e., a separation from other elements emitting α-particles of similar energies. Also the final sample is deposited on a stainless steel disc for α-spectrometry analysis[124]. The demands set for an ICP-MS analysis is different, that is, the analytes have to be separated from elements interfering on the masses of interest, and the final sample has to be an aqueous solution with a low salt content. Therefore a re-development of the sample preparation procedure specific for ICP-MS analysis might be beneficial. Also improvements of the ICP-SFMS technique should be explored in order to increase the sensitivity. First of all the investigation of different sample introduction systems has to be considered even though USN, which was also used in this study, was found to generate the best sensitivity for ICP-QMS[119]. The sample introduction system is one of the main factors limiting the sensitivity of the ICP-MS technique, since at a maximum (ultrasonic nebuliser) 20 % of the sample solution is transported into the plasma by most sample introduction systems. Another possibility is to use a shielded torch. Maintaining the very low background of the PT2 ICP-SFMS instrument, a 50-fold increase of the sensitivity relative to the normal set-up (concentric nebulisation) has been achieved[61]. Potentially the application of a shielded torch in combination with an ultrasonic nebuliser would significantly increase the sensitivity of the method presented here.

5.4 Measurement of technetium by ICP-SFMS

The fission of ^{235}U and ^{239}Pu produce ^{99}Tc, which is subsequently released into the environment by nuclear fuel reprocessing and nuclear weapons testing primarily. ^{99}Tc is an β-emitter and as such is it traditionally determined by β-ray counting. During the last decade several papers have been published on the measurement of technetium by ICP-MS[102-106,113,116,117]. Using the PT2 ICP-SFMS instrument and an ultrasonic nebulisation the development of a method for the determination of ^{99}Tc is in progress in collaboration with the Nuclear Safety Research and Facilities Department at Risø National Laboratory. The development is still in progress and no final analytical method has

yet been developed. Therefore only a few preliminary results regarding the ICP-SFMS analysis of technetium will be presented.

^{97}Tc is not released into the environment, therefore potentially ^{97}Tc can be used as a yield tracer in the sample preparation process and for quantification by isotope dilution the same way as ^{242}Pu is used in the method described for plutonium[II]. The first step in the method development was therefore measurement of the ^{97}Tc/^{99}Tc ratio. While the mass range above m/z = 235, where the plutonium and neptunium isotopes are found, is almost free from spectral interference, numerous spectral interferences are present on m/z = 97 and m/z = 99. The potential interferences on the two isotopes are shown in Table 5.4.

Isotope	Spectral Interferences
^{97}Tc	$^{97}Mo^{+}$ (260753), $^{38}Ar^{50}Co^{+}$ (9605), $^{40}Ar^{57}Fe^{+}$ (11761), $^{81}Br^{16}O^{+}$ (18683), $^{40}Ar_2{}^{16}OH^{+}$ (4516), $^{194}Pt^{2+}$ (1288)
^{99}Tc	$^{99}Ru^{+}$ (315287), $^{98}RuH^{+}$ (14410), $^{98}MoH^{+}$ (14163), $^{64}Zn^{35}Cl^{+}$ (12000), $^{63}Cu^{36}Ar^{+}$ (10867), $^{62}Ni^{37}Cl^{+}$ (8285), $^{59}Co^{40}Ar^{+}$ (9278), $^{49}Ti^{50}Ti^{+}$ (7285)

Table 5.4 *Potential interferences on ^{97}Tc and ^{99}Tc*

The aim is to measure ultratrace levels of technetium, which requires low mass resolution. Possible interferences therefore must be eliminated during the sample preparation procedure or by the application of mathematical corrections. As for the analysis of molybdenum on m/z = 97 the analysis of technetium is interfered by Ar_2OH^{+}, which cannot be eliminated during the sample preparation, since the interference are formed from Ar, H and O, which are present in the plasma in large amounts. Also a mathematically correction is impossible, since no reliable measurements of $Ar_2{}^{17}OH^{+}$, $Ar_2{}^{18}OH^{+}$ or $Ar_2O^{2}H^{+}$ is possible. The interference can be eliminated using a mass resolution setting of 6000, but at higher mass resolution the sensitivity is dramatically reduced and ultratrace determination of ^{97}Tc becomes impossible. It was therefore concluded that ultratrace analysis of ^{97}Tc is not possible with the instrumentation used in this work. As a consequence no further measurements of ^{97}Tc was conducted. However, there are still possibilities to measure ultratrace levels of ^{97}Tc by ICP-MS, although they are outside the scope of this thesis. The first possibility is the use an ultrasonic nebuliser in conjugation with a membrane desolvater, which almost completely eliminate O and H containing interferences. The second possibility is to use an ICP-CC-MS instrument by which the argon based interferences can be completely eliminated. Wether these two approaches posses sufficient sensitivity and detection limits still have to be investigated.

No spectral interferences were positively identified on m/z = 99, but a significant background signal was found in both blanks and samples. Part of this signal originates form ^{99}Ru, therefore a correction using ^{100}Ru were applied, but still a significant background signal remained, which cannot be accounted for. The unknown interferences are very close to

^{99}Tc in mass since they can not be identified applying a mass resolution setting of 10000. The most obvious interferences from Table 5.4 are $^{98}MoH^+$, $^{64}Zn^{35}Cl^+$ and $^{63}Cu^{36}Ar^+$ even though other studies have shown that these interferences are not significant[113,116]. The work on molybdenum isotopes ratios presented in chapter 4.4 showed that a molybdenum background signal on m/z = 98 was found throughout the work, indicating that a $^{98}MoH^+$ peak at m/z = 99 is possible. But a more thorough investigation of the interferences is needed in order to clarify the interference pattern.

Even though a low background signal could not be obtained ^{99}Tc measurements were performed on standard solutions. A calibration curve for the 0.05 -1.00 pg/ml ^{99}Tc range were determined; $I_{Tc} = 3653 \cdot C_{Tc} + 123$, $r = 0.9999$, where I_{Tc} is the signal and C_{Tc} is the ^{99}Tc concentration in pg/ml. The sensitivity is excellent, that is, $3.7 \cdot 10^9$ counts per µg/ml, which is similar to that of plutonium and neptunium. Also the correlation is excellent. But the presence of a significant background signal affects the detection limit. The limit of detection was calculated from the linear regression using the standard deviation on the estimation of I_{Tc}-values as outlined by Miller and Miller[95]. Applying this approach a detection limit of 16 fg/ml was found. Which compared with the detection limits obtained for plutonium and neptunium below 1 fg/ml it is rather high. The reason for this is the variation on the background signal and the noise induced performing the correction for ^{99}Ru. The detection limit is still among the best ever published for ^{99}Tc with ICP-MS techniques, only surpassed by the 13 fg/ml found by Yamamoto et al.[104] using another ICP-SFMS instrument. Using USN ICP-QMS normally higher detection limits are found. Eroglu et al.[113] reports 30 fg/ml, while Ramebäck et al.[116] reports 450 fg/ml. But it has to be kept in mind that the data presented here are preliminary, not fully validated and that the detection limits in real samples is not known.

The USN ICP-SFMS method developed so far is sensitive and low levels of technetium can be measured, but still some problems need to be solved before the method can be used for reliable and robust measurements of technetium in environmental samples. First of all the background/interference problem must be solved. Secondly a tracer for ^{99}Tc, which can be used as a yield tracer in the sample preparation and for calibration in the detection by ICP-SFMS, would be very helpful in order to achieve sufficient accuracy on the results. In conclusion more developments are needed before ICP-SFMS can be used for robust and reliable determination of ^{99}Tc in environmental samples.

6 Measurement of lead isotope ratios using ICP-SFMS

Lead is probably that element for which the isotope ratios have been measured most frequently using ICP-MS techniques. The reason for this is twofold. First of all that the mass spectrum of the lead isotopes is simple and well defined; only the ^{204}Pb isotope are interfered by ^{204}Hg, while the remaining three isotopes are free of interferences. This makes the lead spectrum and the lead isotope ratios ideal for method development and optimisation, which they have also been used for in this study. Secondly the variation in the isotopic composition of lead in nature is large. The lead isotope ratios are therefore often used to determine the origin of lead pollution. The majority of the papers published on the measurement of lead isotope ratios therefore can be divided into two groups, that is method developments[16,17,32,34-42,50,57,127-130] and applications[131-147]. Among the more spectacular applications are the use of ^{206}Pb/^{207}Pb ratios measured in tree rings as a monitor for environmental changes[145], determination of the origin of medieval swords based on lead isotope ratios[146], and identification of lead from Carthaginian and roman Spanish mines in Greenland ice using the ^{206}Pb/^{207}Pb ratio[139]. Most applications are based on the identification of sources of lead pollution using ^{206}Pb/^{207}Pb ratio measured in sediments or atmospheric particles[132-135,138,142-144,147]. The aim of the work in this thesis was not to develop sensitive ICP-SFMS methods for the measurement of lead isotope ratios, as ICP-SFMS as an analytical technique does not add something new, which cannot be achieved using other analytical techniques such as TIMS, MC-ICP-SFMS, ICP-CC-MS or ICP-QMS. The aim was first of all to use the lead isotope ratios in the development and optimisation of the general procedures. Secondly, to show that lead isotope ratios can be measured in real samples with relative good figures of merit, and therefore used along with the above mentioned techniques.

From the data in Appendix 2, it is seen that the precision on the measurement of lead isotope ratios using ICP-SFMS is close to the theoretical precision if the right scanning mode is chosen, e.g. voltage scanning ($\%RSD_m$ = 0.5 % at 2 ng/ml lead). Increasing the lead concentration to 10 ng/ml in the sample solution a measurement precision of 0.1 – 0.2 % was achieved. A measurement precision below 0.1% as reported by Vanhaecke et al.[54] and Latkoczy et al.[148] for ICP-SFMS methods should therefore be within reach analysing more concentrated sample solutions. Also the accuracy on the measurement of lead isotope ratios are good as shown for the measurement of reference materials in Table 6.1 below.

		$^{204}Pb/^{206}Pb$	$^{207}Pb/^{206}Pb$	$^{208}Pb/^{206}Pb$
NIST 981	Measured	0.0600 ± 0.0004	0.9116 ± 0.0050	2.1903 ± 0.0060
(natural lead)	Certified	0.059042 ± 0.000037	0.91464 ± 0.00033	2.1681±0.0008
NIST 982	Measured	0.0277 ± 0.0002	0.4684 ± 0.0020	1.0171 ± 0.0062
	Certified	0.027219 ± 0.000027	0.46707 ± 0.00020	1.00016 ± 0.00036
Enrich. ^{204}Pb	Measured	5.5446 ± 0.0202	0.4998 ± 0.0050	0.8012 ± 0.0026
(70.94%)	Certified	5.5946 ± 0.0448	0.5063 ± 0.0088	0.7855 ± 0.0100

Table 6.1 *Measurement of lead isotope ratios in reference materials. The results are given as mean ± 2 standard deviation (n = 3)*

The results show that lead isotope ratios can be measured with good accuracy over a broad range of ratio values.

Finally the $^{206}Pb/^{207}Pb$ ratios was measured in Baltic Sea sediments with the purpose of following the changes over time (1879 to 1996) and to show that the ICP-SFMS can be applied for the measurement of lead isotope ratios in environmental samples. Six digested sediment samples from a sediment core from the Baltic Sea was provided by Dr. H. Kunzendorf, Plantbiology and Biogeochemistry Department, Risø National Laboratory. The $^{206}Pb/^{207}Pb$ ratio and the total lead content were measured in the samples. The ratio was measured using voltage scanning, with the acquisition parameters given in Appendix 2. The total lead content was determined in a different run as the sum of all four lead isotopes. The result of the analysis is presented in Figure 6.1. The uncertainty on the ratio measurement is shown as ± 1 standard deviation. The standard deviation is calculated from the assumption that the measurement precision is 0.5 %. From the figure it can be seen that a measurement precision of 0.5 % is sufficient to see the difference in the $^{206}Pb/^{207}Pb$ ratio with time.

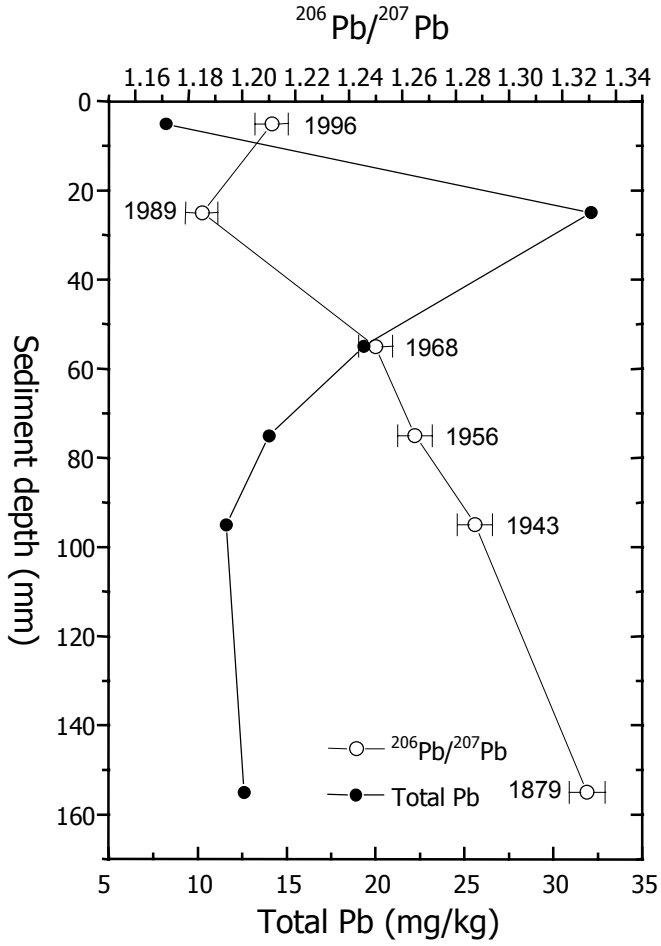

Figure 6.1 *Lead isotope ratios and total lead in sediment*

The lowest ratio and the highest total content was found in the sample from 1989, where the input of lead from gasoline into the environment was high due the use of leaded gasoline. Lead in gasoline (imported lead) has a different isotopic composition (low abundance of ^{206}Pb) than natural occurring lead in the northern part of Europe[133]. The original core was divided into 15 samples of which only 6 so far have been analysed, which makes it possible to obtain a more detailed picture of the change in lead isotope ratios and total lead during time than the one presented here.

In conclusion the above results show that the ICP-SFMS instrument can be used for the measurement of lead isotope ratios with good accuracy and a precision down to 0.1 %, and also that the real analytical problems can be solved using this technique. However, this can, as mentioned, also be achieved with long range of other analytical techniques and as such ICP-SFMS does not posses features that makes it a better choice for the measurement of lead isotope ratios than the other mass spectrometric techniques.

7 Conclusions and suggestions for future research

7.1 Conclusions

The main goal of this thesis was to investigate the potential of the ICP-SFMS technique for the measurement of isotope ratios. In the preceding chapters the development, optimisation and application of ICP-SFMS methods for the measurement of isotope ratios in biological and environmental samples has been described, whereby it has been clearly demonstrated that isotope ratios can be measured using the ICP-SFMS technique with good accuracy and good precision. The investigations led to the following more detailed conclusions:

By applying a high mass resolution setting analyte peaks can be separated from the otherwise interfering spectral interferences, which enables the measurement of isotope ratios of a long range of elements for which the measurement normally is very complex and time-consuming, because a prior matrix separation step is needed before the actual isotope ratio measurement. Another advantage is that the spectral interferences can be positively identified and monitored, which is essential during the method development.

When applying a low mass resolution setting the precision on the measurement of isotope ratios is mainly controlled by counting statistics with absolute values approaching 0.1 % RSD, while a precision of 1-3 times the theoretical precision was obtained when a high mass resolution setting was applied with absolute values generally in the range of 0.3 – 1.0 % RSD.

The main factors limiting the accuracy and precision are mass discrimination, detector dead time, signal noise and choice of acquisition parameters. Best results were obtained applying a rapid scanning alternating between the different isotopes, i.e. a low dwell time (< 10 ms) and many sweeps (> 50). It was also found that the correction for detector dead time affects both accuracy and precision. Therefore it is an advantage that samples is diluted to produce count rates significantly below 10^6 cps, thus no detector dead time correction is needed. No mathematical relationship between mass difference and mass discrimination was found, therefore the correction for mass discrimination was performed using external correction The above findings were used to generate a general procedure for the development of ICP-SFMS methods for the measurement of isotope ratios.
Because of the many sweeps applied a long measurement time of 5 – 10 min per sample solution is necessary in order to accumulate a sufficient number of counts. The main reason for this being that the scanning the magnet is a slow process and that true peak hopping is not possible,

which again prolongs the measurement time, as the hole peak then have to be scanned.

ICP-SFMS methods for the measurements of calcium, zinc, molybdenum and iron isotope ratios in human samples were developed. It has been demonstrated that isotope ratios can be measured with good accuracy and good precision. Spectral interferences can be eliminated, therefore there is no need for a matrix separation step in the sample preparation procedure, making the ICP-SFMS methods for measurement of isotope ratios less time-consuming than corresponding TIMS, FAB-MS and ICP-QMS methods. It was shown that when all isotopes of an element can be measured free of interferences, the total element content can be determined independently of the isotopic composition as the sum of counts for all the isotopes.

The usefulness of ICP-SFMS for the measurement of isotope ratios in samples originating from nutritional tracer experiments was demonstrated by comparison with a radioisotope method and by analysis of human urine and faeces samples enriched with stable isotopes. Also means of optimising the ICP-SFMS and the set-up of nutritional experiments using uncertainty analysis have been investigated, and proved to be a useful way to improve the overall quality of the resulting data.

USN ICP-SFMS methods for the measurement of isotope ratios and ultratrace levels of radionuclides was developed. The figures of merit are excellent, detection limits in the low fg/ml range and sensitivities in the order of 10^9 counts per μg/ml, figures surpassing traditional radiometric methods. However, one limitation is that when applying a low mass resolution all possible interferences have to be eliminated during the sample preparation procedure, which makes the sample preparation is very complex and time-consuming.

The greatest potential of ICP-SFMS in the measurement of isotope ratios lies within the two above-mentioned areas of applications. For the elements of nutritional interest the ICP-SFMS possess sufficient precision and accuracy, at the same time the problem with spectral interferences is solved, isotope ratios and total elements content can be measurement simultaneously, the sample throughput is relatively high and the sample preparation is simple. All in all figures of merit, which is not surpassed by any other analytical technique. The advantage of ICP-SFMS for measurement of radionuclides on the other hand lies in the very low background signals and the high sensitivity in the low mass resolution mode. Very few other analytical techniques have similar detection limits.

In other areas of applications the ICP-SFMS technique does not meet the demands. For example in geochronology, where precision better than 0.05 %RSD is demanded, this cannot be obtained with ICP-SFMS on a routine basis, and other techniques like TIMS and MC-ICP-SFMS should

be preferred. ICP-SFMS can also be used for applications where there is few spectral interferences and where extreme sensitivities are not needed, but other techniques can also be used (e.g. ICP-QMS, ICP-CC-MS or FAB-MS) and often at a lower cost.

7.2 Suggestions for future research

The results of the Ph.D. project provided several ideas for further research to investigate and improve the measurement of isotope ratios using ICP-SFMS. Some of the most important ideas are presented below.

Signal noise is one of the factors limiting the measurement precision. Therefore a further investigation into the different noise components is important. First of all it would be of interest to investigate the significant change of the noise when changing from low to high mass resolution, and an analysis of noise power spectra would be beneficial. Secondly, it is of interest to investigate if the signal noise reduction that can be achieved by the application of a syringe pump system will improve the measurement precision significantly.

Applying ICP-SFMS not only the analyte peaks, but also the spectral interferences can be monitored. Therefore more fundamental studies on the formation of spectral interference are possible and could reveal important and useful results.

It would also be of interest to develop a method for the accurate and precise measurement of the detector dead time, as that would improve the overall accuracy and precision, when concentrated sample solutions are analysed. Alternatively the use of different detector types, which are not affected by dead time, like the Daly detector, should be investigated.

As the precision is partly limited by the sensitivity of the ICP-SFMS instrument both for the measurement of nutritional elements and radioisotopes, an improvement of the precision applying an ultrasonic nebuliser for the nutritional elements and a shielded torch for the radioisotopes, respectively, would be of interest.

Finally, further research into the application of uncertainty analysis for the simultaneously optimisation of both the analytical method and the tracer experiment parameters in human nutrition are of interest, as it would probably improve the overall quality of many data.

8 References

I. Stürup S, Hansen M, Mølgaard C., Measurement of ^{44}Ca:^{43}Ca and ^{42}Ca:^{43}Ca isotopic ratios in urine using HR-ICPMS. *J. Anal. Atom. Spectrom*., 1997, 12, 919-923.

II. Stürup S, Dahlgaard H, Nielsen SC., High Resolution Inductively Coupled Plasma Mass Spectrometry (HR-ICPMS) for Trace Determination of Plutonium Isotopes and Isotope Ratios in Environmental Samples. *J. Anal. Atom. Spectrom*., 1998, 13, 1321-1326.

III. Stürup S., Application of HR-ICPMS for the simoultaneouos measurement of zinc isotope ratios and total zinc content in human samples. *J. Anal. Atom. Spectrom*., 2000, 15, 315-321.

1. Rosman, K.J.R., & Taylor, P.D.P., *Pure & Applied Chemistry*, 1998, 70*,* 217-235.
2. Shukolyukov, A., & Lugmair, G.W., *Science*, 1998, 282, 927-929.
3. Gregoire, D.C., *Analytical Chemistry*, 1987, 59, 2479-2491.
4. Becker, J.S., & Dietze, H.J., *Journal of Analytical Atomic Spectrometry*, 1998, 13, 1057-1063.
5. De Bievre, P., *Advances in Mass Spectrometry*, 1978, 7, 395-447.
6. Cornides, I., Mass spectrometric analysis of inorganic solids - the historical background. In F. Adams, R. Gilbels, & R. Van Greicken (Eds.), *Inorganic mass spectrometry.* (pp. 1-15). New York: John Wiley & Sons, 1988.
7. Solyom, D.A., Burgoyne, T.W., & Hieftje, G.M., *Journal of Analytical Atomic Spectrometry*, 1999, 14, 1101-1110.
8. Thomson, J.J., *Rays of positive electricity and their application to chemical analyses.* London: Longmans Green, 1913.
9. Menegario, A.A., Gine, M.F., Bendassolli, J.A., Bellato, A.C.S., & Trivelin, P.C.O., *Journal of Analytical Atomic Spectrometry*, 1998, 13, 1065-1067.
10. Prohaska, T., Latkoczy, C., & Stingeder, G., *Novel instrumentation for HR-ICP-SMS for precise determination of isotopic ratios in tracer studies*. Book of abstracts, 1999 Winter Conference on Plasma Spectrochemistry, Pau France.
11. Mason, P.R.D., Kaspers, K., & Van Bergen, M.J., *Journal of Analytical Atomic Spectrometry*, 1999, 14, 1067-1074.
12. Turner, P.J., Measurement of isotope ratios using ICP-MS. In G. Holland & A.N. Eaton (Eds.), *Applications of plasma source mass spectrometry II.* (pp. 175-185). Cambridge, The Royal Society of Chemistry, 1993.
13. Crews, H.M., & Mellon, F.A., Mass spectrometry - general considerations. In B. Sandström & F.A. Mellon (Eds.), *Stable isotopes in human nutrition - Inorganic nutrient metabolism.* (pp. 59-60). London: Academic Press, 1996.
14. Kastenmayer, P. , Thermal Ionization Mass Spectrometry (TIMS). In F.A. Mellon & B. Sandström (Eds.), *Stable Isotopes in Human Nutrition, Inorganic Nutrient Metabolism.* London: Academic Press, 1996.
15. Walder, A.J., & Freedman, P.A., *Journal of Analytical Atomic Spectrometry*, 1992, 7, 571-575.
16. Walder, A.J., Platzner, I., & Freedman, P.A., *Journal of Analytical Atomic Spectrometry*, 1993, 8, 19-23.
17. Walder, A.J., & Furuta, N., *Analytical Sciences*, 1993, 9, 675-680.

18. Houk, R.S., Fassel, V.A., Flesch, G.D., Svec, H.J., Gray, A.L., & Taylor, C.E., *Analytical Chemistry*, 1980, 52, 2283-2289.
19. Montaser, A., McLean, J.A., Liu, H., & Mermet, J., An introduction to ICP spectrometers for elemental analysis. In A. Montaser (Ed.), *Inductively coupled plasma mass spectrometry.* (pp. 1-31). New York: Wiley-VCH, 1998.
20. Bamforth, P., Micromass Ltd, Manchester UK, Personal communication, 1999.
21. PlasmaTrace 2, Instrument & Maintenance Manual. *1st ed,* Micromass Ltd, UK, 1996.
22. Johnson, E.G., & Nier, A.O., *Analytical Chemistry*, 1953, 91, 10-17.
23. Van Straaten, M., Ph.D. Thesis. Analytical glow discharge mass spectrometry: physical aspects and applications. University of Antwerpen, 1993.
24. Turner, P.J., Mills, D.J., Schröder, E., Lapitajs, G., Jung, G., Iacone, L.A., Haydar, D.A., & Montaser, A., Instrumentation for low- and high-resolution ICPMS. In A. Montaser (Ed.), *Inductively coupled plasma mass spectrometry.* (pp. 421-501). New York: Wiley-VCH, 1998.
25. Porter, M., Micromass Ltd, Manchester, UK., Personal communication, 1999.
26. Vanhaecke, F., Wannemacker, G., Moens, L., Dams, R., Latkoczy, C., Prohaska, T., & Stingeder, G., *Journal of Analytical Atomic Spectrometry*, 1998, 13, 567-571.
27. Koirtyohann, S.R., *Spectrochimica Acta*, 1994, 49B*,* 1305-1311.
28. Russ, G.P.I., & Bazan, J.M., *Spectrochimica Acta*, 1987, 42B, 49-62.
29. Hamester, M., Wiederin, D.R., Wills, J., Kerl, W., & Douthitt, C.B., *Fresenius Journal of Analytical Chemistry*, 1999, 364*,* 495-497.
30. Taylor, P.D.P., De Bievre, P., Walder, A.J., & Entwistle, A. *Journal of Analytical Atomic Spectrometry*, 1995, 10, 395-398.
31. Kerl, W., Becker, J.S., Dietze, H.J., & Dannecker, W., *Fresenius Journal of Analytical Chemistry*, 1997, 359, 407-409.
32. longerich, H.P., Fryer, B.J., & Strong, D.F., *Spectrochimica Acta*, 1987, 42B, 39-48.
33. Roehl, R., Gomez, J., & Woodhouse, L.R., *Journal of Analytical Atomic Spectrometry*, 1995, 10, 15-23.
34. Begley, I.S., & Sharp, B.L., *Journal of Analytical Atomic Spectrometry*, 1997, 12, 395-402.
35. Ketterer, M.E., Peters, M.J., & Tisdale, P.J., *Journal of Analytical Atomic Spectrometry*, 1991, 6, 439-443.
36. Halicz, L., Erel, Y., & Veron, A., *Atomic Spectroscopy*, 1996, 17, 186-189.
37. Hinners, T.A., Heithmar, E.M., Spittler, T.M., & Henshaw, J.M., *Analytical Chemistry*, 1987, 59, 2658-2662.
38. Campbell, M.J., & Delves, H.T., *Journal of Analytical Atomic Spectrometry*, 1989, 4, 235-236.
39. Quetel, C.R., Thomas, B., Donard, O.F.X., & Grousset, F.E., *Spectrochimica Acta*, 1997, B52*,* 177-187.
40. Yoshinaga, J., *Tohoku J Exp Med*, 1996, 178, 37-47.
41. Woolard, D., Franks, R., & Smith, D.R., *Journal of Analytical Atomic Spectrometry*, 1998, 13, 1015-1019.
42. Gwiazda, R., Woolard, D., & Smith, D., *Journal of Analytical Atomic Spectrometry*, 1998, 13, 1233-1238.
43. Albarede, F., Telouk, P., Toft, J.B., Luais, B., Marechal, C., & Lecuyer, C., *From thermal ionization to plasma source mass spectrometry: a new*

era in isotopic analysis. Book of abstracts, *1999 Winter Conference on Plasma Spectrochemistry*, Pau, France.
44. Douglas, D.J., & Tanner, S.D., Fundamental considerations in ICPMS. In A. Montaser (Ed.), *Inductively coupled plasma mass spectrometry.* (pp. 615-680). New York: Wiley-VCH, 1998.
45. Jakubowski, N., & Stuewer, D., *Reviews on Analytical Chemistry - Euroanalysis VIII*, 1994, 121-144.
46. Moens, L., & Jakubowski, N., *Analytical Chemistry*, 1998, 251A-256A.
47. Allen, L.A., Leach, J.J., & Houk, R.S., *Analytical Chemistry*, 1997, 69, 2384-2391.
48. Burgoyne, T.W., Hieftje, G.M., & Hites, R.A., *Analytical Chemistry*, 1997, 69*,* 485-489.
49. Heumann, K.G., Gallus, S.M., Rädlinger, G., & Vogl, J., *Journal of Analytical Atomic Spectrometry*, 1998, 13, 1001-1008.
50. Delves, H.T., & Campbell, M.J., *Journal of Analytical Atomic Spectrometry*, 1988, 3, 343-348.
51. Alonso, J.I.G., *Analytica Chimica Acta*, 1995, 312, 57-78.
52. Alonso, J.I.G., Camblor, M.G., Bayon, M.M., Marchante-Gayon, J.M., & Sanz-Medel, A., *Journal of Mass Spectrometry*, 1997, 32*,* 556-564.
53. Alonso, J.I.G., Sena, F., Arbore, P., Betti, M., & Koch, L., *Journal of Analytical Atomic Spectrometry*, 1995, 10, 381-393.
54. Vanhaecke, F., Moens, L., Dams, R., & Taylor, P., *Analytical Chemistry*, 1996, 68, 567-569.
55. Friel, J.K., longerich, H.P., & Jackson, S.E., *Biological Trace Element Research*, 1993, 37, 123-136.
56. Begley, I.S., & Sharp, B.L., *Journal of Analytical Atomic Spectrometry*, 1994, 9, 171-176.
57. Furuta, N., *Journal of Analytical Atomic Spectrometry*, 1991, 6, 199-203.
58. Montaser, A., Minnich, M.G., Liu, H., Gustavsson, A.G.T., & Browner, R.F., Fundamental aspects of sample introduction in ICP spectrometry. In A. Montaser (Ed.), *Inductively coupled plasma mass spectrometry.* (pp. 335-420). New York: Wiley-VCH, 1998.
59. Arpe, T., Garbe-Schönberg, C., & Sievers, E., *Determination of major, trace and ultratrace elements inhuman serum and urine with ICP-SFMS*. Book of abstracts. *1998 Winter Conference on Plasma Spectrochemistry*, Scottsdale, Arizona, USA.
60. Nielsen, S.C., Stürup, S., Spliid, H., & Hansen, E.H., *Talanta*, 1999, 49, 1027-1044.
61. Eaton, A.N., & Porter, M., A shielded torch upgrade for plasmaTrace2. *1st ed,* Manchester, UK. Micromass Ltd., 1999.
62. Turnlund, J.R., General introduction. In B. Sandström & F.A. Mellon (Eds.), *Stable Isotopes in human nutrition - inorganic nutrient metabolism.* London: Academic Press, 1996.
63. Ting, B.T.G., & Janghorbani, M., *Journal of Analytical Atomic Spectrometry*, 1988, 3, 325-336.
64. Whittaker, P.G., Lind, T., Williams, J.G., & Gray, A.L., *Analyst*, 1989, 114, 675-678.
65. Ting, B.T.G., Mooers, C.S., & Janghorbani, M., *Analyst*, 1989, 114, 667-674.
66. Schuette, S., Vereault, D., Ting, B.T.G., & Janghorbani, M., *Analyst*, 1988, 113, 1837-1842.
67. Smith, F.G., Wiederin, D.R., Houk, R.S., Egan, C.B., & Serfass, R.E., *Analytica Chimica Acta*, 1991, 248, 229-234.
68. Whittaker, P.G., Barret, J.F.R., & Williams, J.G., *Journal of Analytical Atomic Spectrometry*, 1992, 7, 109-113.

69. Lyon, T.D.B., & Fell, G.S., *Journal of Analytical Atomic Spectrometry*, 1990, 5, 135-137.
70. Durrant, S.F., Krushevska, A., Amarasiriwardena, D., Argentine, M.D., Romon-Guesnier, S., & Barnes, R.M., *Journal of Analytical Atomic Spectrometry*, 1994, 9, 199-204.
71. Woodhouse, L.R., Morgan, P.N., & King, J.C., *Inductively coupled plasma mass spectrometry analysis of zinc stable isotopes in urine to determine dietary zinc absorption*, Book of abstracts, *1994 Winter Conference of Plasma Spectrochemistry*, San Diego, California, USA.
72. Amarasiriwardena, C.J., Krushevska, A., Foner, H., Argentine, M.D., & Barnes, R.M., *Journal of Analytical Atomic Spectrometry*, 1992, 7, 915-921.
73. Serfass, R.E., Thompson, J.J., & Houk, R.S., *Analytica Chimica Acta*, 1986, 188, 73-84.
74. Buckley, W.T., Budac, J.J., Godfrey, D.V., & Koenig, K.M., *Biological Mass Spectrometry*, 1992, 21, 473-478.
75. Ting, B.T.G., & Janghorbani, M., *Spectrochimica Acta*, 1987, 42B, 21-27.
76. Janghorbani, M., & Ting, B.T.G., *J Nut Biochem*, 1990, 1, 19.
77. Janghorbani, M., & Ting, B.T.G., *Analytical Chemistry*, 1989, 61, 701-708.
78. Barnes, R.M., *Analytica Chimica Acta*, 1993, 283, 115-130.
79. Application note, *Practical considerations for rapid scanning with the high resolution ICP-MS, 1st ed,* Micromass Ltd*,* Manchester, UK.
80. Crews, H.M., Luten, J.B., & McGaw, B.A., Inductively coupled plasma mass spectroemtry (ICP-MS). In B. Sandström & F.A. Mellon (Eds.), *Stable isotopes in human nutrition - inorganic nutrient metabolism.* (pp. 97-115). London: Academic Press, 1996.
81. Vanhaecke, F., Moens, L., Dams, R., Papadakis, I., & Taylor, P., *Analytical Chemistry*, 1997, 69, 268-273.
82. Hansen, M., Stürup, S., M¢lgaard, C., Jensen, M., Sörensen, S.S., & Sandström, B., Submitted for publication 1999.
83. Yergey, A.L., Vieira, N.E., & Covell, D.G., *Biomedical and Environmental Mass Spectrometry*, 1987, 14, 603-607.
84. Williams, A., De Halleux, B., Diamondstone, B., Ellison, S., Haesselbarth, W., Kaarls, R., Mansson, M., M¢ller, H., Taylor, P., Thomas, B., Wegschneider, W., & Wood, R., *Quantifying uncertainty in analytical measurement.* Eurochem., 1995.
85. Hansen, M., Stürup, S., & Sandström, B., *The influence of dietary fat on clacium absorption*. Book of abstracts, *Experimental Biology*, 1998.
86. Thompson, M., & Fearn, T., *Analyst*, 1996, 121, 275-278.
87. Van Dokkum, W., Fairweather-Tait, S., Hurrel, R., & Sandström, B., Study Techniques. In F.A. Mellon & B. Sandström (Eds.), *Stable Isotopes in Human Nutrition, Inorganic Nutrient Metabolism.* (pp. 23-42). London: Academic Press, 1996.
88. Caroli, S., Alimonti, A., Coni, E., Petrucci, F., Senofonte, O., & Violante, N., *Critical reviews in Analytical Chemistry*, 1994, 24, 363-398.
89. Soltani-Neshan, M.A., Garbe-Schönberg, C., Dörner, K., & Schaub, J., *Isotopenpraxis*, 1992, 28, 101-106.
90. Soltani-Neshan, M.A., Garbe-Schönberg, C., Dörner, K., & Schaub, J., *Akute und chronische toxiz Spurenelem*, 1993, 61-64.
91. Turnlund, J.R., Keyes, W.R., & Peiffer, G.L., *Analytical Chemistry*, 1993, 65, 1717-1722.
92. Sandström, B., Overview of isotope methods and inorganic nutrient metabolism. In F.A. Mellon & B. Sandström (Eds.), *Stable Isotopes in*

Human Nutrition, Inorganic Nutrient Metabolism. (pp. 3-9). London: Academic Press, 1996.
93. MacTaggart, D.L., & Farwell, S.O., *Journal of AOAC International*, 1992, 75, 594-608.
94. MacTaggart, D.L., & Farwell, S.O., *Journal of AOAC International*, 1992, 75, 608-614.
95. Miller, J.C., & Miller, J.N., *Statistics for analytical chemistry.* New York: Ellis Horwood, 1993.
96. Kastenmayer, P., Davidsson, L., Galan, P., Cherouvrier, F., Hercberg, S., & Hurrel, R.F., *British Journal of Nutrition*, 1994, 71, 411-424.
97. Kim, C., Seki, R., Morita, S., Yamasaki, S., Tsumura, A., Takadu, Y., Igarashi, Y., & Yamamoto, M., *Journal of Analytical Atomic Spectrometry*, 1991, 6, 205-209.
98. Chiappini, R., Taillade, J., & Brebion, S., *Journal of Analytical Atomic Spectrometry*, 1996, 11, 497-503.
99. Aldstadt, J.H., Kuo, J.M., Smith, L.L., & Erickson, M.D., *Analytica Chimica Acta*, 1996, 319, 135-143.
100. Allain, P., Berre, S., Premel-Cabic, A., Mauras, Y., Delaporte, T., & Cournot, A., *Analytica Chimica Acta*, 1991, 251, 183-185.
101. Alonso, J.I.G., Thoby-Schultzendorff, D., Giovanonne, B., Koch, L., & Wiesmann, H., *Journal of Analytical Atomic Spectrometry*, 1993, 8, 673-679.
102. Beals, D.M., *Journal of Radioanalytical and Nuclear Chemistry*, 1996, 204, 253-263.
103. Momoshima, N., Sayad, M., & Takashima, Y., *Radiochimica Acta*, 1993, 63, 73-78.
104. Yamamoto, M., Yarbaini, S., Kofuji, K., Tsumura, A., Komura, K., Ueno, K., & Assinder, D.J., *Journal of Radioanalytical and Nuclear Chemistry*,1995, 197, 185-194.
105. Tagami, K., & Uchida, S., *Journal of Radioanalytical and Nuclear Chemistry*, 1995, 197, 409-416.
106. Momoshima, N., Sayad, M., & Takashima, Y., *Journal of Radioanalytical and Nuclear Chemistry*, 1995, 197, 245-251.
107. Wildner, H., & Hearn, R., *Fresenius Journal of Analytical Chemistry*, 1998, 360, 800-803.
108. Manninen, P.K.G., *Journal of Radioanalytical and Nuclear Chemistry*, 1995, 201, 71-80.
109. Momoshima, N., Kakiuchi, H., Maeda, Y., Hirai, E., & Ono, T., *Journal of Radioanalytical and Nuclear Chemistry*, 1997, 221, 213-217.
110. Jerome, S.M., Smith, D., Woods, M.J., & Woods, S.A., *Appl Radiat Isot*, 1995, 46, 1145-1150.
111. Kershaw, P.J., Sampson, K.E., McCarthy, W., & Scott, R.D., *Journal of Radioanalytical and Nuclear Chemistry*, 1995, 198, 113-124.
112. Kim, C., Oura, Y., Takaku, Y., Nitta, H., Igarashi, Y., & Ikeda, N., *Journal of Radioanalytical and Nuclear Chemistry*, 1989, 136, 353-362.
113. Eroglu, A.E., McLeod, C.W., Leonard, K.S., & McCubbin, D., *Journal of Analytical Atomic Spectrometry*, 1998, 13, 875-878.
114. Wyse, E.J., MacLellan, J.A., Lindenmeier, C.W., Bramson, J.P., & Koppenaal, D.W., *Journal of Radioanalytical and Nuclear Chemistry*, 1998, 234, 165-170.
115. Platzner, T., Becker, J.S., & Dietze, H.J., *Atomic Spectroscopy*, 1999, 20, 6-12.
116. Ramebäck, H., Albinsson, Y., Skålberg, M., & Eklund, U.B., *Fresenius Journal of Analytical Chemistry*, 1998, 362, 391-394.
117. Uchida, S., & Tagami, K., *Analytica Chimica Acta*, 1997, 357, 1-3.

118. Becker, J.S., Dietze, H.J., McLean, J.A., & Montaser, A., *Analytical Chemistry*, 1999, 71, 3077-3084.
119. Becker, J.S., Soman, R.S., Sutton, K.L., Caruso, J.A., & Dietze, H.J., *Journal of Analytical Atomic Spectrometry*, 1999, 14, 933-937.
120. Becker, J.S., & Dietze, H.J., *Fresenius Journal of Analytical Chemistry*, 1999, 364, 482-488.
121. Bruneau, F., Garraud, H., Boust, D., & Donard, O.F.X., *Simultaneous measurement of ^{239}Pu, ^{240}Pu, ^{241}Pu, ^{242}Pu and ^{237}Np by high resolution inductively coupled plasma mass spectrometer (HR-ICPMS) in marine sediments*. Book of abstracts, *1999 Winter Conference on Plasmaspectrochemistry*, Pau, France.
122. Rosenberg, R.J., *Journal of Radioanalytical and Nuclear Chemistry*, 1993, 171, 465-482.
123. Mitchell, P.I., Leon Vintro, L., Dahlgaard, H., Gasco, C., & Sanchez-Cabeza, J.A., *The Science of the Total Environment*, 1997, 202, 147-153.
124. Chen, Q., Aarkrog, A., Nielsen, S.P., Dahlgaard, H., Nies, H., Yu, Y., & Mandrup, K. *Journal of Radioanalytical and Nuclear Chemistry*, 1993, 172, 281-288.
125. Dahlgaard, H., Chen, Q.J., Stürup, S., Eroksson, M., & Nielsen, S.P., *Plutonium isotope ratios in environmental samples from thule (Greenland) and the Techa river (Russia) measured by ICPMS and alpha-spectrometry*. Book of abstracts, *IAEA marine pollution meeting in Monaco*, 1998.
126. Dahlgaard, H., Nuclear Safety Research and Facilities Department, Risø National Laboratory, Personal communication, 1999.
127. Halicz, L., Lam, J.W.H., & McLaren, J.W., *Spectrochimica Acta*, 1994, 49B, 637-647.
128. Gelinas, Y., & Schmit, J., *Environmental Science & Technology*, 1997, 31, 1968-1972.
129. Charles, J.L., III., *Journal of Analytical Atomic Spectrometry*, 1994, 9, 599-603.
130. Cocherie, A., Negrel, P., Roy, S., & Guerrot, C., *Journal of Analytical Atomic Spectrometry*, 1998, 13, 1069-1073.
131. Hurst, R.W., Davis, T.E., & Chinn, B.D., *Environmental Science & Technology*, 1996, 30, 304A-307A.
132. Bacon, J.R., Jones, K.C., McGarth, S.P., & Johnston, A.E., *Environmental Science & Technology*, 1996, 30, 2511-2518.
133. Farmer, J.G., Eades, L.J., Mackenzie, A.B., Kirika, A., & Bailey-Watts, T.E., A.D. *Environmental Science & Technology*, 1996, 30, 3080-3083.
134. Moor, H.C., Schaller, T., & Sturm, M., *Environmental Science & Technology*, 1996, 30, 2928-2933.
135. Kersten, M., Garbe-Schönberg, C., Thomsen, S., Anagnostou, C., & Sioulas, A., *Environmental Science & Technology*, 1997, 31, 1295-1301.
136. Viczian, M., Lasztity, A., & Barnes, R.M., *Journal of Analytical Atomic Spectrometry*, 1990, 5, 293-300.
137. Augagneur, S., Medina, B., & Grousset, F., *Fresenius Journal of Analytical Chemistry*, 1997, 357, 1149-1152.
138. Monna, F., Lancelot, J., Croudace, I.W., Cundy, A.B., & Lewis, J.T., *Environmental Science & Technology*, 1997, 31, 2277-2286.
139. Rosman, K.J.R., Chisholm, W., Hong, S., Candelone, J., & Boutron, C.F., *Environmental Science & Technology*, 1997, 31, 3413-3416.
140. Gulson, B.L., Mizon, K.J., Law, A.J., Korsch, M.J., Davis, J.J., & Howarth, D., *Economic Geology*, 1994, 89, 889-908.
141. Hall, E.S., & Murphy, E., *Journal of Radioanalytical and Nuclear Chemistry*, 1993, 175, 129-138.

142. Veron, A., Flament, P., Bertho, M.L., Alleman, L., Flegal, R., & Hamelin, B., *Atmospheric Environment*, 1999, 33, 3377-3388.
143. Åberg, G., Pacyna, J.M., Stray, H., & Skjelkvåle, B.L., *Atmospheric Environment*, 1999, 33, 3335-3344.
144. Weiss, D., Shotyk, W., Appleby, P.G., Kramers, J.D., & Cheburkin, A.K., *Environmental Science & Technology*, 1999, 33, 1340-1352.
145. Watmough, S.A., Hughes, R.J., & Hutchinson, T.C., *Environmental Science & Technology*, 1999, 33, 670-673.
146. Alonso, J.I.G., Encinar, J.R., Martinez, J.A., & Criado, A.J. (1999). *Spectroscopy Europe*, *11,* 10-14.
147. Krause, P., Kriews, M., Dannecker, W., Garbe-Schönberg, C., & Kersten, M., *Fresenius Journal of Analytical Chemistry*, 1999, 347, 324-329.
148. Latkoczy, C., Prohaska, T., Stingeder, G., & Teschler-Nicola, M., *Journal of Analytical Atomic Spectrometry*, 1998, 13, 561-566.

Appendix 1: Peak hopping with the PT2 ICP-SFMS instrument

The accuracy and precision of peak hopping was evaluated by the analysis of a 10 ng/ml Pb standard solution. The standard solution contained no mercury, therefore no spectral interferences were seen in the spectra. The counts rates were all well below 10^6 counts per second, no detector dead time correction was therefore applied. Before the experiments were started the instrument was carefully mass calibrated. The simultaneous magnetic and voltage scanning mode (sprint) was used for all 4 analysis sequences, only the number of peak widths was varied, which controls the number of points acquired for each peak. Peak widths of 1.7, 0.5, 0.3 and 0.15 were applied, corresponding to a full peak, 5, 3 and 1 points per peak, respectively. In each analysis sequence five replicates were performed. The following acquisition parameters were applied.

Acquisition parameters	
Mass range	202 – 208
Runs	5
Sweeps	600
Mass resolution	400
Dwell time	0.5 ms
Small jump settle time	0
Large jump settle time	10 ms
High hysteresis time	10000 µs
Low hysteresis time	10000 µs
Peak widths	1.7, 0.5, 0.3, 0.15

In the following 4 tables the experimental data is given.

Experimental data					**Isotope ratios**			
Run	^{204}Pb	^{206}Pb	^{207}Pb	^{208}Pb		^{204}Pb/^{206}Pb	^{207}Pb/^{206}Pb	^{208}Pb/^{206}Pb
1	58574	1138087	903252	2460344		0.0515	0.7937	2.1618
2	56918	1101468	873665	2384455		0.0517	0.7932	2.1648
3	57594	1118265	887705	2414564		0.0515	0.7938	2.1592
4	54766	1069863	847272	2308750		0.0512	0.7919	2.1580
5	56367	1102385	872552	2383309		0.0511	0.7915	2.1620
$\overline{X}$	56843	1106014	876889	2390284	$\overline{X}$	0.0514	0.7928	2.1612
					SD	0.0002	0.0010	0.0027
					%RSD	0.44	0.13	0.12
					R_p	1.02	0.93	1.00

Table 1.1 *Full peak scanned*

Experimental data					Isotope ratios			
Run	^{204}Pb	^{206}Pb	^{207}Pb	^{208}Pb		^{204}Pb/^{206}Pb	^{207}Pb/^{206}Pb	^{208}Pb/^{206}Pb
1	77407	1479633	1143588	2974377		0.0523	0.7729	2.0102
2	77541	1480466	1140458	2966807		0.0524	0.7703	2.0040
3	72257	1380094	1068389	2772147		0.0524	0.7741	2.0087
4	73450	1402643	1080473	2813678		0.0524	0.7703	2.0060
5	72588	1398955	1081957	2808260		0.0519	0.7734	2.0074
$\overline{X}$	74649	1428358	1102973	2867054	$\overline{X}$	0.0523	0.7722	2.0072
					SD	0.0002	0.0018	0.0024
					%RSD	0.40	0.23	0.12
					R_p	1.05	1.77	1.20

Table 1.2 *5 Points per peak*

Experimental data					Isotope ratios			
Run	^{204}Pb	^{206}Pb	^{207}Pb	^{208}Pb		^{204}Pb/^{206}Pb	^{207}Pb/^{206}Pb	^{208}Pb/^{206}Pb
1	73895	1436004	1133522	2849353		0.0515	0.7894	1.9842
2	73707	1433029	1131275	2843994		0.0514	0.7894	1.9846
3	77435	1514108	1191602	3003110		0.0511	0.7870	1.9834
4	74934	1453278	1149175	2882524		0.0516	0.7907	1.9835
5	73951	1425549	1124242	2839402		0.0519	0.7886	1.9918
$\overline{X}$	74784	1452394	1145963	2883677	$\overline{X}$	0.0515	0.7890	1.9855
					SD	0.0003	0.0014	0.0036
					%RSD	0.51	0.17	0.18
					R_p	1.38	1.45	1.79

Table 1.3 *3 Points per peak*

Experimental data					Isotope ratios			
Run	^{204}Pb	^{206}Pb	^{207}Pb	^{208}Pb		^{204}Pb/^{206}Pb	^{207}Pb/^{206}Pb	^{208}Pb/^{206}Pb
1	75692	1480192	1179079	2932251		0.0511	0.7966	1.9810
2	76147	1492129	1187423	2952487		0.0510	0.7958	1.9787
3	81591	1592239	1266158	3145820		0.0512	0.7952	1.9757
4	76269	1492054	1189965	2955363		0.0511	0.7975	1.9807
5	77246	1506938	1197687	2978726		0.0513	0.7948	1.9767
$\overline{X}$	77389	1512710	1204062	2992929	$\overline{X}$	0.0512	0.7960	1.9786
					SD	0.0001	0.0011	0.0024
					%RSD	0.18	0.14	0.12
					R_p	0.50	1.17	1.20

Table 1.4 *1 points per peak*

Changing the scanning from a full peak to a small number of points the total number of counts acquired increases as expected, since all measurement time is spend at the top of the peak, when only a few points per peak are used. When the full peak is scanned the precision approaches the theoretical precision $R_p \approx 1$, while R_p values are greater than 1, when only a few point per peak are acquired. The reason is probably that the peak profiles are not truly flat-topped and vary with time, which induce noise on the signals. If the jumping between peaks is not very accurate and peaks are not truly flat-topped noise will increase, since the measurement in not taken in the exact same point every time. Furthermore, the absolute value of the ^{208}Pb/^{206}Pb ratio decreases as the peak widths are narrowed, indicating that the peak profile has an

influence on the measurement. This is probably because the measurement is not taken at the true peak top leading to an erroneously low number of counts acquired for ^{208}Pb. This finding is confirmed by the fact that the ^{204}Pb, ^{206}Pb and ^{207}Pb signals increase by 27 % going from full peaks scanning to 1 point per peak, while only 20 % increase is seen for ^{208}Pb. In conclusion, the best results in terms of precision and accuracy are obtained when the full peak is scanned even though the absolute number of counts acquired are reduced by approximately 25 %.

Appendix 2: Experimental evaluation of scanning rates

Five different whole peak scanning modes were evaluated for the measurement of lead isotope ratios in a 2 µg/l nitric acid solution of CRM 981 (common lead isotopic standard). This concentration was chosen, since counts rate then are well below 10^6 counts per second, and detector dead time then does not have a significant impact on the measurements. The five different modes being magnetic scanning, voltages scanning, combined and simultaneous magnetic and voltage scanning. For the combined magnetic and voltage scanning two different dwell times were applied a short (5 ms) and a long (250 ms) in order to check if a long dwell time can be applied to cancel out the noise in a similar to the application of many successive scan does it. The five different scanning modes were set up to measure an equal amount of ions of the individual isotopes in order to make a comparison of the results more straightforward. The exception being that with combined scanning a longer dwell time was used for ^{204}Pb the isotope of lowest abundance. In the following chapters the experimental details are given.

The results are discussed in the chapter 3.3.2.

Magnetic scanning:

Acquisition parameters	
Mass range	204 – 208
Point/peak width	15
Sweeps	50
Mass resolution	400
Dwell time	5 ms
Small jump settle time	1 ms
Large jump settle time	100 ms
High hysteresis time	10000 µs
Low hysteresis time	5000 µs
Measurement time	190 s
Replicates	10

Experimental data					**Isotope ratios**			
Run	^{204}Pb	^{206}Pb	^{207}Pb	^{208}Pb		^{204}Pb/^{206}Pb	^{207}Pb/^{206}Pb	^{208}Pb/^{206}Pb
1	5961	100044	91788	218692		0.0596	0.917	2.186
2	6210	100087	90851	218494		0.0620	0.908	2.183
3	6288	100275	92038	218498		0.0627	0.918	2.179
4	6054	99532	91373	217298		0.0608	0.918	2.183
5	6181	99765	92105	219176		0.0620	0.923	2.197
6	6230	100391	91696	218229		0.0621	0.913	2.174
7	6257	101977	93225	219946		0.0614	0.914	2.157
8	6248	101994	93284	222344		0.0613	0.915	2.180
9	5944	100913	92307	219819		0.0589	0.915	2.178
10	6175	100962	92856	218680		0.0612	0.920	2.166
$\overline{X}$	6155	100594	92152	219118	$\overline{X}$	0.0612	0.916	2.178
					SD	0.0012	0.004	0.011
					%RSD	1.91	0.46	0.51
					R_p	1.46	1.00	1.29
					CRM	0.059042	0.91464	2.1681
					f_{md}	0.965	0.998	0.995

Table 2.1 *Magnetic scanning*

Voltage scanning:

Acquisition parameters	
Mass range	206 – 208
Point/peak width	15
Sweeps	50
Mass resolution	400
Dwell time	5 ms
Small jump settle time	0 ms
Large jump settle time	100 ms
High hysteresis time	10000 µs
Low hysteresis time	5000 µs
Measurement time	150 s
Replicates	10

Experimental data				**Isotope ratios**			
Run	^{204}Pb	^{206}Pb	^{207}Pb	^{208}Pb		^{204}Pb/^{206}Pb	^{207}Pb/^{206}Pb	^{208}Pb/^{206}Pb
1		92487	84937	192805			0.918	2.085
2		92796	84481	192980			0.910	2.080
3		93267	84920	193889			0.911	2.079
4		92556	85119	192751			0.920	2.083
5		92504	84242	192898			0.911	2.085
6		93298	85582	192970			0.917	2.068
7		93210	84546	193132			0.907	2.072
8		94155	85990	194727			0.913	2.068
9		94373	86015	194427			0.911	2.060
10		93638	85348	193849			0.911	2.070
$\overline{X}$		93228	85118	193443	$\overline{X}$		0.913	2.075
					SD		0.004	0.008
					%RSD		0.45	0.40
					R_p		0.94	0.98
					CRM	0.059042	0.91464	2.1681
					f_{md}		1.002	1.045

Table 2.2 *Voltage scanning*

Combined magnetic and voltage scanning (5 ms):

Acquisition parameters	
Masses	204, 206, 207, 208
Peak widths	3
Point/peak width	15
Sweeps	50
Mass resolution	400
Dwell time	5 ms 25 ms on ^{204}Pb
Small jump settle time	1 ms
Large jump settle time	100 ms
High hysteresis time	10000 µs
Low hysteresis time	5000 µs
Measurement time	275 s
Replicates	10

Experimental data					**Isotope ratios**			
Run	^{204}Pb	^{206}Pb	^{207}Pb	^{208}Pb		^{204}Pb/^{206}Pb	^{207}Pb/^{206}Pb	^{208}Pb/^{206}Pb
1	29436	97685	89040	212689		0.0603	0.912	2.177
2	29200	96249	88262	209864		0.0607	0.917	2.180
3	28671	93733	86425	205102		0.0612	0.922	2.188
4	28640	94773	86578	205389		0.0604	0.914	2.167
5	29123	94461	86913	207246		0.0617	0.920	2.194
6	28422	94599	86009	205120		0.0601	0.909	2.168
7	27828	91760	84192	199797		0.0607	0.918	2.177
8	28176	92349	85099	201417		0.0610	0.921	2.181
9	28034	91124	84098	200356		0.0615	0.923	2.199
10	28159	90528	83588	198860		0.0622	0.923	2.197
$\overline{X}$	28569	93726	86020	204584	$\overline{X}$	0.0610	0.918	2.183
					SD	0.0007	0.005	0.011
					%RSD	1.11	0.55	0.51
					R_p	1.64	1.16	1.26
					CRM	0.059042	0.91464	2.1681
					f_{md}	0.968	0.996	0.993

Table 2.3 *Combined scanning, low dwell time*

Combined magnetic and voltage scanning (250 ms):

Acquisition parameters	
Masses	204, 206, 207, 208
Peak widths	3
Point/peak width	15
Sweeps	1
Mass resolution	400
Dwell time	250 ms 1250 ms on ^{204}Pb
Small jump settle time	1 ms
Large jump settle time	100 ms
High hysteresis time	10000 µs
Low hysteresis time	5000 µs
Measurement time	65 s
Replicates	10

Experimental data					**Isotope ratios**			
Run	^{204}Pb	^{206}Pb	^{207}Pb	^{208}Pb		^{204}Pb/^{206}Pb	^{207}Pb/^{206}Pb	^{208}Pb/^{206}Pb
1	27796	90790	83303	195811		0.0612	0.918	2.157
2	27284	90017	83186	193006		0.0606	0.924	2.144
3	27280	90611	82324	201566		0.0602	0.909	2.225
4	27721	90159	83820	194744		0.0615	0.930	2.160
5	28313	90642	83117	199114		0.0625	0.917	2.197
6	27665	91248	84453	200531		0.0606	0.926	2.198
7	27694	89941	82065	200148		0.0616	0.912	2.225
8	27751	91738	83400	192967		0.0605	0.909	2.103
9	27883	89658	80566	193246		0.0622	0.899	2.155
10	27766	90614	83511	196689		0.0613	0.922	2.171
$\overline{X}$	27715	90542	82975	196782	$\overline{X}$	0.0612	0.916	2.173
					SD	0.0007	0.009	0.038
					%RSD	1.21	1.03	1.75
					R_p	1.77	2.14	4.22
					CRM	0.059042	0.91464	2.1681
					f_{md}	0.964	0.998	0.998

Table 2.4 *Combined scanning, long dwell time*

Simultaneously magnetic and voltage scanning (Sprint):

Acquisition parameters	
Mass range	204-208
Peak widths	2
Point/peak width	15
Sweeps	500
Mass resolution	400
Dwell time	0.5 ms
Small jump settle time	0 ms
Large jump settle time	10 ms
High hysteresis time	10000 µs
Low hysteresis time	5000 µs
Measurement time	90 s
Replicates	10

Experimental data					**Isotope ratios**			
Run	^{204}Pb	^{206}Pb	^{207}Pb	^{208}Pb		^{204}Pb/^{206}Pb	^{207}Pb/^{206}Pb	^{208}Pb/^{206}Pb
1	6184	101070	92997	235224		0.0612	0.920	2.327
2	6007	101777	92303	234551		0.0590	0.907	2.305
3	5929	101066	91873	233073		0.0587	0.909	2.306
4	6078	101058	91981	235259		0.0601	0.910	2.328
5	6051	100871	91772	233532		0.0600	0.910	2.315
6	6196	101466	92260	234048		0.0611	0.909	2.307
7	6220	102398	92604	237012		0.0607	0.904	2.315
8	6185	102264	93224	236195		0.0605	0.912	2.310
9	6107	101907	92629	237049		0.0599	0.909	2.326
10	6151	102975	94885	238738		0.0597	0.921	2.318
$\overline{X}$	6111	101685	92653	235468	$\overline{X}$	0.0601	0.911	2.316
					SD	0.0008	0.005	0.009
					%RSD	1.37	0.60	0.39
					R_p	1.04	1.31	1.01
					CRM	0.059042	0.91464	2.1681
					f_{md}	0.982	1.004	0.936

Table 2.5 *Simultaneous scanning*

Appendix 3: Mass discrimination factors

In the table below the observed mass discrimination factors for the iron, zinc and lead isotope ratios are shown. The f_{md} values were determined over 8 days for iron, 4 for zinc and 3 for lead. The isotope ratios for the different elements were not determined on the same day.

Ratio	Day 1	Day 2	Day 3	Day 4	Day 5	Day 6	Day 7	Day 8
$^{54}Fe/^{56}Fe$	0.9985	1.0028	1.0038	0.9921	0.9963	0.9993	0.9936	1.0025
$^{56}Fe/^{57}Fe$	0.9843	0.9808	0.9836	0.9910	1.0062	1.0000	0.9925	0.9883
$^{64}Zn/^{66}Zn$	0.9991	0.9867	1.0022	0.9847				
$^{66}Zn/^{67}Zn$	0.9945	0.9912	1.0014	0.9905				
$^{66}Zn/^{68}Zn$	0.9967	0.9973	0.9960	0.9984				
$^{66}Zn/^{70}Zn$	1.0090	0.9989	1.0101	0.9996				
$^{204}Pb/^{206}Pb$	0.9840	0.9826	1.0090					
$^{206}Pb/^{207}Pb$	0.9967	1.0028	0.9872					
$^{206}Pb/^{208}Pb$	1.0102	1.0170	1.0200					

Table 3.1 *f_{md} values for the PT2 ICP-SFMS instrument*

All f_{md} values are in the range of 0.98 – 1.02, indicating that the absolute mass discrimination at all times is below 2 %, both positive and negative biases are seen. For a particular isotope ratio the magnitude of f_{md} varies between days and for most ratios values both below and above 1 are found. No pattern can be found in any day that indicates a mathematical relationship between Δm and f_{md}. The fact that both values above and below 1 are found on the same day indicates that the mass discrimination processes acting in opposite directions are almost cancelled out, so possibly the remaining variation seen reflects small changes in the mass discrimination processes or merely noise on the signals. Also, no trend indicates that the mass discrimination is larger for the low mass elements than for the heavy elements. Also 1-2 % mass discrimination was found for the calcium isotope ratios[I]. For a more detailed discussion on mass discrimination seen chapter 3.3.

Appendix 4:

Correction for mass discrimination on iron isotope ratios

Mathematical and external corrections for mass discrimination were compared through the determination of iron isotope ratios in faecal sample solutions. The iron isotope ratios ($^{54}Fe/^{56}Fe$ and $^{56}Fe/^{57}Fe$) were measured in accordance with the method described in chapter 4.5. The measurements were performed over two days. From the $^{54}Fe/^{56}Fe$ ratios measured in four 30 ng/ml iron standards analysed on the first day ε_{lin}, ε_{pow} and ε_{exp} were calculated. The ε values were then used to calculate the corrected $^{56}Fe/^{57}Fe$ ratios measured in the same standards solutions. The results obtained using the power law correction were slightly better than the others, see Table 4.1. The power law correction was therefore applied to correct the iron isotope ratios measured in faecal sample solutions. These results are shown in Table 4.2 and 4.3.

Std.	^{54}Fe	^{56}Fe	^{57}Fe	$^{54}Fe/^{56}Fe$	$(^{56}Fe/^{57}Fe)_{lin}$	$(^{56}Fe/^{57}Fe)_{pow}$	$(^{56}Fe/^{57}Fe)_{exp}$
1	55604	890586	20836	0.0624	43.7226	43.7170	43.7226
2	61241	978744	23067	0.0626	43.4032	43.3977	43.4032
3	57282	927655	21590	0.0617	43.9519	43.9463	43.9519
4	55911	896960	20762	0.0623	44.1924	44.1868	44.1924
		Average		0.0623	43.8175	43.8120	43.8175
		True		0.0637	43.3006	43.3006	43.3006
		f_{md}		1.0229	0.9882	0.9883	0.9882
		ε_{lin}		0.0115			
		ε_{pow}		0.0114			
		ε_{exp}		0.0113			

Table 4.1 *Mathematically correction for mass discrimination*

The determined ε_{pow} value was then used to correct the iron isotope ratios measured over two days, on the first day 10 faecal sample solutions were analysed, and 5 sample solutions were analysed on the second day. The following results were obtained.

	Day 1		Day 1	
	$^{54}Fe/^{56}Fe$	$^{56}Fe/^{57}Fe$	$^{54}Fe/^{56}Fe$	$^{56}Fe/^{57}Fe$
$Ratio_{corr}$	0.0638	42.8629	0.0645	43.4592
True	0.0637	43.3006	0.0637	43.3006
f_{md}	0.999	1.010	0.987	0.996

Table 4.2 *Faecal samples mathematical correction*

The same results were also corrected using the external correction. The observed isotope ratios were corrected using the average observed isotope ratio of two 30 ng/ml iron standard solutions bracketing the unknown samples (faecal sample solutions) in the analysis sequence.

The following results were obtained.

	Day 1		Day 2	
	$^{54}Fe/^{56}Fe$	$^{56}Fe/^{57}Fe$	$^{54}Fe/^{56}Fe$	$^{56}Fe/^{57}Fe$
$Ratio_{corr}$	0.0638	42.8384	0.0634	43.4592
True	0.0637	43.3006	0.0637	43.3006
f_{md}	0.999	1.011	1.004	1.010

Table 4.3 *Faecal samples external correction*

The results for day 1 are almost identical despite the different correction schemes. The best result, judged on the f_{md} values, for the $^{54}Fe/^{56}Fe$ ratio on day 2 was obtained with the external correction, while the best result for the $^{56}Fe/^{57}Fe$ ratio was obtained with the mathematical correction. However, the differences are small and based on the above results, it is impossible to conclude which correction scheme is the best. The choice of correction scheme therefore can be made on the basis of practical considerations.

Appendix 5: Determination of detector dead time

The detector dead time was determined for the $^{42}Ca/^{43}Ca$ ratio using both the graphical method and the least square fitting method. Both determinations were performed on the same data set originating from the measurement of calcium isotopes in standard solutions with concentrations of 500, 1000 and 2000 ng/ml. Since the standard solutions also contain low levels of strontium, the data were corrected for overlap from doubly charged strontium ions. The data is shown in Table 5.1, also the observed and the final dead time corrected ratios are presented. The final ratios were corrected using the detector dead time of 10.5 ns determined by both methods. The observed $^{42}Ca^{+}/^{43}Ca^{+}$ ratios are dependant on the total calcium concentration, due to an increasing loss of counts on $^{42}Ca^{+}$ with increasing calcium concentration, as an increasing number of $^{42}Ca^{+}$ ions reach the detector, while the detector is still processing the signal from the previous ion.

Conc. (ng/ml)	$^{42}Ca^{+}$	$^{43}Ca^{+}$	$^{42}Ca^{+}/^{43}Ca^{+}$	
			Observed	*Corrected*
500	885768	170190	5.2046	5.2441
1000	2827368	552666	5.1159	5.2418
2000	4710276	935709	5.0339	5.2438

Table 5.1 *Observed $^{42}Ca^{+}/^{43}Ca^{+}$ ratios*

Normally more than three different standard solutions are used, but this presentation is a description of the principles and therefore only three solutions are used throughout the example in order not to complicate graphs and calculations unnecessarily.

Graphical determination of detector dead time

The normalised isotope ratios for the three concentration levels are calculated for the graphical determination of detector dead time. The normalised ratio is calculated as the observed isotope ratio corrected for dead time divided by the natural isotope ratio. The normalised ratios are then plotted against the dead time producing a curve for each concentration level, see graph in Figure 5.1. The detector dead time at which the curves intersect is the correct dead time for the detector, which for the example given is approximately 10 ns. In this case all three curves apparently intersect in the same point, but a closer inspection of the curves reveals that this is not entirely true. In Figure 5.2, three different intersects are seen (10.25, 10.50 and 10.75 ns). The average dead time is then used as the best estimate of the detector dead time. The difference between the estimated values can then be used as a measure of the precision of the determination of the detector dead time. For this example

the standard deviation on the three estimates is 0.25 ns. The estimated detector dead time is then 10.50 ± 0.25 ns ($\bar{x}$ ± SD). The value of the normalised ratios corresponding to the curve intersects is a measure for the observed mass discrimination. For the example given here the normalised ratio is approximately 1.0935, which is similar to a f_{md} value of 0.91, a rather large mass discrimination.

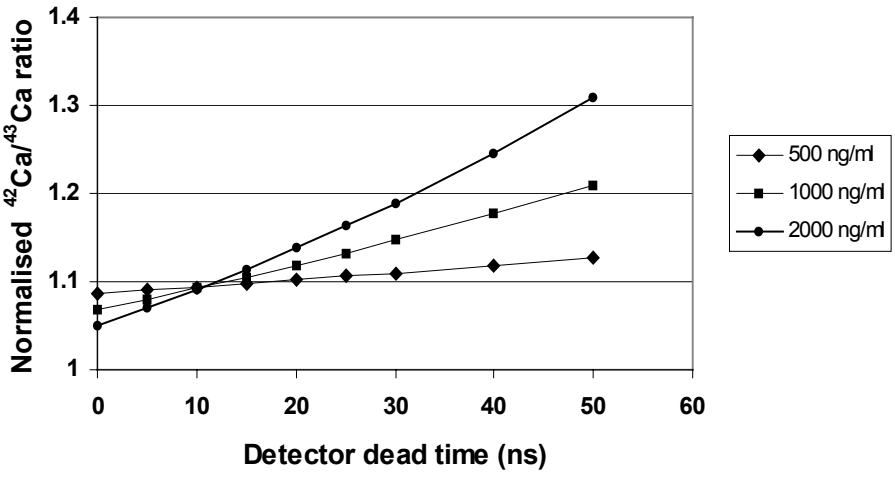

Figure 5.1 *Graphical determination of detector dead time*

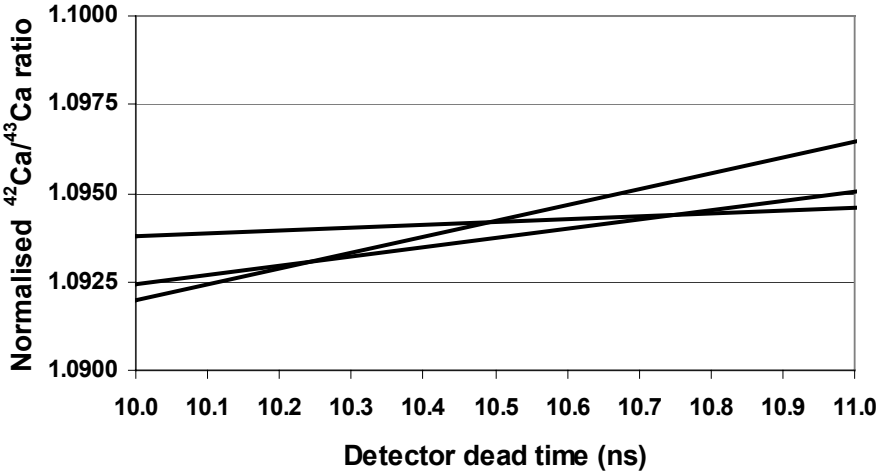

Figure 5.2 *Precise graphical detector dead time determination*

Determination of detector dead time by minimisation of the standard deviation

Using this approach the detector dead time is determined as the dead time that results in minimum standard deviation of the isotope ratios measured in the standard solutions of different concentration levels. An iterative procedure, which at the same time corrects for detector dead time, calculates the ratios and the standard deviation can easily be performed in

a spreadsheet. Figure 5.3 shows the excel spreadsheet made to determine the detector dead time for the above experiments. The correct value is easily found by trying different values for the detector dead time. A typical iterative procedure is shown in Table 5.2. As with the graphical method a detector dead time of 10.5 ns was found. Using this procedure there is no estimate of the precision of the determination. An estimate of the mass discrimination (f_{md}) can be calculated from the average ratio.

	A	B	C	D	E	F	G	H
1	**Detector dead time by minimisation of the standard deviation**							
2								
3	***Experimental data***							
4	**Standard**	**$^{42}Ca^{+}$**	**$^{43}Ca^{+}$**					
5	500	***885767.8***	***170189.5***					
6	1000	***2827368***	***552666***					
7	2000	***4710276***	***935709***					
8								
9	**Dead time (ns)**	***10.5***						
10	Dead time (s)	1.05E-08		**(conversion into seconds)**				
11								
12	**Standard**	**$^{42}Ca/^{43}Ca$**		**(correction for dead time and calculation of ratio)**				
12	500	5.2441		=(B5/C5)*(1-B10*C5)/(1-B10*B5)				
14	1000	5.2418		=(B6/C6)*(1-B10*C6)/(1-B10*B6)				
15	2000	5.2438		=(B7/C7)*(1-B10*C7)/(1-B10*B7)				
16								
17				**(calculation of average and standard deviation)**				
18	Average	5.2432		=AVERAGE(B13:B15)				
19	**SD**	**0.0012**		=STDEV(B13:B15)				

Figure 5.3 *Excel spreadsheet for determination of detector dead time*

Dead time (ns)	Standard deviation
20	0.0865
15	0.0397
10	0.0046
5	0.0461
11	0.0044
12	0.0130
10.5	0.0012
10.7	0.0020
10.4	0.0016
10.6	0.0014

Table 5.2 *Sequence for determination of detector dead time*

The application of the correct detector dead time is crucial when unknown samples are analysed and high count rates are encountered. If for instance, a detector dead time of 20 was applied instead of the correct value of 10.5 the $^{42}Ca^{+}/^{43}Ca^{+}$ ratio measured in the 500 ng/ml calcium standard solution would change from 5.2441 to 5.2804. A relative change of 0.7 %, which is a significant change considering that the measurement precision is approximately 0.4 %.

Appendix 6: Uncertainty on calcium absorption rates

Using the laws of error propagation and the procedure outlined by Eurochem[84] it is possible to estimate the uncertainty on the different terms in the equations used to calculate calcium absorption from double stable isotope experiments. These equations, presented in chapter 4 are:

$$Absorption(\%) = 100 \cdot \frac{na^{44}Ca}{na^{42}Ca} \cdot \frac{^{42}Ca(i.v)}{^{44}Ca(oral)} \cdot \frac{\%XS^{44}Ca}{\%XS^{42}Ca} \qquad (4.1)$$

Where $na^{44}Ca$ and $na^{42}Ca$ are the natural abundances of ^{44}Ca and ^{42}Ca, respectively, $^{42}Ca(i.v.)$ and $^{44}Ca(oral)$ are the doses of the isotopes administered in mmol and $\%XS^{44}Ca$ and $\%XS^{42}Ca$ are the % atom enrichment defined as:

$$\%XS = \frac{(R_{enriched} - R_{baseline})}{R_{baseline}} \qquad (4.2)$$

Here $R_{enriched}$ and $R_{baseline}$ are the isotope ratios (^{42}Ca/^{43}Ca or ^{44}Ca/^{43}Ca) in the enriched and baseline sample, respectively.

The uncertainty on the individual terms in equation 4.1 can be estimated, and from these estimates the combined uncertainty on the absorption rate can be estimated. The combined uncertainty is calculated with the original set-up as an example, see chapter 4.1. Two rules are applied to estimate the combined uncertainty of analytical results. The rules, quoted from Eurochem[84] are as follows. Rules 1, which is used for models involving only a sum or difference of quantities, e.g. $y = k \cdot (p + q + r + ..)$ where k is a constant, the combined standard uncertainty $u_c(y)$ is given by:

$$u_c(y(p,q..)) = k \cdot \sqrt{u(p)^2 + u(q)^2 + ...} \quad \text{(Rule 1)}$$

The second rule for models involving a product or quotient, e.g. $y = k(pqr..)$, where k is a constant, the combined standard uncertainty $u_c(y)$ is given by:

$$u_c(y) = y \cdot k \cdot \sqrt{\left(\frac{u(p)}{\bar{p}}\right)^2 + \left(\frac{u(q)}{\bar{q}}\right)^2 + ...} \qquad \text{(Rule 2)}$$

The original mathematical model is then broken down into expressions that consist solely of operations covered by one of the above rules.

The combined uncertainty on the first term ($na^{44}Ca/na^{42}Ca$) of equation 4.1 can be estimated using rule 2. The uncertainties (standard deviation) on the natural abundance of the calcium isotopes are stated in IUPACs table over the isotopic compositions of the elements 1997[1]. The following uncertainty is found:

$$u_c(na^{44}Ca/na^{42}Ca) = \frac{2.086}{0.647}\cdot\sqrt{\left(\frac{0.002}{2.086}\right)^2+\left(\frac{0.0015}{0.647}\right)^2} = 0.0081$$

The combined uncertainty on the second term ($^{42}Ca(i.v.)/^{44}Ca(oral)$) can again be estimated using rule 2. The standard deviation on the preparation of the two doses can be estimated from the uncertainty on the weight or volume of a given amount of stable isotope. The standard deviation is estimated assuming that doses of 3.3 mg ^{42}Ca and 16.7 mg ^{44}Ca, as the high doses in the original experiment, chapter 4.1. For the ^{42}Ca dose approximately 8.900 g of a solution contain 0.380152 mg ^{42}Ca/ml and density of 0.9804 g/ml is used. The dose is weighed with three significant decimal places. The uncertainty being ± 0.0005 g, since the distribution of the uncertainty is unknown it is assumed that it follows a rectangular distribution[84]. The uncertainty is then $u(w) = 0.0005/\sqrt{3} = 0.0003g$, it is assumed that the uncertainties on the other quantities are negligible. The quantities $y(^{42}Ca(i.v))$ and $u_c(^{42}Ca(i.v))$ can then be calculated as:

$$y(^{42}Ca(i.v.)) = \frac{8.900g\cdot 0.9804ml/g\cdot 0.380152mg/ml}{41.9586g/mol} = 0.0791mmol$$

$$u_c(^{42}Ca(i.v.)) = \frac{0.0003g\cdot 0.9804ml/g\cdot 0.380152mg/ml}{41.9586g/mol} = 2.66\cdot 10^{-6}\ mmol$$

For the ^{44}Ca dose approximately 4.3 ml of a solution containing 3.886064 mg/ml is used. The uncertainty on the pipette is ± 0.03 ml. A rectangular distribution is assumed producing a standard deviation of $u(v) = 0.03/\sqrt{3} = 0.0173g$. The quantities $y(^{44}Ca(oral))$ and $u_c(^{44}Ca(oral))$ can then be calculated as:

$$y(^{44}Ca(oral)) = \frac{4.3\ ml\cdot 3.886064\ mg/ml}{43.9555\ g/mol} = 0.3802\ mmol$$

$$u_c(^{44}Ca(oral)) = \frac{0.0173\ ml\cdot 3.886064\ mg/ml}{43.9555\ g/mol} = 0.0015\ mmol$$

The combined uncertainty on the second term can now be calculated using rule 2:

$$y\left(\frac{^{42}Ca(i.v.)}{^{44}Ca(oral)}\right)=\frac{0.0791}{0.3802}=0.2080$$

$$u_c\left(\frac{^{42}Ca(i.v.)}{^{44}Ca(oral)}\right)=\frac{0.0791}{0.3802}\cdot\sqrt{\left(\frac{2.66\cdot10^{-6}}{0.0791}\right)^2+\left(\frac{0.0015}{0.3802}\right)^2}=0.0008$$

For the calculation of the combined uncertainty of the third term it is assumed that $\%XS^{44}Ca$ and $\%XS^{42}Ca$ are 2 and 4 respectively and that three replicates are performed, i.e. similar to the original experiment[82]. The term is split into two parts $\%XS^{44}Ca$ and $\%XS^{42}Ca$, the uncertainty is then calculated for the two part-terms and finally combined using rule 2. Given the above assumption the following quantities are given:

$$\begin{aligned}
&^{42}R_b = (^{42}Ca/^{43}Ca)_{basis} &&= 4.7926\\
&^{42}R_e = 1.04\cdot{}^{42}R_b = (^{42}Ca/^{43}Ca)_{enriched} &&= 4.9843\\
&^{42}S_3 = \%RSD_{42}/\sqrt{3} &&= 0.24\\
&\\
&^{44}R_b = (^{44}Ca/^{43}Ca)_{basis} &&= 15.4519\\
&^{44}R_e = 1.02\cdot{}^{44}R_b = (^{44}Ca/^{43}Ca)_{enriched} &&= 15.7609\\
&^{44}S_3 = \%RSD_{44}/\sqrt{3} &&= 0.19
\end{aligned}$$

Where R_b and R_e are the baseline and enriched ratios and S_3 is the %SEM for 3 replicates. The uncertainty on $\%XS^{42}Ca$ can then be calculated combining rule 1 and 2 as follows:

$$y(\%XS^{42}Ca)=100\cdot\frac{^{42}R_e-{}^{42}R_b}{^{42}R_b}=100\cdot\frac{0.1917}{4.7926}=4$$

$$u_c(\%XS^{42}Ca)=100\cdot\frac{^{42}R_e-{}^{42}R_b}{^{42}R_b}\cdot\sqrt{\left(\frac{\sqrt{\left(^{42}R_e\cdot{}^{42}S_3/100\right)^2+\left(^{42}R_b\cdot{}^{42}S_3/100\right)^2}}{\left(^{42}R_e-{}^{42}R_b\right)}\right)^2+\left(\frac{^{42}R_b\cdot{}^{42}S_3/100}{^{42}R_b}\right)^2}$$

$$u_c(\%XS^{42}Ca)=4\cdot\sqrt{\left(\frac{\sqrt{(0.0120)^2+(0.0115)^2}}{0.1917}\right)^2+\left(\frac{0.0115}{4.7926}\right)^2}=4\cdot\sqrt{0.0075+5.76\cdot10^{-6}}=0.3465$$

Similarly for ^{44}Ca values of 2 and 0.2714 was calculated for $y(\%XS^{44}Ca)$ and $u(\%XS^{44}Ca)$, respectively. The combined uncertainty of the third term can now be calculated as:

$$u_c\left(\frac{\%XS^{44}Ca}{\%XS^{42}Ca}\right) = \frac{2}{4}\cdot\sqrt{\left(\frac{0.2714}{2}\right)^2 + \left(\frac{0.3465}{4}\right)^2} = 0.0805$$

Now the values and uncertainty of all the term in equation 4.1 is known, they are presented in the table below.

Term	Y	$u_c(y)$	$(u_c(y)/y)^2$
$na^{44}Ca/na^{42}Ca$	3.2241	0.0081	$6.3\cdot10^{-6}$
$^{42}Ca(i.v.)/^{44}Ca(oral)$	0.2080	0.0008	$1.5\cdot10^{-5}$

Table 6.1 *uncertainty on equation 4.1*

From the values in table 6.1 a calcium absorption (%Abs) of 33.53 is calculated. The u_c(%Abs) is calculated as shown below applying rule 2:

$$u_c(\%Abs) = 33.53\cdot\sqrt{6.3\cdot10^{-6} + 1.5\cdot10^{-5} + 0.0259} = 5.40$$

This corresponds to a relative standard deviation (% RSD_{abs}) of 16.11 %. Since the uncertainty on the third term is much larger than the uncertainty on the first two terms, the uncertainty on these two terms are left out, resulting in a $\%RSD_{abs}$ of 16.09 %. Showing that 99.9 % of the total uncertainty originates from the third term, the assumption that the first two terms can be set to zero is valid. Taking a closer look on the equation used to calculate $u_c(\%XS^{42}Ca)$ above, it can be seen that the second term under the square root is much smaller than the first term (0.0075 compared with $5.76\cdot10^{-6}$) ignoring this term in both the calculation of $\%XS^{42}Ca$ and $\%XS^{44}Ca$ a $u_c(XS\%^{44}Ca/\%XS^{42}Ca)$ of 0.0805 is still found, therefore the assumption that the second term can be set to zero is valid. Taking into account these two assumptions a more simple set of equations can be set-up for the calculation of $\%RSD_{abs}$, see box 1. Where S_n is the %SEM for n replicates, calculates as $\%RSD_{44}/\sqrt{n}$.

$$u_c(\%XS^{42}Ca) = \frac{100 \cdot \sqrt{\left(\frac{^{42}R_e \cdot ^{42}S_n}{100}\right)^2 + \left(\frac{^{42}R_b \cdot ^{42}S_n}{100}\right)^2}}{^{42}R_b}$$

$$u_c(\%XS^{44}Ca) = \frac{100 \cdot \sqrt{\left(\frac{^{44}R_e \cdot ^{44}S_n}{100}\right)^2 + \left(\frac{^{44}R_b \cdot ^{44}S_n}{100}\right)^2}}{^{44}R_b}$$

$$\%RSD_{abs} = 100 \cdot \sqrt{\left(\frac{u_c(\%XS^{42}Ca)}{\%XS^{42}Ca}\right)^2 + \left(\frac{u_c(\%XS^{44}Ca)}{\%XS^{44}Ca}\right)^2}$$

***Box 1**. Equations for calculation of $\%RSD_{abs}$*

For a given set of %XS values and S_n values, the latter determined by the number of replicates applied, the estimated relative standard deviation on the calcium absorption can be estimated. In Table 6.2 below three examples are given, in example 1 the $\%RSD_{abs}$ is calculated for the food oil experiment[85], while example 2 and 3 are those used for the economical considerations in chapter 4.1. The calculations are performed under the assumption that the measurement precision (%RSD) is 0.41 and 0.33 for $^{42}Ca^+/^{43}Ca^+$ and $^{44}Ca^+/^{43}Ca^+$, respectively, as in the method published in paper I.

	Example 1	**Example 2**	**Example 3**
$\%XS^{44}Ca$	5	6	8
$\%XS^{42}Ca$	4	4	6
Replicates	3	6	3
$\%RSD_{abs}$	10.2	6.9	6.8

***Table 6.2** calculated $\%RSD_{abs}$ values*

The $\%RSD_{abs}$ calculated for the food oil experiment has also been measured experimentally. The $^{42}Ca^+/^{43}Ca^+$ and $^{44}Ca^+/^{43}Ca^+$ ratios and the resulting calcium absorption rates were determined in the urine samples from one subject on four different days. One the four days absorption rates of 40.2, 46.2, 49.0 and 44.6 were determined corresponding to a $\%RSD_{abs}$ of 8.2. A value in good agreement with the estimated value of 10.2, showing that the procedure for estimation of $\%RSD_{abs}$ produce valid results.

In general if the $u_c(y)$ values is multiplied by a factor of two the combined expanded uncertainty is produced, which corresponds to a 95% confidence interval, providing that the underlying distribution approach a normal distribution[84].

Paper I

Measurement of ^{44}Ca: ^{43}Ca and ^{42}Ca:^{43}Ca isotopic ratios in urine using high resolution inductively coupled plasma mass spectrometry.

Published in:

Journal of Analytical Atomic Spectrometry, 1997, 12, 919-923

Authors:

Stefan Stürup, Marianne Hansen, and Christian Mølgaard

Paper II

High resolution inductively coupled plasma mass spectrometry for the trace determination of plutonium isotopes and isotope ratios in environmental samples

Published in:

Journal of Analytical Atomic Spectrometry, 1998, 13, 1321-1326

Authors:

Stefan Stürup, Henning Dahlgaard, and Steffen Chen Nielsen

Paper III

Application of HR-ICPMS for the simultaneous measurement of zinc isotope ratios and total zinc in human samples.

Published in:

Journal of Analytical Atomic Spectrometry, 2000, 15, 315-321.

Author:

Stefan Stürup

Bibliographic Data Sheet **Risø-R-1192(EN)**

Title and authors

Development, optimisation, and application of ICP-SFMS methods for the measurement of isotope ratios

Stefan Stürup

ISBN	ISSN
87-550-2715-6 87-550-2738-5 (Internet)	0106-2840

Department or group	Date
Plant Biology and Biogeochemistry Department	July 2000

Groups own reg. number(s)	Project/contract No(s)

Pages	Tables	Illustrations	References
126	29	19	151

Abstract (max. 2000 characters)

The measurement of isotopic composition and isotope ratios in biological and environmental samples requires sensitive, precise, and accurate analytical techniques. The analytical techniques used are traditionally based on mass spectrometry, among these techniques is the ICP-SFMS technique, which became commercially available in the mid 1990s. This technique is characterised by high sensitivity, low background, and the ability to separate analyte signals from spectral interferences. These features are beneficial for the measurement of isotope ratios and enable the measurement of isotope ratios of elements, which it has not previously been possible to measure due to either spectral interferences or poor sensitivity.

The overall purpose of the project was to investigate the potential of the single detector ICP-SFMS technique for the measurement of isotope ratios in biological and environmental samples. One part of the work has focused on the fundamental aspects of the ICP-SFMS technique with special emphasize on the features important to the measurement of isotope ratios, while another part has focused on the development, optimisation and application of specific methods for the measurement of isotope ratios of elements of nutritional interest and radionuclides.

The fundamental aspects of the ICP-SFMS technique were investigated theoretically and experimentally by the measurement of isotope ratios applying different experimental conditions. It was demonstrated that isotope ratios could be measured reliably using ICP-SFMS by educated choice of acquisition parameters, scanning mode, mass discrimination correction, and by eliminating the influence of detector dead time.

Applying the knowledge gained through the fundamental study, ICP-SFMS methods for the measurement of isotope ratios of calcium, zinc, molybdenum and iron in human samples and a method for the measurement of plutonium isotope ratios and ultratrace levels of plutonium and neptunium in environmental samples were developed. The figures of merit of these methods demonstrated that isotope ratios could be measured with good precision and accuracy by ICP-SFMS.

Descriptors INIS/EDB

BIOLOGICAL MATERIALS; CALCIUM ISOTOPES; DATA COVARIANCES; ICP-MASS SPECTROSCOPY; IRON ISOTOPES; ISOTOPE RATIO; LEAD ISOTOPES; MAN; MOLYBDENUM ISOTOPES: NEPTUNIUM ISOTOPES; NUTRITION; OPTIMIZATION; PLUTONIUM ISOTOPES; RADIOECOLOGICAL CONCENTRATION; TECHNETIUM ISOTOPES; ZINC ISOTOPES

Available on request from Information Service Department, Risø National Laboratory,
(Afdelingen for Informationsservice, Forskningscenter Risø), P.O.Box 49, DK-4000 Roskilde, Denmark.
Telephone +45 4677 4004, Telefax +45 4677 4013